

A comparative analysis of the chemical composition of linear low density polyethylene polymers synthesised with 1-hexene comonomer under different catalytic conditions.

By

Preloshni Naidoo

Thesis presented in partial fulfilment of the requirements for the degree of Master of Science
at the University of Stellenbosch.

Study leader: Prof A. J. Van Reenen

March 2013



Dedication

To my parents, Pushparanie and Peter Utting, for their devotion and loyal support throughout my academic career. To Peter, for his constant encouragement and inspiration to excel in all that I do.

Abstract

A comparative study of the chemical composition of linear low density polyethylene polymers, synthesised with 1 - hexene as comonomer was conducted. Catalyst trials were conducted on the linear low density 1 - hexene polymer grade material to evaluate alternative catalysts. A comparative analysis was performed in order to investigate if the samples synthesised under catalyst trial conditions showed any significant differences in terms of crystallinity and mechanical properties with the reference sample that was synthesised using the reference catalyst.

The results showed that the macro product properties, namely melt flow Index, density, and level of hexene extractables are different for the trial samples in comparison with the reference sample. The differences observed implied that the trial samples were synthesised with differences on a molecular level. The differences in the chemical composition between the reference sample and the comparative samples were fully explored using a wide range of analytical techniques, namely crystallisation analysis by fractionation (CRYSTAF), temperature rising elution fractionation (TREF), differential scanning calorimetry (DSC), Carbon 13 nuclear magnetic resonance (^{13}C NMR), Size exclusion chromatography (SEC), Positron analysis lifetime spectroscopy (PALS) and micro hardness analysis. The results of the characterisation studies indicated the following:

- Crystallinity and hardness analysis of the reference sample, catalyst trial sample 1 and catalyst trial sample 2 indicate that the catalyst trial sample 2 having a low cocatalyst concentration is the most crystalline of all the samples.
- The reference sample, catalyst trial sample 1 and catalyst trial sample 2 were further fractionated using TREF at fractionation temperature intervals of 10 $^{\circ}\text{C}$. TREF analysis indicates that the bulk of the material is observed to elute between 70 $^{\circ}\text{C}$ - 100 $^{\circ}\text{C}$.
- ^{13}C NMR analyses of the TREF fractions identified four populations of fractions that could be selectively removed, allowing the bulk of the material to be recombined. As these highly crystalline fractions were removed, there was an observed decrease in the total crystallinity of the bulk recombined material. This trend was further verified by the free volume analysis.
- Free volume analysis indicated of the bulk recombined material indicated a general increase in the τ_3 lifetime and τ_4 lifetime intervals. Free volume analysis further confirmed a decrease in crystallinity of the bulk recombined material as highly crystalline material was removed.

- Micro hardness analysis of the polymers further verified the crystallinity trends observed. As the molecular composition of the polymer changed due to removal of highly crystalline fractions, the total mechanical strength of the material indicated by the hardness value decreased.

The study showed that by changing the chemical composition of the polymer by removing highly crystalline fractions, there was an observed change in the mechanical properties of the polymer. It can be concluded that the samples synthesised under catalytic conditions show significant differences in terms of crystallinity and mechanical properties in comparison with the sample that was synthesised using the standard reference catalyst.

Opsomming

'n Vergelykende analise studie is onderneem van die chemiese samestellings van lineêre lae digtheid poliëtileen polimere, gesintetiseer met 1-hekseen as ko-monomeer. Alternatiewe kataliste is ge-evalueer ten opsigte van lineêre lae digtheid 1-hekseen Sasol polimeer graad materiaal. Die vergelykende analise is uitgevoer om die monsters onder katalis proef kondisies te evalueer en te merk of enige beduidende verskille in terme van kristalliniteit en meganiese eienskappe met die verwysings monster voorkom.

Die resultate toon dat die makro-produk eienskappe, naamlik smelt vloeï indeks, digtheid en vlak van hekseen onttrekking, verskillend is vir die proef monsters in vergelyking met die verwysings monster. Die waargenome verskille impliseer dat die proef monsters op molekulêre vlak verskil. Die verskille in chemiese samestelling tussen die verwysings monster en die vergelykende monsters is ten volle ondersoek deur gebruik te maak van 'n wye verskeidenheid van analitiese tegnieke, naamlik kristallisasië analise fraksionering (CRYSTAF), temperatuur stygende eluering fraksionering (TREF), differensiële skandeer kalorimetrie (DSC), koolstof 13 kernmagnetiese resonansie (^{13}C KMR), gelpermeasie chromatografie (SEC), positron analise leeftyd spektroskopie (PALS) en mikro-hardheid analise. Die resultate van die karakterisering studies het die volgende aangedui:

- Kristalliniteit en hardheid analyses van die verwysings monster en katalis proef monsters 1 en 2 het getoon dat katalis proef monster 2, wat 'n lae ko-katalis konsentrasie bevat, die mees kristallyn is.
- Die verwysings monster en katalis proef monster 1 en 2 is gefraksioneer met behulp van 'n TREF met temperatuur tussenposes van 10 °C. TREF analise toon dat oormaat materiaal ge-elueer word tussen 70 °C en 100 °C.
- ^{13}C KMR analise van die TREF fraksies het 4 verskillende fraksies geïdentifiseer wat selektief verwyder kan word. Dit laat ook toe dat die grootste deel van die materiaal weer geherkombineer kan word. Soos die hoogs kristallyne fraksies verwyder is, is 'n afname in die totale kristalliniteit van die geherkombineerde materiaal waargeneem. Hierdie tendens is bevestig deur vrye volume analyses.
- Vrye volume analyses van die geherkombineerde materiaal toon 'n algemene toename in die τ_3 en τ_4 leeftyd aan. Vrye volume analyses toon verder dat 'n afname in die kristalliniteit van die geherkombineerde materiaal plaasvind soos meer kristallyne fraksies verwyder word.

- Verdere mikro-hardheid analises van die polimere bevestig die waargenome kristalliniteit tendense. Soos die molekulêre samestelling van die polimere verander as gevolg van die verwydering van die hoogs kristallyne fraksies, so neem die totale meganiese sterkte van die materiaal af; soos aangedui deur die afname in hardheid waarde.

Die studie toon dat die verandering van die chemiese samestelling van die polimeer, deur die verwydering van hoogs kristallyne fraksies, 'n waargenome verandering in die meganiese eienskappe van die polimeer laat plaasvind. Daar kan afgelei word dat die monsters, vervaardig onder die katalis proef voorwaardes, beduidende verskille toon in terme van kristalliniteit en meganiese eienskappe in vergelyking met die monster vervaardig deur die huidige verwysings katalis.

Acknowledgements

I wish to express my appreciation to the following people for their support and assistance during my studies:

My Managers (John Mellor, Monja Smith and Jenny Green): For their continued support and sponsorship during the course of the study.

My supervisors (Prof A. J. Van Reenen and Prof P. Mallon): For their supervision and support during the course of the study.

Gareth Harding: For his valued advice and willingness to assist.

To the Stellenbosch University administration Staff and Polyolefin research team:
Lisel Keulder, Tiaan Basson, Magaretha Brand, Mohammed Sweed, Jaco Brand for their assistance during the course of study.

Dr Tracy Bromfield: For her highly appreciated and valued mentorship, unwavering support and constant encouragement during the course of the study.

Nyambeni Luruli: For his valued guidance during the study review period.

Rojashree Beigley: For her effective networking skills.

Jerrie Vermeulen: For his assistance with the analytical work.

The Webber family : Isabel and Ray Webber: For their hospitality and friendship during my visits to the Cape. Gordon Andrew Webber: For his kindness. He will always be well loved and remembered by Gummi and Niki.

To my friends: For their encouragement and support during the course of the study.

Table of Contents

1	INTRODUCTION.....	1
1.1	General overview and scope of work.....	1
1.2	Aim	1
1.3	Objectives	2
1.4	Tasks	3
1.5	Layout of thesis	4
1.6	References	5
2	POLYETHYLENE	6
2.1	Polyethylene (a brief overview)	6
2.2	History of polyethylene	8
2.2.1	Low density Polyethylene (LDPE).....	9
2.2.2	Linear low density Polyethylene (LLDPE)	17
2.2.3	Polymerisation chemistry of LLDPE	17
2.3	The effect of catalyst chemistry on the crystallinity of LLDPE	22
2.4	Production of LLDPE via a low pressure gas phase polymerisation process 23	
2.5	Production of LLDPE via a solution phase polymerisation process	28
2.6	Production of LLDPE via slurry phase polymerisation process	30
2.7	Characterisation of LLDPE through fractionation.....	34
2.8	Temperature rising elution fractionation (TREF).....	34
2.9	Crystallisation analysis fractionation (CRYSTAF).....	36
2.10	Bulk characterisation techniques.....	37
2.11	Differential scanning calorimetry (DSC)	37
2.12	Size exclusion chromatography (SEC)	38
2.13	Positron annihilation spectroscopy (PALS)	40
2.14	Micro Hardness analysis.....	42
2.15	Carbon 13 nuclear magnetic resonance spectroscopy (¹³ C NMR).....	43
2.16	Solid state nuclear magnetic resonance spectroscopy (¹³ C NMR)	44
2.17	References	45
3	EXPERIMENTAL TECHNIQUES	48
3.1	Materials.....	48
3.1.1	Polymer	48
3.1.2	Stabiliser.....	48
3.1.3	Solvent	49
3.2	Analytical techniques.....	49
3.2.1	Temperature rising elution fractionation (TREF).....	49
3.2.2	CRYSTAF	51
3.2.3	Differential scanning calorimetry	51

3.2.4	Size exclusion chromatography	52
3.2.5	Solution state carbon 13 nuclear magnetic resonance (NMR).....	52
3.2.6	Solid state carbon 13 nuclear magnetic resonance (NMR)	53
3.2.7	Micro hardness analysis	53
3.2.8	Positron annihilation lifetime spectroscopy (PALS)	54
3.3	References	54
4	RESULTS AND DISCUSSION.....	55
4.1	Characterisation of bulk material	56
4.1.1	CRYSTAF analyses.....	56
4.1.2	TREF analysis	57
4.1.3	DSC analysis	62
4.1.4	SEC analysis	65
4.1.5	¹³ C NMR analyses	68
4.2	Characterisation of bulk material recombined with fractions removed.....	71
4.2.1	TREF analysis: Removal of TREF fractions	71
4.2.2	Molecular weight and dispersity index distribution.....	72
4.2.3	Crystallinity and comonomer content	73
4.2.4	Crystallinity and melting	74
4.2.5	Free volume analysis	77
4.2.6	Hardness analysis analysis.....	79
4.3	References	80
5	CONCLUSIONS.....	83
5.1	Conclusions.....	83
5.2	Future work.....	84

APPENDICES

Appendix A: DSC Data	85
Appendix B: NMR Data	90
Appendix C: SEC Data	95

TABLE OF FIGURES

Figure 2.1: LDPE autoclave production process [10].....	12
Figure 2.2: Tubular LDPE process summary [10].....	14
Figure 2.3: LDPE reactor profile design [10].....	16
Figure 2.5: SEC separation chromatograph for LLDPE sample [29].....	39
Figure 3.1: Tris (2, 4 - di-tert-butylphenyl) phosphate Irgafos 168 [1]	48
Figure 3.2: Irganox 1010 [1]	49
Figure 3.3: Illustration of the packing of a single TREF column [3]	50
Figure 4.1: CRYSTAF analysis of bulk LLDPE samples.....	57
Figure 4.2: TREF elution weight distribution for the reference sample.....	59

Figure 4.3: TREF elution profile for the catalyst trial sample 1.....	60
Figure 4.4: TREF fractionation data for the catalyst trial sample 2.....	61
Figure 4.5: TREF profile comparisons for reference sample, catalyst trial sample 1 and catalyst trial sample 2	62
Figure 4.6: DSC analyses of reference sample, catalyst trial sample 1, catalyst trial sample 2	64
Figure 4.7: Melting temperature of the reference sample, catalyst trial sample 1 and catalyst trial sample 2	65
Figure 4.8: Molecular weight trends for reference sample, catalyst trial sample 1 and catalyst trial sample 2	66
Figure 4.9: Molecular weight distribution across fractions	67
Figure 4.10: Distribution of DI across fractions	67
Figure 4.11: Suggested mechanism for active site formation activated by alkyl aluminium type (X: -Cl, A, B or C; ethyl, n-hexyl or Cl) [12]	71
Figure 4.12: % Crystallinity of recombined material with selective fractions removed.....	76

TABLE OF TABLES

Table 2.1: Differences between the tubular and autoclave LDPE technologies [10]	17
Table 2.2: Comparison of gas phase, solution phase and slurry-loop phases for the production of LLDPE [10].....	34
Table 4.1: Macro product properties for bulk reference sample, bulk catalyst trial sample 1 and bulk catalyst trial sample 2	56
Table 4.2: CRYSTAF results of bulk Reference sample, Catalyst Trial sample 1 and Catalyst Trial sample 2	57
Table 4.3: TREF fractionation results of reference sample	58
Table 4.4: TREF fractionation results for catalyst trial sample 1	60
Table 4.5: TREF fractionation data for catalyst trial sample 2.....	61
Table 4.6: DSC results of bulk samples	63
Table 4.7: Molecular weight and dispersity index of bulk samples.....	65
Table 4.8: Comonomer content of bulk samples	68
Table 4.9: Fitting parameters for the deconvolution of the CP MAS spectra of the LLDPE polymers and the determined values of crystallinity	69
Table 4.10: Comonomer content of fractions of samples.....	70
Table 4.11: Weight percentages of selected fractions removed for the reference case sample, catalyst trial sample 1 and catalyst trial sample 2	72
Table 4.12: Molecular weight distributions for the reference sample	72
Table 4.13: Molecular weight distributions for the catalyst trial sample 1	73
Table 4.14: Molecular weight distributions for the catalyst trial sample 2.....	73
Table 4.15: Comonomer content of reference sample fractions and bulk recombined material.....	74
Table 4.16: Comonomer content of catalyst trial sample 1 fractions and bulk recombined ...	74
Table 4.17: Comonomer content of catalyst trial sample 2 fractions and bulk recombined ...	74
Table 4.18: DSC data of fractions removed for the reference sample	75

Table 4.19: DSC data of fractions removed for the catalyst trial sample 1	75
Table 4.20: DSC data of fractions removed for the catalyst trial sample 2	75
Table 4.21: PALS data for reference sample, catalyst trial sample 1 and catalyst trial sample 2	77
Table 4.22: PALS data for the reference sample recombined with selected fractions removed	78
Table 4.23: PALS data for the catalyst trial sample 1 recombined with selected fractions removed.....	78
Table 4.24: PALS data for the catalyst trial sample 2 recombined with selected fractions removed.....	79
Table 4.25: Micro hardness results of bulk LLDPE samples.....	79
Table 4.26: Micro hardness results of the bulk recombined LLDPE samples with selective fractions removed	80

List of Abbreviations

LLDPE	Linear low density polyethylene
LDPE	Low density polyethylene
PE	Polyethylene
CRYSTAF	Crystallisation analysis fractionation
TREF	Temperature rising elution fractionation
PALS	Positron annihilation lifetime spectroscopy
DSC	Differential scanning calorimetry
CP MAS	Cross polarisation magic angle spinning
SEC	Size exclusion chromatography
¹³ C	Carbon thirteen
¹ H	Proton one
NMR	Nuclear magnetic resonance
Δ T	Difference in temperature
V _t	Total volume
V ₀	Free volume outside
V _g	Volume of polymer gel
e ⁺	Positron
e ⁻	Electron
γ	Gamma
IR	Infra red
o - Ps	Ortho - positronium
p - Ps	Para - positronium
MFI	Melt flow index

DMA	Dynamic mechanical analysis
VLDPE	Very low density polyethylene
MDPE	Medium density polyethylene
HDPE	High density polyethylene
UHMWPE	Ultra high molecular weight polyethylene
CSTR	Continuous stirred tank reactor
MAO	Methylaluminoxane
APC	Advanced process control
TMS	Tetramethylsilane
BHT	2,6 –di-tert-butyl-4-methylphenol
TEAL	Tri- ethyl aluminium
DI	Dispersity Index
θ	Teta
τ_3	Tau three lifetime intervals
τ_4	Tau four lifetime intervals

CHAPTER 1: INTRODUCTION

1.1 General overview and scope of work

LLDPE polymer can be produced by slurry, gas phase and solution phase production technologies. Not all polyolefin production companies maintain both pilot scale and commercial scale production facilities. During the commercial production of LLDPE, various process changes can be made to test new catalysts or make changes to the existing catalyst systems in order to improve the performance of the production process. Dynamic changes in the production process conditions such as changes to reaction temperature, reaction pressure, chain transfer agent concentration, catalyst concentration and rate of production can have a pronounced effect on the final polymer produced. During commercial scale production trials, process control attempts are made to control process variables to ensure that the final polymer product that is produced has similar macro product properties to the product made under standard conditions. However, in certain cases although there may be no significant changes to the polymer on a macro product property level, the polymer can be produced with changes on the molecular product property level. These changes affect the molecular architecture of the polymer resulting in the polymer having a different chemical composition and molecular structure to the polymer produced under standard conditions. Changes in the process conditions can have a significant effect on the molecular architecture of the polymer and can affect the thermal and crystalline polymer profiles, molecular weight, molecular-weight distribution, degree of comonomer branching, and the overall molecular heterogeneity of the final polymer.

This study focuses on the molecular architecture of linear low density polyethylene (LLDPE) polymer synthesised with 1-hexene as comonomer. The study shows how the removal of crystalline material results in an observed change in the molecular architecture of the polymer. The study is also comparative in nature, comparing linear low density polymer samples produced with different catalyst systems, to a reference polymer sample produced with a reference catalyst.

1.2 Aim

Previous work conducted by Keulder studied linear low density polyethylene synthesised with the butene as comonomer [1]. The concluding notes from the study indicated that similar investigative type work should be performed on LLDPE synthesised with a different

α -olefin comonomer. The recommendation was to check if the results obtained from the Keulder investigation could act as a model for all LLDPE polymers. The aim of this study is not a direct comparison to the Keulder work. This study is unique and different from the Keulder *et al* work in that a polymer with different comonomer, namely hexene, was studied and that a comparative study of LLDPE polymers synthesised with changes to the catalyst system were made. The aims of this study were to perform a characterisation study of LLDPE polymer and to compare LLDPE samples produced with changes to the catalyst system against a reference LLDPE sample produced under standard production conditions. In addition, further objectives were to ascertain whether selectively removing different polymer fractions from the bulk polymer material would result in significant changes in the product properties. Due to the heterogeneous nature of the LLDPE polymer, the molecular architecture is significantly affected by the comonomer concentration and degree of comonomer distribution and branching along the backbone of the polymer chain. The comonomer content has a profound effect on the crystallinity and the subsequent mechanical strength of polyolefin polymers [2]. The characterisation study through fractionation entailed the use of the high temperature preparative temperature rising elution fractionation (TREF) technique. TREF is a useful technique that fractionates semi crystalline polymers according to their ability to crystallise from solution which is dependent on the crystallisable sequence length of the polymer chains [2]. The technique was extensively used in this study to selectively fractionate the bulk samples. The DSC technique and the solid state ^{13}C NMR technique was used to measure the degree of crystallinity of the fractions isolated from the TREF experiments. Based on the measurements obtained, selectively distinct fractions could be identified and removed. The bulk of the material was thereafter recombined and the product property testing was conducted on the bulk of the material to assess if the removal of the crystalline fractions significantly affected the crystalline and mechanical properties of the polymer. The Positron annihilation lifetime spectroscopic technique (PALS) was used to measure the free volume content of the recombined bulk material to further gain an understanding of the internal free volume in the crystalline and the amorphous areas in the semi crystalline polymer. The individual objectives of the study are listed in Section 1.3.

1.3 Objectives

- Previous work conducted by Keulder investigated the effect of the molecular composition on the mechanical properties of LLDPE - 1-butene using preparative

TREF as a fractionation technique. This study was extended to the LLDPE- 1-hexene polymer to see if similar results could be obtained.

- Three LLDPE samples synthesised under different catalytic conditions were compared in order to investigate if all the samples showed the same degree of crystallinity or if there were differences in crystallinity due to the differences in the catalytic conditions.
- To investigate the effect on the mechanical properties of the LLDPEs by the individual (crystalline) fractions of the material.

1.4 Tasks

The following tasks were identified to perform in order to realise the objectives listed above.

- Fractionate the bulk reference LLDPE sample, bulk catalyst trial LLDPE sample 1 and bulk catalyst trial LLDPE sample 2 using preparative TREF.
- Characterise each fraction by using DSC, SEC and ^{13}C NMR.
- Remove the selective fractions from the bulk samples and recombine the rest of the fractions to form the recombined bulk materials in order to see the influence of certain fractions on the bulk polymer properties.
- Characterise the recombined bulk materials by using DSC, SEC and ^{13}C NMR analytical techniques.
- Measure the free volume content of the bulk recombined material with the PALS technique.
- Measure the mechanical strength of the bulk recombined material with the micro hardness technique.
- Upon completing the comparative analyses between the reference sample and the catalyst trial samples, evaluate if the changes in the catalyst systems significantly affected the polymer product properties.

1.5 Layout of thesis

Chapter 1

Chapter 1 identifies the aim and the objectives of the study.

Chapter 2

Chapter 2 presents a brief discussion on the historical and theoretical background of the production of polyethylene. The commercial scale production processes for LLDPE and LDPE polymers are discussed. The polymerisation chemistry for LDPE and LLDPE polymerisation reactions are discussed. The molecular properties of the LLDPE are also discussed, with the emphasis on crystallinity, branching, molecular weight and thermal properties. The chapter concludes with a discussion on the fractionation and analytical techniques used in the study.

Chapter 3

The chapter discusses the experimental procedures for the fractionation and analytical techniques used in the study. This includes TREF, CRYSTAF, DSC, ^{13}C NMR, SEC, PALS and DMA.

Chapter 4

The chapter focuses on a detailed discussion of the characterisation and the fractionation of the bulk LLDPE samples. The results from the various analytical techniques and free volume analyses are also discussed.

Chapter 5

The chapter presents the conclusions drawn from the results obtained from the study as well as the recommendations for future work.

1.6 References

1. Keulder L., The effect of molecular composition on the properties of linear low density polyethylene. MSc Thesis, University of Stellenbosch: Stellenbosch 2008
2. Harding, G. W and A. J Van Reenen, Fractionation and characterisation of propylene ethylene copolymers: Effect of comonomer on crystallisation of poly(propylene) in the γ – phase. Journal of macromolecular chemistry and physics 2006. 207: p. 1680 - 1690
3. Wild, L., Temperature rising elution fractionation. Advances in polymer science, 1990. 98: p. 1 - 47.

CHAPTER 2

2 POLYETHYLENE

2.1 Polyethylene (a brief overview)

Polyethylene is the largest volume synthetic commodity polymer in the world [1]. The polymer can be classified into the following types namely; very low density polyethylene (VLDPE), low density polyethylene (LDPE), linear low density polyethylene, (LLDPE), medium density polyethylene (MDPE), high density polyethylene (HDPE), ultra-high molecular weight polyethylene (UHMWPE) and elastomers.

VLDPE is defined by a density range of 0.880 - 0.915 g/cm³ and is a substantially linear polymer with high levels of short-chain branches, commonly made by copolymerisation of ethylene with short-chain alpha-olefins (for example, 1-butene, 1-hexene and 1-octene). VLDPE is most commonly produced using metallocene catalysts due to the greater comonomer incorporation possible when using these catalysts. Metallocene catalysts have a much better distribution of the comonomer. The distribution is much more uniform as compared to the Ziegler catalysts where the distribution is more heterogenous. VLDPEs are used for hose and tubing, ice and frozen food bags, food packaging and stretch wrap as well as impact modifiers when blended with other polymers.

Low density polyethylene (LDPE) has density ranging from 0.910 - 0.930 g/cm³ and is characterised by a high degree of short and long chain branching, which prevents the packing of the chains into a defined crystal structure. As a consequence, the polymer has weaker intermolecular forces as the instantaneous dipole induced-dipole attraction is less in comparison to LLDPE which is more crystalline than the LDPE polymer. This results in the polymer having a lower tensile strength and increased ductility. The high degree of branching with long chains gives molten LDPE unique and desirable flow properties. LDPE is used for both rigid containers and plastic film applications such as plastic bags and film wrap. The global demand for LDPE in 2011 was approximately 45% of the total demand for polyethylene (LDPE + LLDPE) [1]. The world LDPE production capacity is projected to increase at an average rate of about 3% per year through 2016 [1].

Linear low density polyethylene (LLDPE) has density ranging from 0.915 - 0.940 g/cm³. LLDPE is a substantially linear polymer in comparison to LDPE. The polymer is characterised by a significant number of short chain branches, commonly made by copolymerisation of ethylene with short-chain alpha-olefins (for example, 1-butene, 1-hexene and 1-octene). Although LLDPE has a significant number of short chain branches, it exhibits a much lower tensile strength than VLDPE. This is due to the highly branched structure of the VLDPE. In comparison, LLDPE has higher tensile strength than LDPE due to the linear structure of the LLDPE polymer. LLDPE exhibits higher impact and puncture resistance than LDPE. Lower thickness (gauge) LLDPE films can be blown in comparison to LDPE. These resins have better environmental stress cracking resistance but are not as easy to process. LLDPE is used in packaging, particularly film for bags and sheets. LLDPE is used in films primarily due to its toughness, flexibility and relative transparency. The product examples range from agricultural films, saran wrap, and bubble wrap, to multilayer and composite films. The global demand for LLDPE continues to increase. LLDPE continues to gain market share in the combined LLDPE/LDPE market. In 2011 the world LLDPE demand share was 30 % of the total demand for polyethylene. The world consumption of LLDPE was projected to reach 29.2 million metric tons by 2012 [2].

MDPE is defined by a density range of 0.926 - 0.940 g/cm³. Depending on the type of production technology used to manufacture the MDPE, chromium/silica catalysts, Ziegler-Natta catalysts or metallocene catalysts can be used in the various production processes. MDPE has good shock and drop resistance properties. It also is less notch sensitive than HDPE, stress cracking resistance is better than HDPE. MDPE is typically used in gas pipes and fittings, sacks, shrink film, packaging film, carrier bags and screw closures. MDPE is widely used in the rotomoulding application processes to manufacture roof top water tanks, toys and kayaks.

High density (HDPE) has density ranging from 0.960 - 0.970 g/cm³. The polymer has a low degree of branching and thus stronger intermolecular forces and tensile strength. HDPE can be produced by chromium/silica catalysts, Ziegler-Natta catalysts or metallocene catalysts. The low degree of branching is determined by an appropriate choice of catalyst (for example, chromium catalysts or Ziegler-Natta catalysts) and reaction conditions. There has recently been much development in the area of bimodal HDPE and the use of dual reactor technology to manufacture bimodal HDPE. Most polymer companies are introducing new catalyst technologies to manufacture bimodal

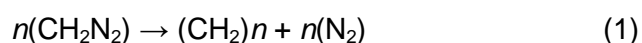
HDPE. HDPE is used in products and packaging such as milk jugs, detergent bottles, margarine tubs, garbage containers and water pipes. One third of all toys are manufactured from HDPE.

Ultra high molecular weight polythene (UHMWPE) is a group of linear polyethylene materials with a molecular weight ranging ten times more than that of commercial high density polyethylene. The high molecular weight makes it a very tough material, but results in less efficient packing of the chains into the crystal structure as evidenced by densities of less than high density polyethylene (for example, 0.930 - 0.935 g/cm³). UHMWPE can be made through any catalyst technology, although Ziegler catalysts are most commonly used in the UHMWPE production process. Because of its outstanding toughness and its cut, wear and excellent chemical resistance, UHMWPE is used in a diverse range of applications. These include can and bottle handling machine parts, gears, artificial joints, edge protection on ice rinks and butchers' chopping boards. It competes with Aramid in bullet-proof vests, under the trade names Spectra and Dyneema, and is commonly used for the construction of articular portions of implants used for hip and knee replacements [3].

Plastomers are linear low density polyethylene type materials which have very low density values as well as low crystallinity. These linear low density polyethylene materials are typically produced in solution by metallocene single site catalyst systems [4].

2.2 History of polyethylene

The discovery of the polyethylene polymer occurred in the 19th century. The discovery was in fact, accidental. The polymer was accidentally synthesised in 1898 by the German chemist, Hans von Pechmann [4]. The synthesis was as a consequence of heating diazomethane and was represented by equation 1 [5]:



The first industrial polyethylene synthesis was again discovered by accident in 1933 by Eric Fawcett and Reginald Gibson at the Imperial Chemical Industries (ICI) works in Northwick, England. This discovery was made by applying high pressure in the region of several hundred atmospheres to a mixture of ethylene and benzaldehyde at 200 °C

[5]. The result was the production of a white waxy material. The reaction was difficult to instantaneously reproduce as the reaction was initiated by trace levels of oxygen which contaminated the apparatus. The mechanism of the polymerisation was not clearly understood. In 1935, another ICI chemist, Michael Perrin, developed this accident into a reproducible experimental reaction. The reproducible reaction became the basis for the industrial scale ICI LDPE production [5].

During World War II, further research was conducted in the United States on the ICI process. In the late 1940's the Bakelite Corporate at Sabine, Texas and Du Pont at Charleston, West Virginia, began a large scale commercial production of polyethylene under a technology license agreement from ICI. Further milestones in the history of the synthesis of polyethylene have revolved around the development of several types of catalysts [6 - 8]. These catalyst systems promote the polymerisation of LLDPE and LDPE at lower temperatures and pressures.

The Phillips catalyst system was discovered in 1951 by Robert Banks and J. Paul Hogan at Phillips Petroleum. This system was a chromium trioxide based catalyst system. In 1953, the German chemist, Karl Ziegler, developed a catalytic system based on titanium halides and organoaluminium compounds that worked at even milder conditions than the Phillips catalyst [6]. Both catalyst systems are used in industry for the production of linear low density polyethylene and HDPE production. The third type of catalytic system based on metallocenes was discovered in 1976 [9]. The discovery was made by Walter Kaminsky and Hansjörg Sinn [9]. The metallocene catalysts are active single site catalysts for ethylene polymerisation. Recent work done by Fujita at the Mitsui Corporation has demonstrated that certain salicyaldimine complexes of Group 4 metals show substantially higher activity than the metallocenes [9].

2.2.1 Low density Polyethylene (LDPE)

Low density Polyethylene can be produced via two production technologies, namely via an autoclave reaction process and via a high pressure tubular reaction process. Both production processes entail the homo polymerisation of ethylene via a free radical polymerisation process.

2.2.1.1 Polymerisation chemistry of LDPE

The polymerisation of ethylene to produce low density polyethylene occurs via a free radical polymerisation process. The main reaction steps involved in the polymerisation of ethylene are initiator decomposition, initiation of polymer chain, propagation of polymer chain, chain transfer reactions and termination of polymer chains. These main reactions determine the overall rate of polymerisation.

Early LDPE processes used oxygen as a source of free radicals but due to the paradoxical nature of oxygen (acting as both an inhibitor and an initiator), oxygen was replaced by organic peroxides. In current high pressure LDPE polymerisation processes, a mixture of peroxides is used to initiate the free radical polymerisation reaction. Typically cocktail mixtures of low temperature peroxyesters and high temperature peroxides components are used to initiate LDPE reactions. The type and concentration of peroxides used in the cocktail formulations is usually determined by the LDPE production technology process.

Free radicals are short lived reactive intermediate species with an unpaired electron. The reaction begins when a free radical reacts with an ethylene molecule, forming a new radical that propagates the chain reaction. A number of side reactions such as short chain branching, long chain branching, chain transfer to polymer, chain transfer to monomer occur before the chain is terminated. These additional side reactions determine the molecular weight and molecular weight distribution of the polymer.

In essence the overall polymerisation reaction may be represented by the equation 2:



At high pressures, the polymerisation proceeds at a very rapid rate with multiple reactions occurring at the same time. Basically the polymerisation process can be described by the classical kinetic description of the free radical polymerisation reaction.

2.2.1.2 Production of tubular LDPE resin via autoclave technology process

Typically the production of LDPE resins via the autoclave and tubular technology processes occur at higher reaction pressures in comparison to the production of LLDPE via the gas phase process.

The autoclave process is adiabatic in nature in that there is no significant heat removal from the reactor during the process. The polymerisation of ethylene is highly exothermic and the exothermic heat of reaction is controlled by the injection of fresh cold ethylene into the reactor at several points.

Modern stirred autoclave reactors have four to six polymerisation zones, each running at a different temperature thus enabling the direct control of the mix of the molecular species and degree of long chain branching. Organic peroxides are used to support the polymerisation process in the autoclaves. A modern autoclave reactor has a conversion of 19.5 to 21 percent per pass depending on the polymer grade being produced [10].

The reactor feed streams are cooled and then fed to the different injection points in the autoclave reactor. In comparison to the tubular reactor, the autoclave reactor can be thought of as a single reaction zone or unit. The autoclave reactor is a continuous-stirred tank reactor (CSTR) with an agitator to promote good mixing. The multiple zones in the reactor allow for adequate control of the final product properties. The process flow diagram for the LDPE autoclave production process is shown in Figure 2.1.

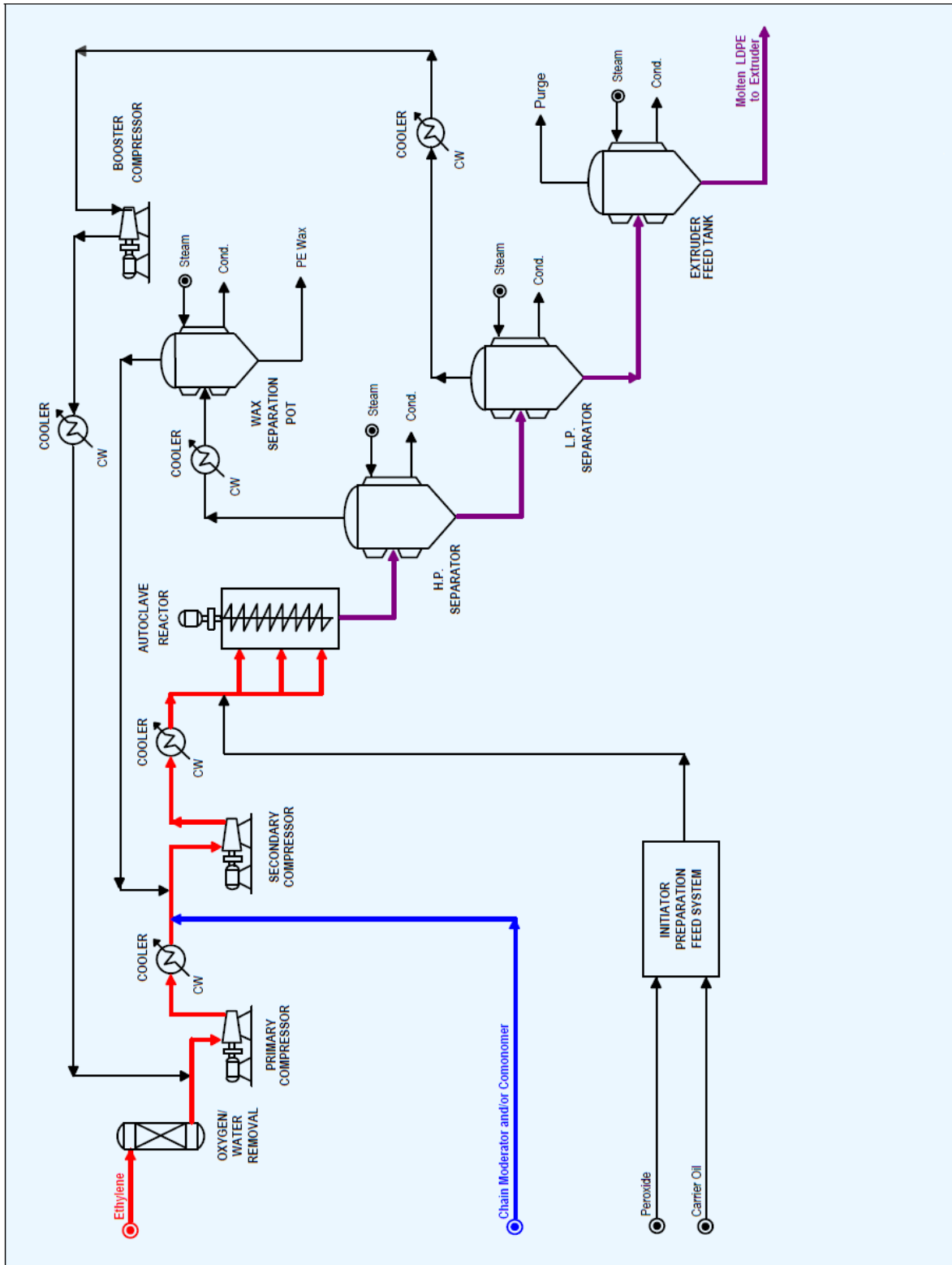


Figure 2.1: LDPE autoclave production process [10]

The autoclave reactor

In the autoclave production process, the multiple zones in the reactor allow for manipulation of the temperature profile. The organic peroxide solutions are injected at multiple points into the reactor to initiate the highly exothermic reaction. The autoclave reactor is an adiabatic CSTR reactor and the addition of the cold ethylene side streams balances the exothermic heat of polymerisation. After the polymerisation process in the reactor, the reactor fluid is decompressed through the high pressure letdown valve to about 800 bar and cooled with the product cooler. The mixture is then fed to the high pressure separator and thereafter to the low pressure separator. The polymer is thereafter extruded, degassed, blended and cooled for being packaged for distribution.

2.2.1.3 Production of tubular LDPE resin via tubular technology process

Tubular technology has recently taken the competitive edge over the autoclave technology in the production of LDPE. Licensors of the tubular technology processes such as ExxonMobil Chemicals, SABTEC and LyondellBasell claim significant benefits of employing the use of tubular reactors in their LDPE production processes. Due to the unique design of the tubular process, ethylene gas is compressed at much higher pressures in comparison to the autoclave process before reaction in the tubular reactor. Typically, the gas is compressed from 1500 bar to 3000 bar before being fed into the tubular reactor. LDPE reaction in the tubular reactor occurs between 2700 - 3000 bar. The compression at high pressure results in an increased percentage conversion of gas to polymer and hence a high production output of polymer. A basic schematic of the high pressure tubular process is indicated in Figure 2.2.

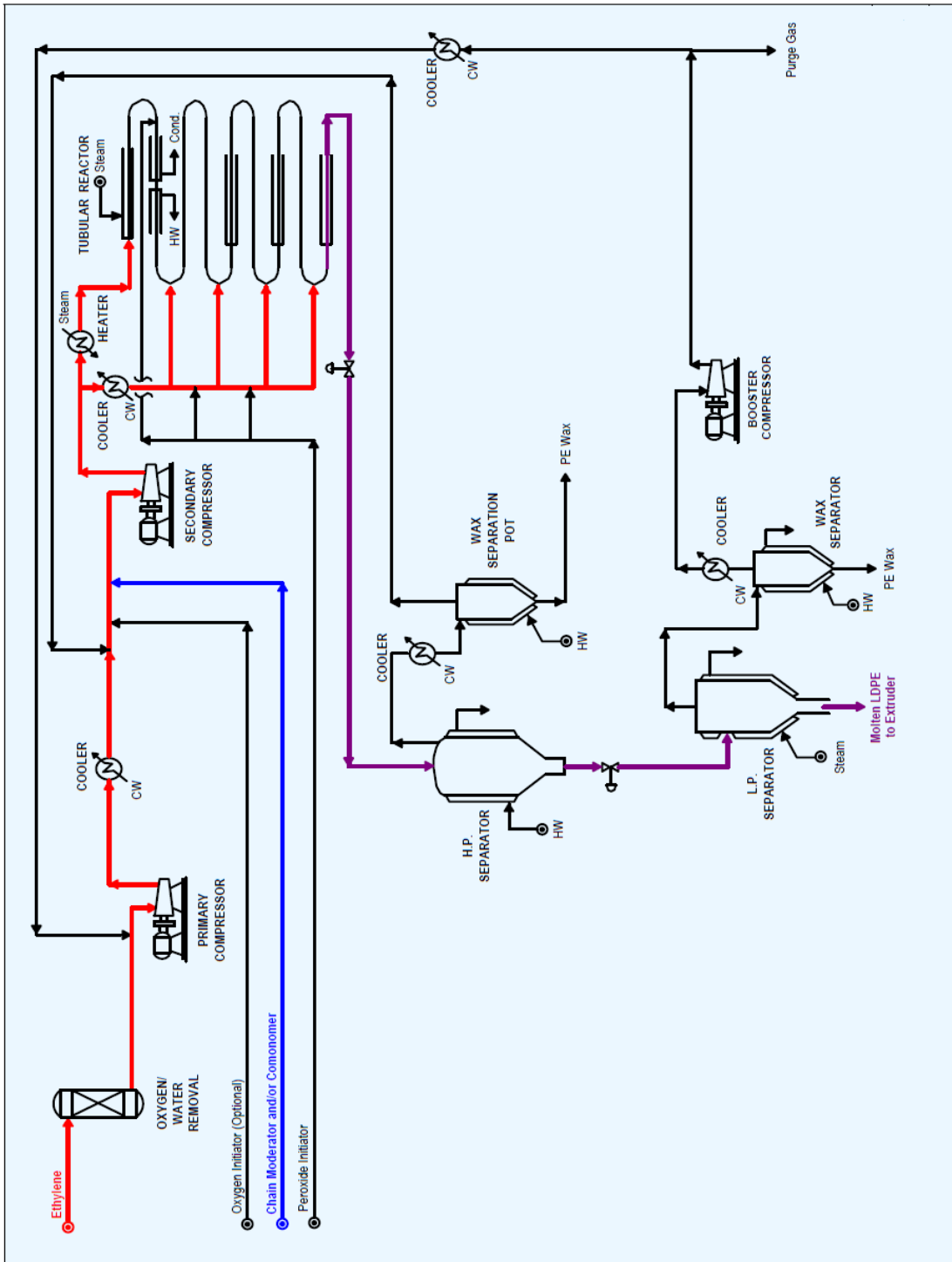


Figure 2.2: Tubular LDPE process summary [10]

Different tubular technology licensors have slight differences in the process design features of the tubular technology. A brief description of the tubular technology process in general is described [10]. There are slight differences with regards to choice of initiators, reactor pressure and temperatures. In typical high pressure LDPE polymerisation processes, polymerisation grade ethylene is supplied to a primary compressor at 300 bar. The gas is compressed in a secondary compressor to 2700 - 3000 bar and then fed into the reactor for polymerisation. Chain transfer agents or modifiers are injected into the suction of the secondary compressor for compression with the ethylene before introduction into the high pressure reactor. Tubular reactors have several zones where fresh ethylene and initiator are added. The addition of fresh ethylene both cools the reactants and agitates the mixture so that the molecular weight distribution of the polymer can be varied. At the injection points, a cocktail of organic peroxides can be added to initiate the reaction at different temperature. The contents of the tubular reactor are cooled either before or after the reactor pressure control valve.

Ethylene exhibits the Joule - Thompson effect in that the temperature rises as the pressure is reduced. Since the ethylene decomposes at 350 °C, it limits the exit temperature of the reaction mixture of ethylene and polymer. To prevent polymer degradation by elevated temperature beside the reactor pressure control valve, a post reactor cooling system is used. The difference between the reactor inlet and outlet temperature sets the conversion rate for the reactor and density of the polymer. For example a polymer grade with MFI of 4 g/10min and density of 0.9240 g/cm³ the conversion per pass is between 34 - 35 %. After the polymer/ gas mixture passes through the letdown control valve after the reactor, the reaction mixture is separated into polymer melt and unreacted monomer in two stages. The stages are a high pressure separator stage and a low pressure separator stage. The unreacted monomer is returned after cooling the wax and the monomer is sent to the suction of the primary compressor and the secondary compressor. The polymer melt is passed to an extruder and then is pelletised, degassed and blended in silos before being packed off.

The tubular reactor

Typical high pressure reactors have multiple reaction zones where polymer is polymerised in the reaction zone. The tubular reactor is in essence a plug flow reactor. Multiple peroxide injection points are used along the length of the reactor to maximise

the conversion of the ethylene to the LDPE. In tubular design the reactants are cooled along the long jacketed tube reactor.

Typically more than three injection points are used in the high pressure tubular reactors. The reactor conversion rates are approximately 40 %, depending on the capacity of the secondary compressor and the number of reaction zones. ExxonMobil and LyondellBassel process technologies use rising and falling maximum peak temperatures whereas SABIC use constant peak temperatures for most reaction zones [10]. The light off temperatures are the initiation temperatures and the peak temperatures are the maximum reaction temperatures. Process parameters such as temperature and pressure control the final product properties, such as Melt flow Index (MFI), Density and Haze (optical clarity). A schematic of the temperature profile for a 5 point LDPE tubular reactor is shown in Figure 2.3.

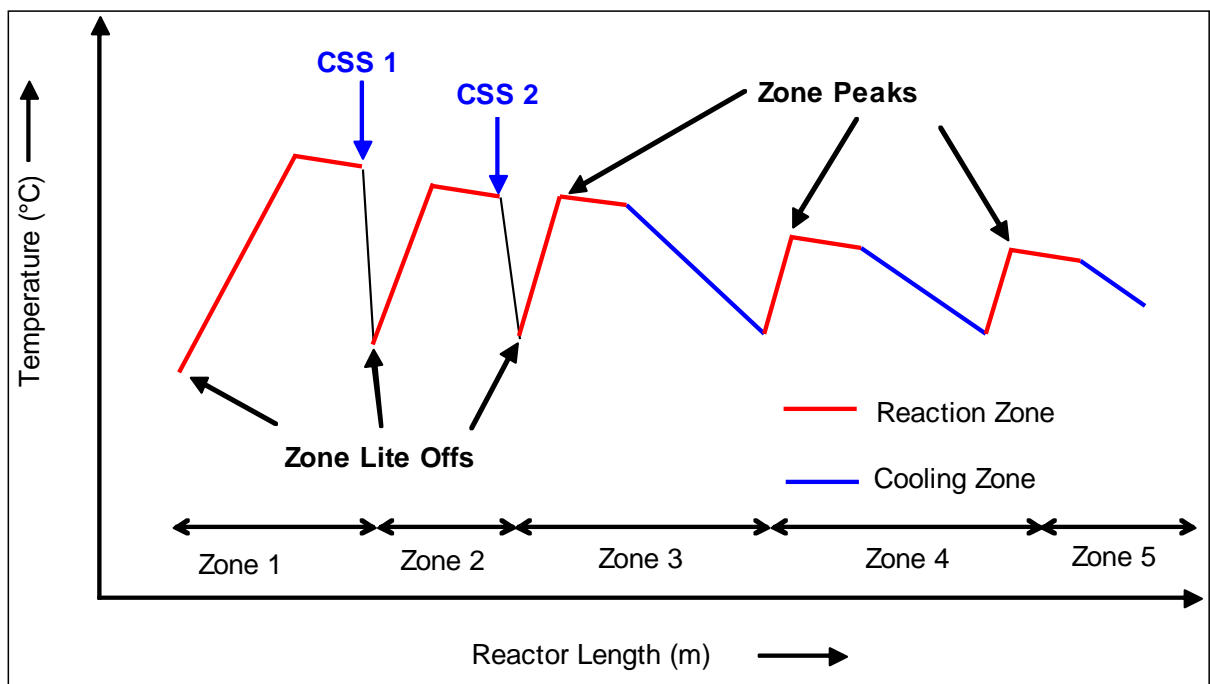


Figure 2.3: LDPE reactor profile design [10]

The fundamental differences between the tubular and the autoclave technologies are indicated in Table 2.1. The comparative data clearly indicates the advantages of using the tubular technology process over the autoclave technology process as a preferred manufacturing process. The main advantage is that the tubular reactor can sustain much higher reaction temperatures and pressures than the autoclave reactor, and as a result, the total monomer conversion from ethylene to polyethylene is higher.

Table 2.1: Differences between the tubular and autoclave LDPE technologies [10]

Design Feature	Tubular process	Autoclave process
Reactor (m ³)	0.6 - 10	0.4 - 2.3
Reactor design	Tube hundreds of meters -Inner diameter	Multi - zone reactor, continuous stirring
Reactor cooling	Yes	No
Monomer injection	Mono or multi- injection	Mono or multi- injection
Oxygen as initiator	Yes	No
Peroxides as initiator	Yes	Yes
Residence time(s)	20 - 80	20 - 80
Pressure (bar)	2200 - 2700	1300 - 2200
Temperature (°C)	130 - 325	160 - 310
Monomer conversion (%)	15 - 30	15 - 20

2.2.2 Linear low density Polyethylene (LLDPE)

Linear low density can be produced via suspension/slurry phase, gas phase and solution phase production processes. The production of LLDPE is initiated by transition metal catalysts such as the Ziegler-Natta catalysts, Phillips catalyst and metallocene catalysts.

2.2.3 Polymerisation chemistry of LLDPE

The LLDPE polymer can be synthesised with three types of catalysts namely Ziegler - Natta, Phillips and metallocene catalysts.

In 1955, Ziegler discovered the first catalyst which was suitable for the polymerisation of ethylene into a crystalline polymer. Giulio Natta used employed the use of these Titanium catalyst to prepare stereo - regular propylene polymers. Ziegler - Natta catalysts have been used in the commercial manufacture of various polyolefins since 1955. The catalyst was a combination of $TiCl_4$ and $Al(C_2H_5)_2Cl$. Modern commercial catalysts of this type are supported catalysts which are bound to a solid surface area. $TiCl_4$ and $TiCl_3$ can be used individually to produce active catalysts respectively. In essence, a Ziegler-Natta catalyst is a catalyst that consists of two components, namely a transition metal compound which can be a halide, alkyl or aryl derivative of the group IV – VIII transition metals. The second component is a methyl alkyl or alkyl halide of group I – III base metals. These two components react to form a catalyst. Many heterogeneous

processes have been developed for polymerizing alkenes using aluminium alkyls in combination with transition metal complexes. Cossee and Arlman have proposed a mechanism for Ziegler-Natta catalyst polymerisation process [11]. The mechanism is shown in Figure 2.4.

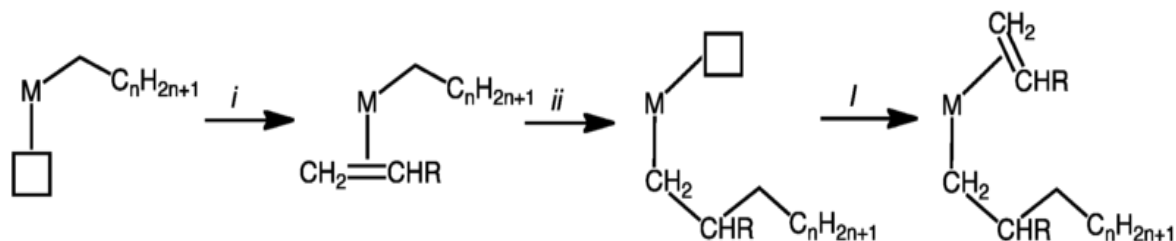


Figure 2.4: Cossee and Arlman mechanism [11]

The reaction of TiCl_4 with the aluminium alkyl gives TiCl_3 . The TiCl_3 reacts with the aluminium alkyl to give the titanium alkyl complex. The monomer, ethylene or propylene can then insert into the titanium-carbon bond to form an alkyl. The alkyl is further susceptible to the insertion of ethylene to lengthen the chain.

The Cossee and Arlman reaction features an intermediate coordination complex that contains both the growing polymer chain and the monomer (alkene). The ligands combine within the coordination sphere of the metal to form a polymer chain that is elongated by two carbons. The box represents a vacant or extremely labile coordination site. Step I involves the binding of the monomer to the metal and step II involves the migratory insertion step. These steps which alternate from one side of the metal centre to the other side are repeated many times for each polymer chain. This mechanism ideally explains the stereoregularity of the polymerisation of the alkenes using the Ziegler-Natta or metallocene catalyst. Stereoregularity is relevant for the unsymmetrical alkenes such as propylene. The coordination sphere of the metal ligands sterically influences which end of the propylene attaches to the growing polymer chain and the relative stereochemistry of the methyl groups on the polymer. The stereoregularity is influenced by the ligands. In general, the Ziegler-Natta catalysts are heterogeneous in nature. For heterogeneous catalysts, the stereoregularity of the catalyst is determined by the surface structure around the active site on the catalyst particle. The surface structure is influenced by additive such as phthalates or succinates which tend to block specific sites allowing other active sites with a different stereoreactivity to catalyse polymerisation. These types of coordination reactions are applicable to the polypropylene polymer.

The main difference between the metallocene catalysts and the Ziegler-Natta catalysts is in the distribution of active sites. Ziegler-Natta catalysts are heterogeneous in nature and have many active sites. The active sites on the Ziegler-Natta catalyst are also important for LLDPE polymerisation. In comparison to polypropylene polymerisation, these active sites on the LLDPE polymer allow for a higher degree of comonomer incorporation due to the decreased steric hindrance. Some of these sites are stereospecific, and some are more accessible to monomers for coordination and subsequent polymerisation. Metallocene catalysts are generally homogeneous in nature with supported metallocenes being heterogeneous in nature. The homogeneous metallocene catalysts produce polymers with a narrow molecular weight distribution and uniform comonomer distribution. Homogeneous metallocene catalysts are organometallic compounds of Ti, Zr and Hf based in organic solvent. The catalytic species is activated by an alkyl aluminium cocatalyst to create the active site for the C – C bond insertion. The cocatalyst is responsible for the formation of the metal-carbon bond. Methylaluminoxane (MAO) is typically used to initiate the homogeneous metallocene catalysis process. Metallocene catalysts are single site catalysts and produce uniform polymers with unique structure and physical properties. The mechanism for metallocene catalysis is shown in Figure 2.5 [13] Water reacts with Triethylaluminium to produce the methylaluminoxane molecule. Step 1 of the reaction entails the metallocene molecule reacting with the MAO molecule and the methyl group replacing the chlorine on the metallocene. MAO then acts as a Lewis acid taking one of the methyl groups from the metallocene to give a negatively charged MAO ion and a positively charged Zirconium ion. In this anionic form, the metallocene catalyses the polymerisation process. Step 2 illustrates the stabilisation of the positive Zirconium ion by sharing the electrons from a C – H bond. The polymerisation process begins when Zirconium ion attracts the olefin monomer through the electrons of the olefin double bond. The new bond starts to form and the double bond breaks. The movement of the electrons continues as the electrons from the double bond now form a new bond with the zirconium and the active site becomes available again for further reaction. This is indicated in step 3.

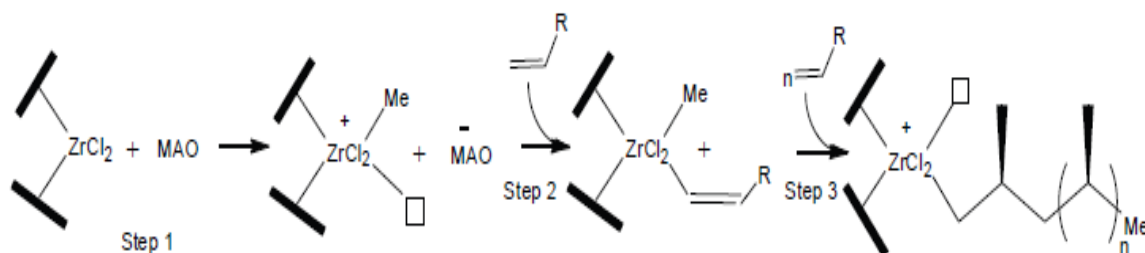


Figure 2.5: Mechanism for metallocene polymerisation [12]

The reaction essentially terminates by a β hydride abstraction [12]. The molecular engineering of the ligand attached to the metal ion, in the metallocene catalyst is used for control of the stereochemistry during the polymerisation reaction. Monomer molecules approaching the Zirconium reaction centre selectively co-ordinate to the reaction centre producing a polymer chain of a specific geometry. Metallocene catalysts can produce polymers with structures of different tacticity. Factors such as the type of ligand, substituents on the ligand, the presence/ absence of bridging influence the degree of tacticity for polypropylene production or the degree of comonomer incorporation for polymerisation of linear low density polyethylene.

Due to the fact that Ziegler-Natta catalysts have different active metal sites, polymers with high molar mass and various tacticity distributions are produced using the Ziegler-Natta catalyst system. In contrast, due to the single active site available on the metallocene catalysts, more uniform polymer chains are produced using the metallocene catalyst system. These polymer chains have a lower molar mass and a more uniform comonomer distribution and tacticity distribution. However, there are disadvantages associated with the use of metallocene catalysts. The main disadvantage of the metallocene catalysts are the extremely high molar Al to transition metal ratios. (Al/M) ratios in the range of (1000 – 15000:1) are required to achieve high activities [12]. In comparison, Ziegler-Natta catalysts require (Al/M) ratios of (50 - 200:1).

Ziegler-Natta catalysts have extensive commercial applications. The catalyst system has been used in the manufacture of various polymeric materials since 1956. The main application area using Ziegler-Natta catalysts is in the polymerisation of monomers specifically. The products are plastics, elastomers and rubber.

Metallocene based compounds have extensive applications in the pharmaceutical industry. To date there has been extensive research into metallopharmaceutical drugs [14, 15]. One area of such research has utilised metallocenes in place of the fluorophenyl group in the haloperidol drug. The haloperidol drug is a typical antipsychotic drug.

Phillips catalysts are also used in the production of LLDPE. Phillips extensively use the catalyst in the slurry loop process. The catalyst is essentially deposited chromium (III) oxide on silica. The catalyst is activated by hydrogen. The exact catalytic mechanism of how the Phillips catalyst works is not clearly understood. It has postulated that the mechanism is based on co-ordination polymerisation. When the catalyst is in the presence of dichloromethane, one ligand is lost to form a 13 electron chromium intermediate species. The polymerisation reaction proceeds via a side on addition of ethylene and the polymer chain grows by the combination of the ligands in the metal complex. The Phillips catalysis mechanism is shown in Figure 2.6.

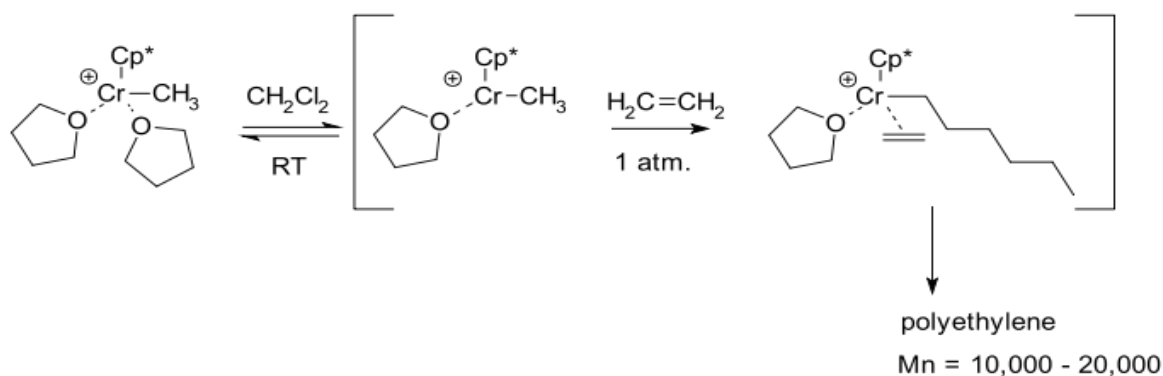


Figure 2.6: Postulation of the Phillips catalysis mechanism [16]

Recent developments in the field of catalyst chemistry in the first half of the 1990s have focused on the development of single site metallocene catalysts for use in the gas phase polymerisation processes. The Univation Chemical Company has done extensive work in the area of metallocene technology for the gas phase process using the UNIPOL PE process technology [17]. Capability has been developed to produce PE resins with bimodal property-attributes manufactured on single UNIPOL reactors. This has replaced the need for two reactor configurations. Catalyst technologies and raw catalysts such as Ziegler-Natta, chromium, metallocene and engineered bimodal catalysts are currently

widely available for commercial usage by polymer technology licensors such as Univation.

2.3 The effect of catalyst chemistry on the crystallinity of LLDPE

Catalyst chemistry plays a significant role in determining the molecular architecture of polyethylene. Recent advancements in technology have improved the ability to selectively synthesise polyethylene with a pre-determined crystalline structure. Molecular structural properties of LLDPE differ when LLDPE is synthesised with different catalyst systems. For instance when Ziegler-Natta catalysts are used in the synthesis of LLDPE as opposed to metallocene catalysts, the tear resistance of the final product is higher than a product synthesised with metallocene catalysts. Apart from using different catalyst systems to change the molecular architecture of the polymer, using a single catalyst system and making changes on the single catalyst system, for example changing cocatalyst amount can significantly impact on the crystallinity of the LLDPE produced.

LLDPE is a semi crystalline polymer. The polymer comprises of crystalline, amorphous and semi crystalline regions. Semi crystalline polymers have lamella structures in which thin ribbon like crystals are constructed from the molecule segments. The molecules fold at the surface and pass through a crystal phase and the amorphous phase. This provides strong adhesion between the two phases. The tie molecules connect the crystal lamellae with the amorphous phase [18]. Figure 2.7 shows the molecular structure of the semi crystalline polymer.

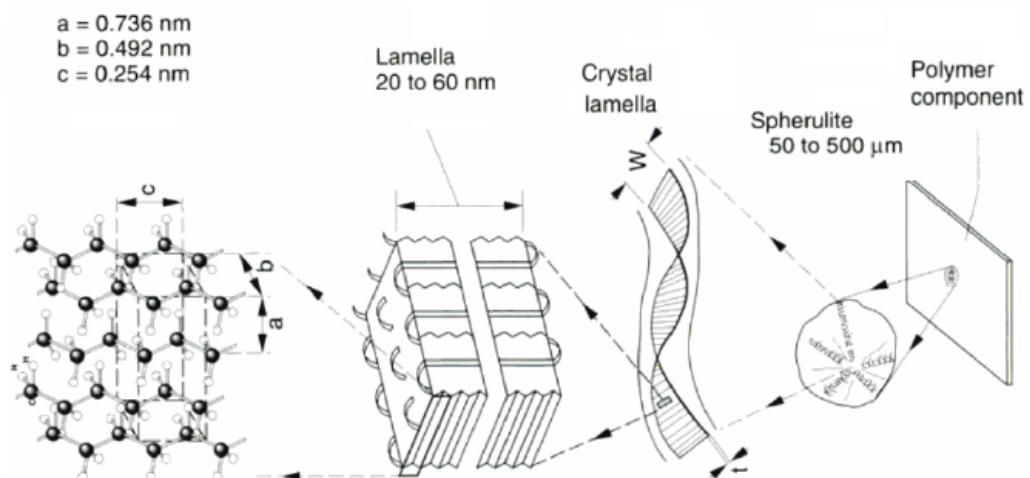


Figure 2.7: Molecular structure of semi crystalline polymer [18]

The amount of comonomer incorporated into the backbone of the polymer chain and the degree of branching of the comonomer significantly impacts on the crystallinity of the polymer. Polymers with uniform distribution of the comonomer along the backbone of the polymer chain are regarded as having a narrow chemical composition. Polymers with uneven comonomer distribution along the backbone of the polymer chain are regarded as having a broad chemical composition [19]. Generally, regions of the LLDPE polymer with high comonomer content are highly branched and are less crystalline, as opposed to regions of the polymer with a low comonomer content and a low degree of branching. Previous TREF fractionation of LLDPE polymerised using 1-butene as comonomer conducted by Keulder *et al* [20] showed that the bulk of the comonomer distribution in the copolymer resided in the soluble and less crystalline fractions of the polymer. Bulk recombination studies conducted also showed that when highly crystalline fractions were removed from the bulk material, there was an observed total decrease in the crystallinity of the bulk recombined material. Work conducted by Harding *et al* also showed a similar trend [21].

2.4 Production of LLDPE via a low pressure gas phase polymerisation process

LLDPE can be produced by gas phase, solution phase and slurry phase production processes. There are several LLDPE licensors that actively compete in the technology licensing area licensing LLDPE production technologies. The companies that license the gas phase production technologies are Ineos (Innovene G process), LyondellBasell (Spherilene process), and Univation (Unipol process). The main advantages of using a gas phase process to manufacture LLDPE polymer is that the process is relatively simple in design and can be scaled to large single line capacities (approx 400 – 650 000 tons per annum). Gas phase processes produce a wide product range and different comonomer types, namely butene -1, hexene -1 and octene-1, can be used. All three catalyst systems (Ziegler-Natta, chromium, single site metallocene) can be used. As a result resins with a broad range of product properties, namely density (0.890 g/cm^3 - 0.965 g/cm^3) and MFI (0.05 g/10min - 155 g/10min), can be used. However, the major disadvantages of the gas phase processes are the long reactor residence times and long product transition times. Some technology developers have optimized features of the gas phase process to reduce the reactor residence and grade transition times by increasing the catalyst activity and heat removal capability.

A process description of the gas phase technology for the production of LLDPE polymer as licensed by Univation Technologies is described [10]. The process discussed below is based on the latest technology namely UNIPOL PE offered by Univation.

The process flow diagram for the UNIPOL PE Process is illustrated in Figure 2.8 and Figure 2.9 respectively [10]. The UNIPOL PE Process is based on the use of Ziegler-Natta, metallocene, chromium and bimodal-type catalysts. Since many types of catalysts are poisoned by moisture and oxygen, the various feeds through the reactor such as ethylene, comonomer, induced condensing agent and nitrogen pass through the guard beds to remove these impurities. The comonomers are degassed prior to being fed to the guard beds.

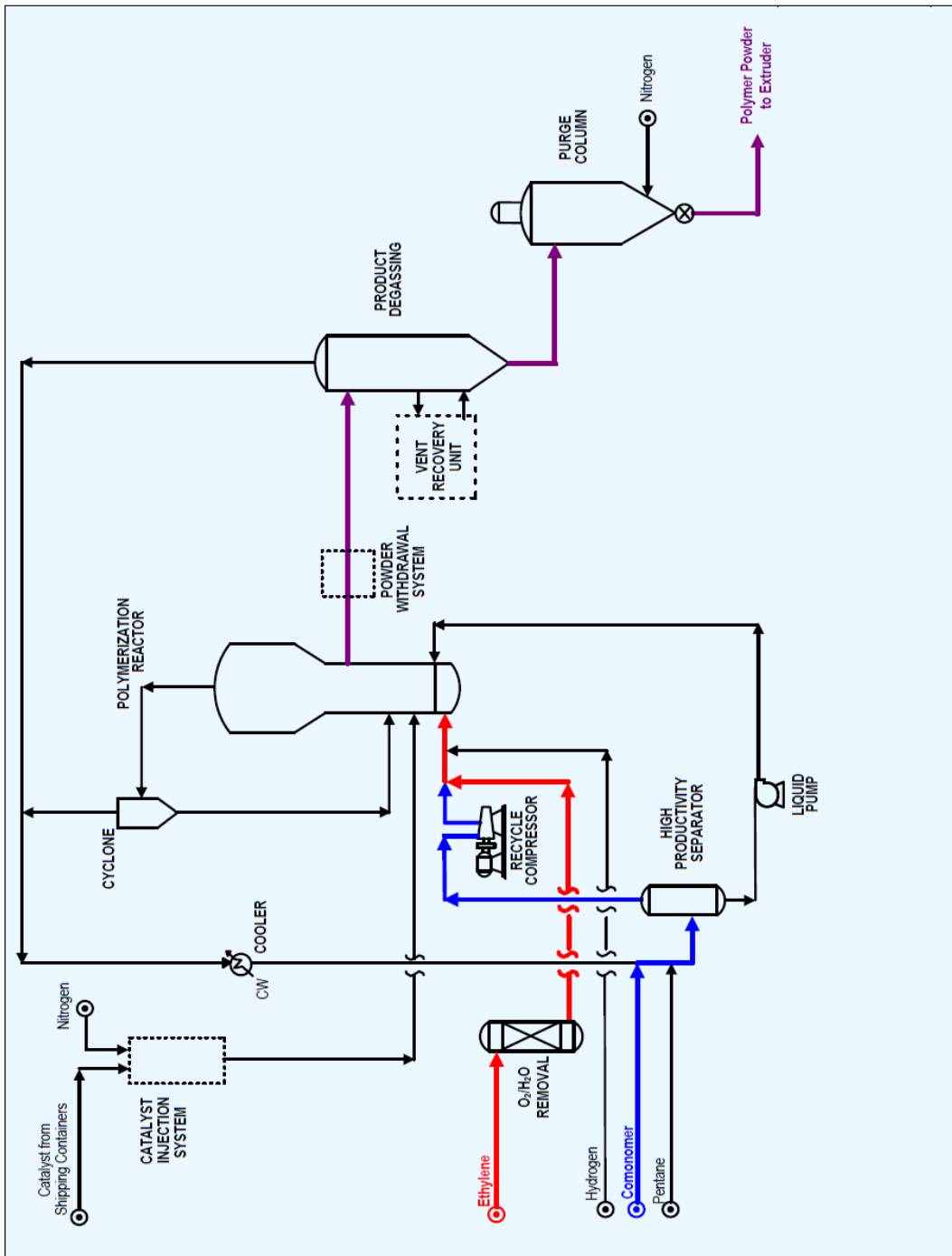


Figure 2.8: UNIPOL fluidized bed Polyethylene process reactor system [10]

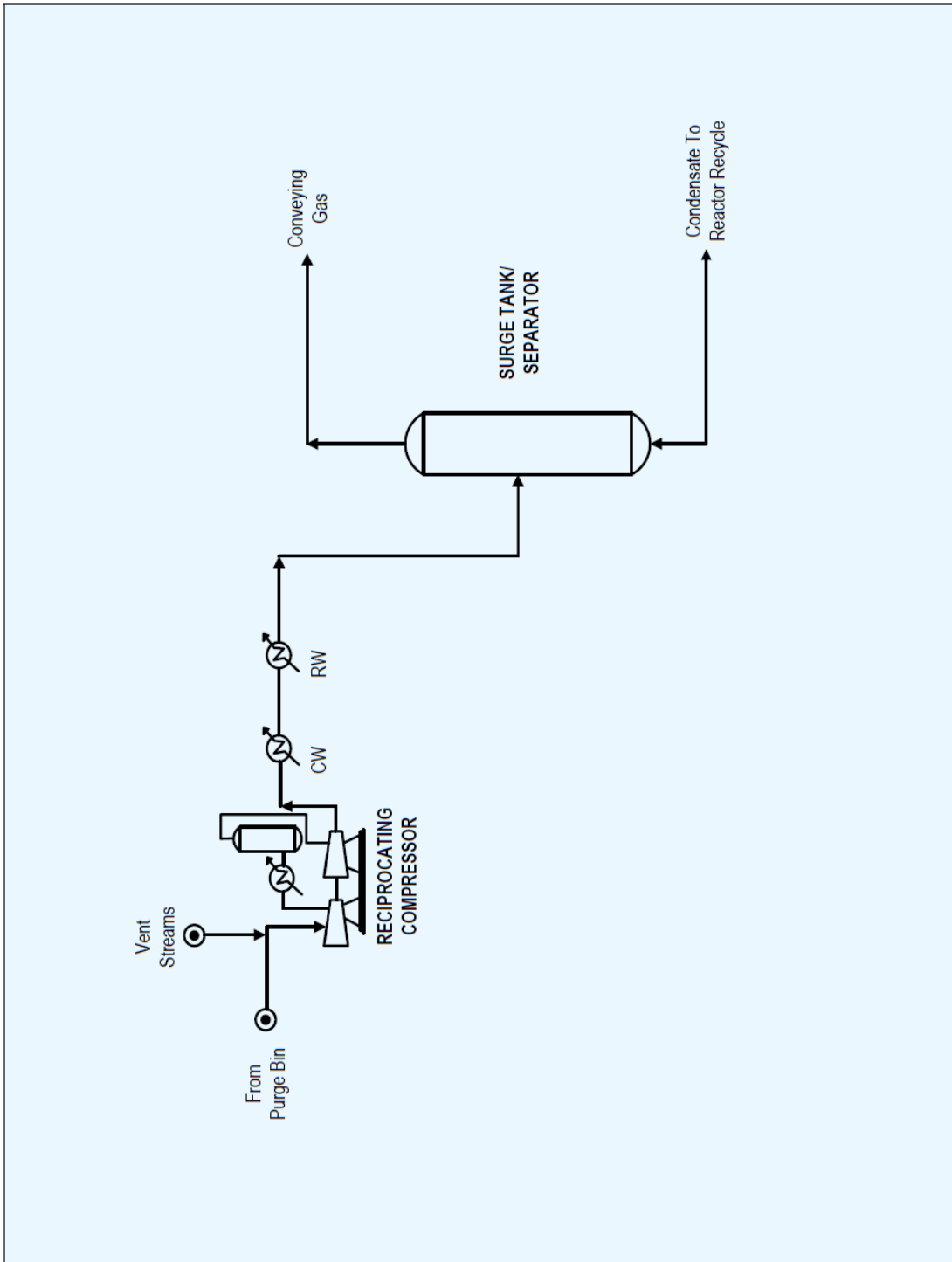


Figure 2.9: UNIPOL Polyethylene process, vent recovery system [10]

In the UNIPOL PE process, the catalyst is added to the reactor via the catalyst feeder. The fluidised-bed reactor system consists of a vertical pressure vessel with an expanded upper section for the de-entrainment of polymer particles. The reactor is operated at 85 °C to 11 °C and at 20 bar. The reactant gas stream circulates through the bed and is cooled in an external heat exchanger thereby removing the exothermic heat of the reaction. A blower in the recycle loop provides the pressure increase to overcome the differential pressure of the fluidised-bed reactor and the cycle gas loop. The control of the reactor conditions is critical as the catalyst is highly temperature sensitive relative to the product properties. Most licensees use advanced process control systems (APC) for the control and optimisation of the LLDPE process. These systems assist with the process-product property control. Initial UNIPOL PE processes maintained the recycle reactants in a gaseous phase at all times. Latest technological developments allow the UNIPOL PE process to now operate with the recycle of liquefied condensing agent in order to significantly expand the production capacity. The removal of latent heat by the evaporation of the induced condensing agent increases output rates by approximately 35 %.

The fluidised bed reaction is characterised by extensive back-mixing which yields a very uniform product. The product polymer is drawn off periodically and depressurised into the product degassing tanks. The existing gas from the degasser is recycled to the reactor. The hydrostatic head across the reactor bed allows for the recycle of the gas to the reactor with the need for gas recompression. The light gas recovery is very efficient and a small intermittent purge stream is required to prevent the build-up of inerts during operating conditions.

The polymer leaving the product-degasser is delivered to the purge bin where the residual hydrocarbons are stripped with the nitrogen and the catalyst is deactivated with a small quantity of steam. The purge gas stream is cooled and sent to a separator where the comonomer is recovered and recycled. The lights are sent to the vent compression system. The polymer from the purge bin in the form of a powder is sent to the finishing section of the plant. In the vent system, the vent stream is collected and fed to the compressor where it is cooled and condensed. It is then fed to the surge tank/separator where the lights are taken overhead and the condensate is fed back to the reactor. There is also an option to perform a secondary recovery step to further reduce the ethylene losses.

For the formation of pellets, the polymer powder is gravity fed to the mixer feed. The process also allows for the feeding of the polymer by pneumatic air supply. The additives are metered by feeders and the flow by gravity to the resin/additive conveyor where they are combined with the main resin stream and fed to the mixer. The pelleting system consists of a twin screw mixer to melt the polymer followed by a gear pump to pressurise the mixture through an underwater die-face cutter. The Univation system takes advantage of the thorough back-mixing in the reactor and the high amount of heat in the powder. These features serve to minimize the amount of homogenisation required in the mixer and reduce the heat requirement for melting. This results in power savings and less potential for the product to be contaminated. The single reactor approach allows this low energy, low investment pelletising to be used to produce the low gel products even with the bimodal HDPE grades.

From the pelletiser, the pellets are dewatered in a centrifugal dryer. The polymer is then transferred to a conventional commercial resin handling system. Normal air conveying is used throughout the resin handling system. The two combination storage / continuous blending bins plus one loading bin per reactor line are recommended for surge capacity and product change/off-grade flexibility.

2.5 Production of LLDPE via a solution phase polymerisation process

Technology licensing companies such as DSM license solution phase process technologies for the production of LLDPE. The processes that are licensed by these companies are Compact, Advanced Sclairtech and Sclairtech process technologies respectively. The solution phase process technology is more suited to the production of high quality LLDPE resins based on octene - 1 as a comonomer. The solution phase process technology is renowned for the feature of very short reactor residence times, thus allowing the process significant flexibility in producing a wide product slate in a short production cycle. The main disadvantage of the solution phase process is the high investment costs involved in maintaining the solution phase technology as well as the costs of the high activity catalysts used in the solution phase process.

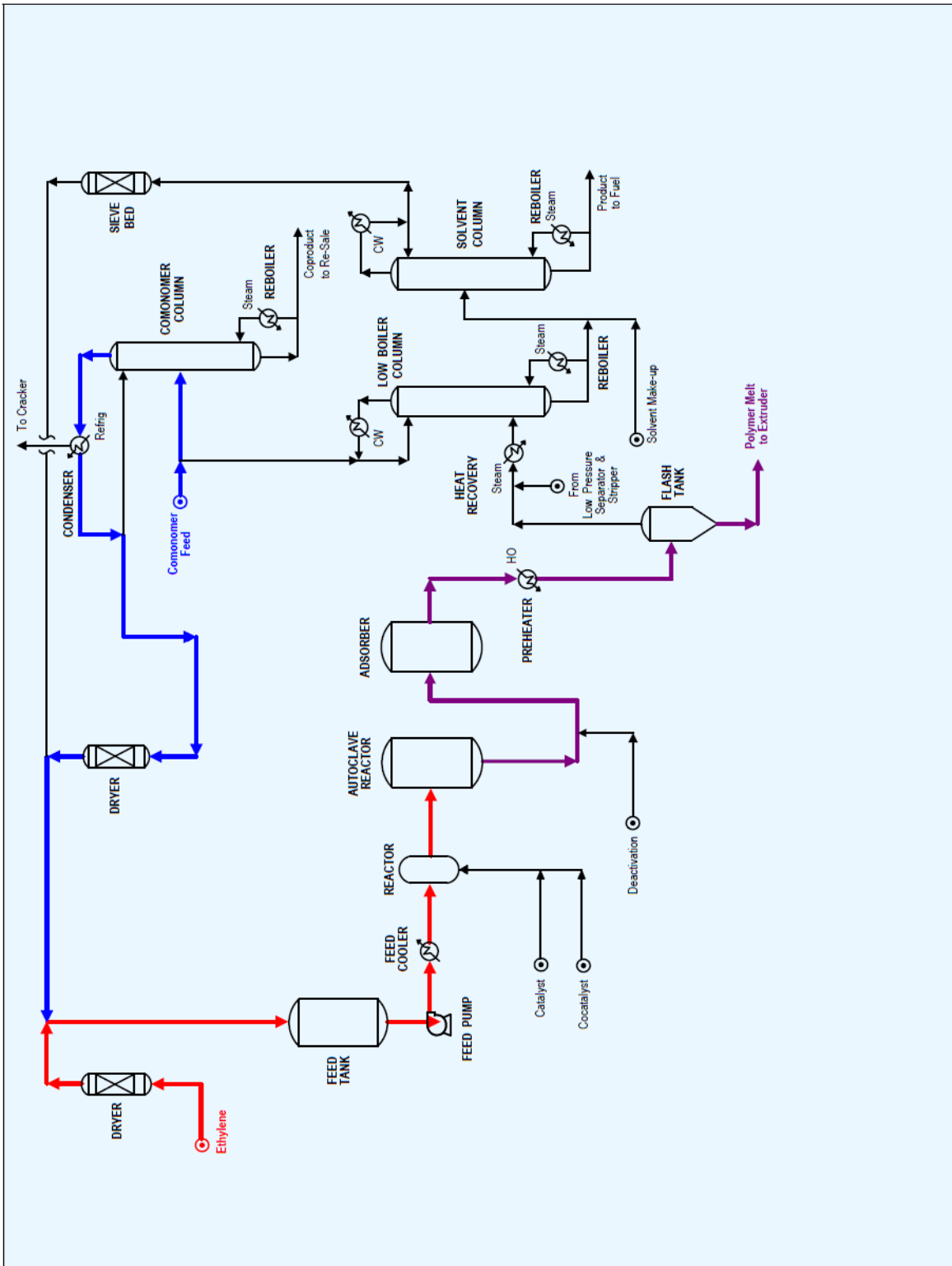


Figure 2.10: Sciairtech solution phase process technology [10]

The process flow diagram for the solution phase technology is illustrated in Figure 2.10. In the process, ethylene is fed directly to the reactor system with the catalyst feed components. Depending on the ethylene feed specification, feed compression and molecular-sieve guard beds may be required. The ethylene is mixed with the solvent and comonomers. The mixture is pressurised and the solution is fed to the reactor. The reactor consists of a single autoclave and tube. After polymerisation a catalyst deactivator is added to the solution stream to terminate the polymerisation reaction. The deactivator renders the catalyst inactive and forms a chelate which is absorbed in the downstream alumina beds. The molten stream is sent to a two stage depressuriser where the solvent and monomers are flashed off. Liquid additives are injected into the molten polymer at the low pressure separator. The polymer is thereafter fed from the low pressure separator into the extruder. The polymer is pelletised by an underwater pelletiser, stripped of water and residual solvent before being pneumatically blended. The combined streams of flash vapours are fed to the low boiler column, where unconverted ethylene and comonomer are removed. The bottom stream is fed to the high boiler column and the pure solvent is taken overhead for recycle and the heavies stream is recovered as bottoms and burned as fuel.

2.6 Production of LLDPE via slurry phase polymerisation process

Technology licensing companies such as Borealis and Chevron Phillips license the slurry loop process technology for the manufacture of LLDPE and HDPE. The process technology is a swing technology between LLDPE and HDPE production technologies.

The Borstar process technology is able to produce a full range of polyethylene resins ranging from LLDPE, MDPE and HDPE in a single process. A key feature of the process technology is the use of multiple reactor systems to broaden the molecular weight distribution of the resins and produce bimodal LLDPE and HDPE. The Borstar process uses liquid propane at a pressure above its critical point. The solubility of polyethylene at higher temperatures in supercritical propane is less than it is in isobutene and hence fouling of the reactor is avoided. The process uses a silica supported Ziegler-Natta catalyst for the commercial production. The catalyst has a very flat activity profile giving good activity for production of polymers across a wide range of molecular weight. The process flow diagram for the slurry loop process technology as licensed by Borstar is illustrated in Figures 2.11 and 2.12 respectively.

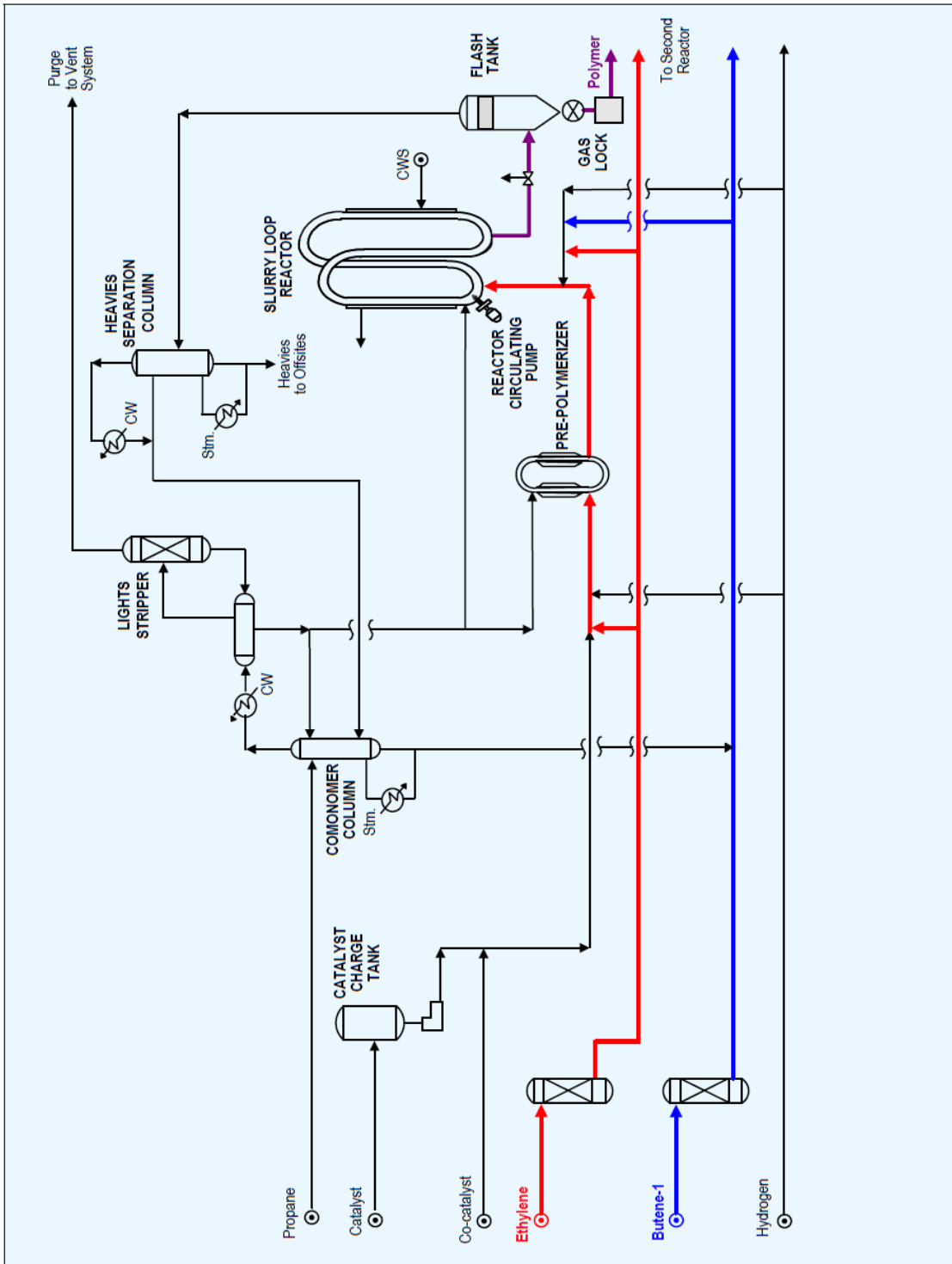


Figure 2.11: Borstar feed and first stage polymerisation process [10]

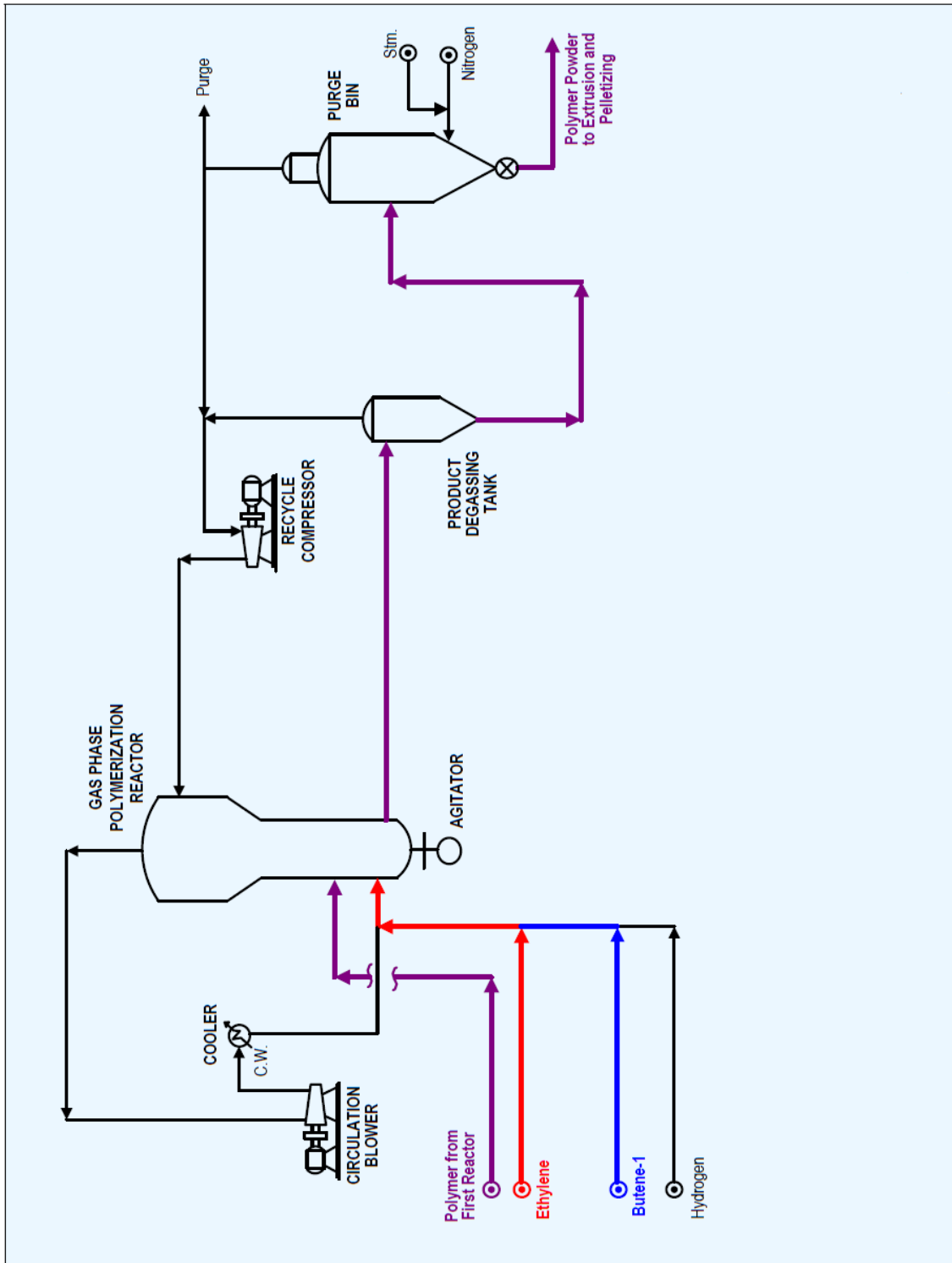


Figure 2.12: Borstar second polymerisation process and recovery system [10]

Raw materials such as catalyst, comonomer and ethylene are sent to the slurry loop reactor. The first reactor produced a low molecular weight resin with MFI ranging between 200 - 600 g/10min. Polymerisation with supercritical propane promotes high catalyst activity at high temperature. The typical operating conditions in the slurry loop reactor range from 85 °C to 100 °C with pressure in the range of 60 bar to 65 bar. The slurry discharge to the flash tank contains approximately 60% polymer solids. The overheads from the flash tank are compressed and sent to the heavies scrubber column where a small amount of heavy components are separated. The overhead from the heavies column is sent to the comonomer column for butene removal when LLDPE is produced. The overhead from the comonomer column is sent to the lights stripper where the light ends are purged and sent to the vent system. The bottoms from the lights stripper containing mainly propane, ethylene and butane are either recycled back to the slurry reactor or sent to the comonomer column. The dried polymer from the flash tank is conveyed through a proprietary gas conveying system to the gas phase fluid-bed reactor. In the second reactor, the partial pressures of ethylene and butene are accurately controlled to give the correct composition of the polymer produced and to maintain the distribution split between the 2 reactors. The polymerisation reactor produced HMW resin fractions with the HLMI typically below 1 g/10min and the densities below 0.922 g/cm³. This reaction produced an overall LLDPE polymer for commercial use with densities below 0.922 g/cm³. The reactor operates at 80 °C and at a pressure of 20 bar.

In the dual reactor system approximately 50% of the polymer is produced in the first reactor and the balance in the second reactor. The slurry material is almost all homopolymer and the second reactor produced the copolymer. The polymer from the gas phase reactor as indicated in Figure 2.11 is discharged to the product degassing tank. The solids are sent to a purge bin in which the polymer is scrubbed with nitrogen to remove the residual hydrocarbons and steam to deactivate the catalyst. The overheads from the purge bin are vented to the flare and the overheads from the product degassing tank are compressed and recycled to the gas phase reactor. The polymer from the purge bin is thereafter conveyed to the downstream extrusion and pelletising steps.

The key features for the comparison of the different technologies available for the production of LLDPE are indicated in Table 2.2.

Table 2.2: Comparison of gas phase, solution phase and slurry-loop phases for the production of LLDPE [10]

	Gas phase	Solution phase	Slurry - loop phase
Operating Temperature (°C)	80 - 90	150 - 200	85 -100
Operating Pressure (mPa)	5 - 10	3 -100	7 - 20
Catalyst Type	Ziegler-Natta/ Metallocene/Chromium	Ziegler-Natta/ Metallocene	Ziegler-Natta/ Metallocene/ Chromium
Product range	Rotomoulding, Film, MDPE and HDPE product range	High clarity film product	Bimodal LLDPE and HDPE product
Costs	Lowest investment costs	High investment costs due to expensive catalyst costs and solvent costs	High investment costs due to several polymer hydrocarbon recovery steps

2.7 Characterisation of LLDPE through fractionation

Due to the heterogeneity of Ziegler-Natta catalysts resulting from the multiple active sites, polymer is produced with differences in comonomer content. The distribution of the comonomer and the degree of branching impacts on the crystallinity of the polymer. TREF was used in the study to fractionate the polymer chains so as to be able to isolate polymer chains produced at similar active sites thus allowing their effect on the properties of the bulk polymer to be evaluated. CRYSTAF was used in the study to gain an indication of the fractionation temperature which could be used in the TREF fractionation process.

2.8 Temperature rising elution fractionation (TREF)

The temperature rising elution fractionation (TREF) technique is used to fractionate polymer chains according to the ability to crystallise from solution. This depends on the

crystallisable chain length sequence length of the polymer chains. The distribution and degree of branching in semi crystalline material gives an indication of the crystallinity of the material. On a molecular level the presence of chain branches decreases the length of the linear crystallisable sequences in the backbone. This modifies the morphology and the degree of crystallinity. The length of the -CH₂- sequences with minimum length to crystallise at a given temperature determines if the lamellar structure is feasible. The fringed micelle structure is formed when the methylene sequences are not long enough to form the lamella structure [22]. Polyolefins containing a high degree of branching are predominantly amorphous in nature. The general trend observed from fractionation using the TREF technique is a decrease in crystallinity of material with an increase in fractionation temperature.

TREF is particularly useful in the analysis of semi crystalline polyolefins for the primary reasons that these polymer materials are crystallisable and dissolve in a few solvents at high temperature (above 100 °C). A schematic representation of the TREF separation mechanism is given in Figure 2.13.

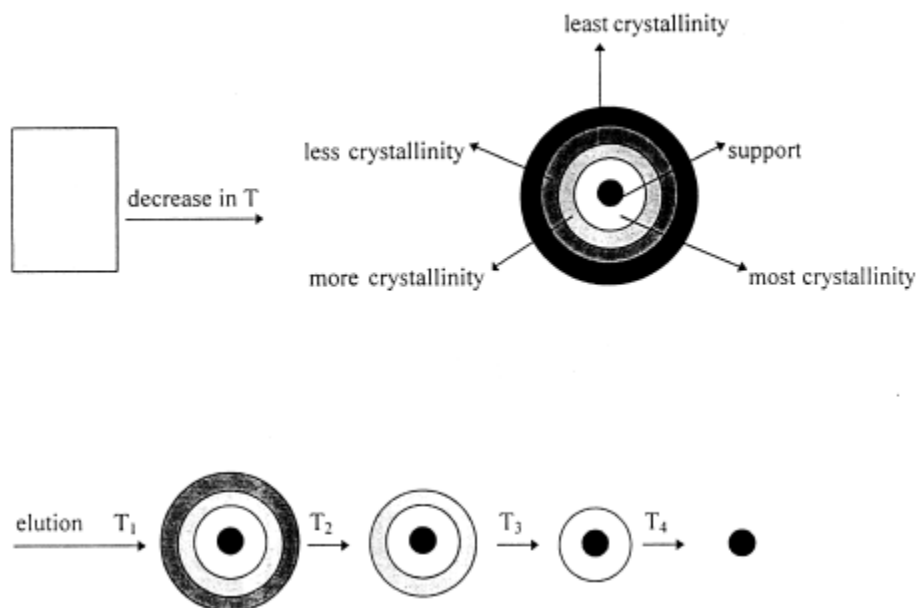


Figure 2.13: TREF experimental separation mechanism [23]

TREF is operated in 2 stages [23]. The first stage entails the dilution of polymer at high temperature as these polymers only dissolve at high temperature. The hot solution is then mixed with an inert support like sand or silica. The mixture is thereafter cooled from 130 °C to room temperature. As the temperature decreases, the polymer chains

precipitate from solution and coat the support in various layers of crystallinity. The polymer chains crystallise onto the support in the various layers according to their crystallisability from solution. Typically, the most easily crystallisable fraction precipitates first and deposits on the support in the innermost layer, whilst the least crystallisable fraction precipitates last and deposits on the outermost layer. In preparative TREF, the rate of cooling is essential as this ensures that the material fractionates according to the crystallinity. A slow cooling rate provides optimal separation which will be free from any interference from molecular weights. The second stage of the experiment entails the elution of the precipitated polymer at increasing temperature. Fractions with the lowest crystallinity dissolve at low temperatures whilst fractions which are more crystalline dissolve at high temperatures.

TREF can be analytical or preparative. Analytical TREF is automated and is generally connected to an IR detector and SEC. It presents the advantage of being able to analyse polymer fractions online. Preparative TREF is used to obtain large amounts of polymer fractions, which can be analysed by different characterisation techniques such as ^{13}C NMR, DSC and SEC.

Several studies have been conducted on the analytical features of TREF and the usage of TREF to study the degree of crystallisability of LDPE and LLDPE polymer chains [23 - 25]. Studies have shown that crystallinity is a function of comonomer distribution and the TREF is instrumental in fractionating material according to the degree of crystallisability and the crystallisable sequence chain length. TREF is an appropriate analytical technique for analysing samples with heterogeneous polymers with complex chemical composition distributions.

2.9 Crystallisation analysis fractionation (CRYSTAF)

Similar to the TREF technique, the CRYSTAF technique is used to determine the crystallisation profile of a polymer solution. The techniques are based on the principle that semi crystalline polymers in solution at high temperature will crystallise and precipitate as the solution temperature is gradually lowered. Polymer chains with high comonomer content (high level of branching) will crystallise from solution at lower temperatures, whereas the polymer chains with low comonomer content (low level of branching) will crystallise from solution at high temperature. CRYSTAF monitors the concentration of polymer in solution during the crystallisation phase. In contrast,

TREF measures the concentration of polymer in solution during the dissolution stage after the crystallisation. As a result, the CRYSTAF technique can be used frequently due to the short analysis time. In most instances, the CRYSTAF analysis is performed first to gain an indication of the crystallisation profile of a sample. This information is then useful in determining the fractionation temperature intervals required for a sample to be quantitatively fractionated on the Preparative TREF.

CRYSTAF determines the crystallisation profile of a polymer solution at a constant cooling rate. The change in the concentration of the solution is monitored during the crystallisation period creating a concentration profile gradient. The integration of the derivative curve indicates the fraction of the polymer crystallised at each temperature interval.

2.10 Bulk characterisation techniques

Several characterisation techniques were used to fully characterise the bulk LLDPE samples, the respective fractions of the LLDPE samples and the bulk recombined LLDPE samples with the selective fractions that were removed. The characterisation techniques that were used in this study are Differential Scanning Calorimetry (DSC), Size exclusion chromatography (SEC), Positron Annihilation lifetime spectroscopy (PALS) and Micro hardness. A theoretical description of the principles of these characterisation techniques is discussed below.

2.11 Differential scanning calorimetry (DSC)

Differential Scanning Calorimetry is one of the thermal analysis techniques that are widely available used to analyse thermal properties of polyolefins.

The principle of thermal analysis is based upon the detection of changes in the enthalpy or heat content of a sample with a change in temperature. When thermal energy is supplied to a sample, its enthalpy increases and its temperature rises proportionately by the amount of heat supplied to the sample. The specific heat of a material changes slowly with temperature in a particular physical state, but alters discontinuously at a change of state. Apart from increasing the sample temperature, the supply of thermal

energy may induce physical or chemical processes in the sample, e.g. melting or decomposition, accompanied by a change in enthalpy.

The DSC technique was developed by E.S. Watson and M.J. O'Neill in 1962 [26]. It was introduced commercially at the 1963 Pittsburgh Conference on Analytical Chemistry and Applied Spectroscopy [27].

In the DSC technique, both the sample and reference experience the same temperature profile. The temperature is maintained throughout the course of analysis even during a thermal event in the sample. The amount of energy which has to be supplied to or withdrawn from the sample to maintain a zero temperature differential between the sample and the reference is the experimental parameter displayed as the ordinate of the thermal analysis curve. The sample and reference are placed in identical environments, metal aluminium pans on individual bases each of which contain a platinum resistance thermocouple and a heater [28].

The temperatures of the two thermocouples are compared, and the electrical power supplied to each heater adjusted so that the temperatures of both the sample and the reference remain equal to the programmed temperature, i.e. any temperature difference which would result from a thermal event in the sample is 'nulled'. The ordinate signal, the rate of energy absorption by the sample (e.g. millicalories/sec.), is proportional to the specific heat of the sample since the specific heat at any temperature determines the amount of thermal energy necessary to change the sample temperature by a given amount. Any transition accompanied by a change in specific heat produces a discontinuity in the power signal, and exothermic or endothermic enthalpy changes give peaks whose areas are proportional to the total enthalpy change.

Thus in DSC analysis, the measuring principle is to compare the rate of heat flow to the pan containing the sample and to an empty pan which are both heated and cooled at the same rate. The change in the sample that is associated with absorption or evolution of heat causes a change in the differential heat flow and is recorded as a peak. The area under the peak is directly proportional to the enthalpic change and its direction indicates whether the thermal event is endothermic or exothermic.

2.12 Size exclusion chromatography (SEC)

Size exclusion Chromatography is a method used to separate polymers chains with varying molecular weights. The SEC experimental result gives an elution chromatograph

which is converted into the molecular weight distribution via a calibration profile. The profile of the elution curve is determined by the molecular weight distribution of the sample. A SEC chromatograph for a LLDPE sample is given in Figure 2.14.

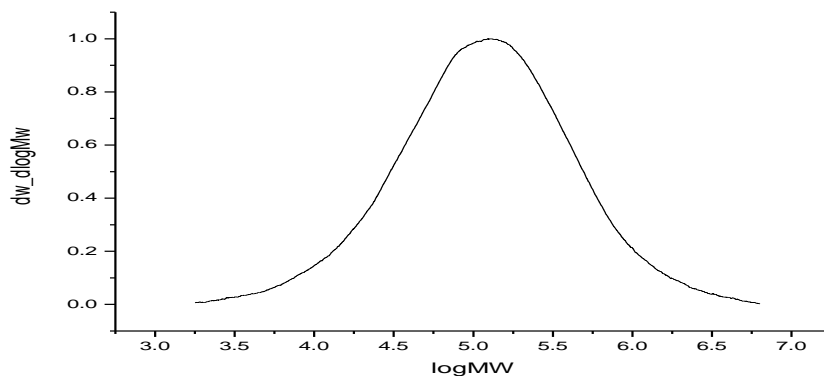


Figure 2.4: SEC separation chromatograph for LLDPE sample [29]

From a theoretical perspective, for a polymer of uniform molecular weight distribution, the maximum peak on the elution profile gives an indication of average molecular weight specific to SEC, M_{SEC} . This variable is dependent on the type of distribution and lies between the average of the number average M_n and the weight average molecular weight M_w [29]. SEC allows for the calculation the molecular mass in a given polymer sample. The DI is calculated at the quotient of the weight average molecular weight to the number average molecular weight. SEC is a form of liquid chromatography and separates according to the hydrodynamic volume of the chains. It differs from other separation techniques which depend upon chemical or physical interactions to separate molecules. Separation occurs between the stationary phase (porous beads packed in column) and the mobile phase (polymer solution). The main features of SEC are characterised by three properties, namely i) separation is effected according to hydrodynamic volume, ii) larger molecules are eluted before smaller molecules and iii) separation takes place in a volume that is smaller than the total volume of the column.

In principle during the phase separation process, the smaller molecules enter the column pores more easily, spend more time in these pores and increase their retention time. Conversely, the larger molecules spend less time in the pores and are eluted quickly. If a molecule is either too large or too small it will be either completely retained or not retained respectively. Molecules that are not retained are eluted with the free volume outside of the particles (V_o), while molecules that are completely retained are eluted with the volume of solvent held in the pores (V_i). The total volume can be

considered by equation 3, where V_g is the volume of the polymer gel and V_t is the total volume [29]:

$$V_t = V_g + V_i + V_o \quad (3)$$

A schematic illustration of the phase separation process is given in Figure 2.15.

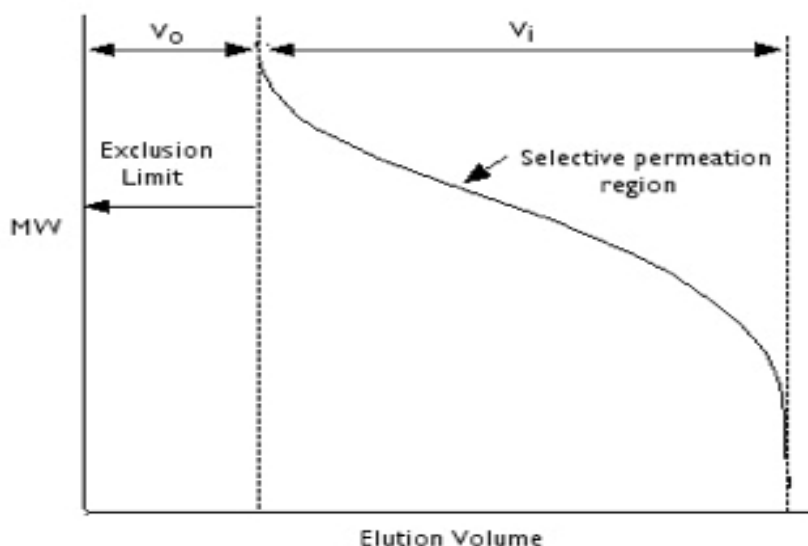


Figure 2.15: Schematic of the phase separation process [29]

Columns can separate a limited range of molecular weights. The size of the column pores for the packing of the column should be selected based on the molecular weight of the polymer which is to be separated. For polymers with broad molecular weight distribution, it may be necessary to use several SEC columns to resolve one sample.

2.13 Positron annihilation spectroscopy (PALS)

The existence of the positron was first predicted theoretically by Dirac in 1931 from the negative solution of electron energy. It was proved experimentally by Anderson from the observation of cosmic ray showers [30]. The positron, represented by e^+ is the antiparticle of the electron, e^- . It has similar properties to that of an electron but carries an opposite charge. Positrons are produced via nuclear reactions such as the production of γ rays with energy greater than $2mc^2$. When the positron encounters an electron, annihilation may take place, and the energy of $2mc^2$ or more is emitted in the form of γ rays radiation. The reaction is indicated in equation 4 [30].



where n is the number of photons created by the annihilation process.

Before annihilating with an electron, the positron may capture an electron to form a bound state called Positronium (Ps). Ps has a similar structure to that of the hydrogen atom. Figure 2.16 gives the schematic comparison between the hydrogen atom and the Ps atom.

Hydrogen	Positronium	
1.0080	Atomic mass (amu)	0.00110
0.99946	Reduced mass (a.u)	1/2
J = 0 (para) J = 1(ortho)	Spin states	S = 0 (para) S = 1(ortho)
∞	Lifetime	125 ps (para) 142 ns (ortho)

Figure 2.16: Hydrogen and Positronium atoms [30]

The positron annihilation lifetime spectroscopic (PALS) technique is used to determine free volume and free volume distributions in semi crystalline materials. Free volume holes in crystalline materials are as a result of irregular molecular packing. The technique explores the free volume phenomena explicitly by measuring changes in the mean lifetime intervals of the ortho-positronium (o-Ps). The ortho-positronium reflects

the size of the free volume hole and is sensitive to the changes of free volume caused by changes of the molecular structure, chain length, temperature and physical aging processes of polymer material [30]. There exists two ground states of the positronium Ps ions. 25% of all Ps atoms are formed in the singlet state or para-positronium (p-Ps) whilst 75% of all Ps atoms are formed in the triple state or ortho-positronium (o-Ps). Many experimental techniques have been performed to correlate the observed changes in positronium lifetime and the intensities I_3 to changes in free volume. In semi crystalline material, the determination of free volume and free volume distributions becomes complex due to the presence of crystallites and of amorphous regions of different mobilities. Sweed *et al* [18] investigated the free volume properties of propylene/1-pentene copolymers prepared with heterogeneous Ziegler-Natta catalytic systems. The copolymers were successfully fractionated using preparative TREF. The fractions were characterised by NMR, DSC and PALS. The studies showed that the ortho-positronium atoms showed systematic variations with degree and nature of short chain branching. Greater variations were observed in propylene co - polymers than with ethylene co polymers which were reflective of a more complex chain structure. Their studies also showed that greater free volume was measured in the amorphous regions of the semi crystalline polymer and in the bulk recombined polymer upon removal of highly crystalline fractions. [18].

2.14 Micro hardness analysis

Micro hardness is a sensitive technique used to measure small differences in samples not detected by other large scale techniques. The technique involves the static penetration of a material with an indenter using a known force. The micro hardness of a material is obtained by dividing the load used by the residual deformation area on the surface of the material. It is a measure of the irreversible deformation processes characterising the material. There are two main types of deformation in the material below the indenter. These zones are the plastic deformation zone and the larger elastic penetration zone. The zones serve to support the stress imposed on the material by the force of the indenter.

There are two main types of indenters used in micro hardness measurements namely the Vickers indenter and the Knoop indenter. The Vickers indenter consists of a square based pyramid of approximately 100 μ m in height. The included angle between the

opposite faces is $\alpha = 130^\circ$. The hardness value is determined according to the equation 5 [31]. P is the applied Newton force.

$$MH_{Vickers} = \frac{2P \sin \frac{\alpha}{2}}{9.807d^2} \quad (5)$$

The Knoop indenter consists of a rhombic base pyramidal opposite a diamond with angle edges of 172° and 130° . The applied force is divided by residential area of impression and is determined by equation 6 [31].

$$MH_{Knoop} = \frac{P}{9.807d^2 C} \quad (6)$$

Sample preparation is an important part of the micro hardness technique. It is important to ensure that the sample has a smooth surface. A smooth and even surface allows for a good indentation where the indentation marks can be visibly seen.

2.15 Carbon 13 nuclear magnetic resonance spectroscopy (^{13}C NMR)

Carbon 13 Nuclear magnetic resonance spectroscopy (NMR) was used in the study to measure the comonomer content (branched carbon content) of the respective individual polymer fractions and bulk recombined material. Nuclear magnetic resonance spectroscopy was first developed in 1946 by research groups at Stanford and M.I.T., in the USA. The principle of NMR is based on the fact that nuclei of atoms have magnetic properties that can be utilised to yield chemical information. The technique is based on the concept of nuclear magnetic resonance. Nuclear magnetic resonance is a physical phenomenon in which magnetic nuclei in a magnetic field absorb and re-emit electromagnetic radiation. This energy is at a specific resonance frequency which depends on the strength of the magnetic field and the magnetic properties of the isotope of the atoms. The energy of the absorption and the intensity of the signal are proportional to the strength of the magnetic field. In essence, a spinning charge generates a magnetic field that results in a magnetic moment proportional to the spin. In the presence of an external magnetic field two spin states exists for the magnetic field. The difference in energy between the spin states increases as the strength of the field increases. Irradiation of the sample with energy corresponding to the exact spin state separation of a specific set of nuclei will cause excitation of those set of nuclei in the lower energy state to the higher energy state. The location of different NMR signals is dependent on the external magnetic field strength and the radio frequency, the signals

are usually reported relative to a reference signal, usually that of TMS (tetramethylsilane). Since the distribution of NMR signals is field dependent, these frequencies are divided by the spectrometer frequency. However since we are dividing Hz by MHz, the resulting number would be too small, and thus it is multiplied by a million. This operation therefore gives a locator number called the chemical shift with units of parts per million. To detect small frequency differences the applied magnetic field must be constant throughout the sample volume. Chemical shifts for protons are highly predictable since the shifts are primarily determined by simpler shielding effects (electron density), but the chemical shifts for many heavier nuclei are more strongly influenced by other factors including excited states. The chemical shift provides information about the structure of the molecule. ^{13}C chemical shifts follow the same principles as those of ^1H , although the typical range of chemical shifts is much larger than for ^1H . The chemical shift reference standard for ^{13}C is the carbons in tetramethylsilane (TMS), whose chemical shift is considered to be 0 ppm for all samples.

2.16 Solid state nuclear magnetic resonance spectroscopy (^{13}C NMR)

The solid state technique is used to measure samples in solid form where analysis in the solution state is not possible. The technique is based on the principle that the radio frequency pulse sequence starts with cross polarisation. This is used to enhance the signal of nuclei with low gyromagnetic ratio to high gyromagnetic ratio where gyromagnetic ratio is the ratio of a magnetic dipole moment to its angular momentum. To establish a magnetic transfer the radio frequency pulses must be applied on the two frequency channels and must fulfill the Hartman- Hahn condition [32]. Magic angle spinning defines the spinning of a sample at a magic angle of θ_m approximately 54.7° with respect to the direction of the magnetic field.

Different solid state ^{13}C NMR approaches are possible making use of the different relaxation behaviour or different distributions of isotropic chemical shifts of carbons in a crystalline or an amorphous environment. The distribution of chemical shifts of carbons is used by lineshape analysis of ^{13}C CP MAS spectra. The solid state ^{13}C CP MAS spectra can be deconvoluted into three Lorentzian lines (position 1-3) for polyethylene polymers. Position 1 and position 3 are signals of carbons in the monoclinic and an orthorhombic crystalline environment. Position 2 is the signal of the carbon on the amorphous environment. The total crystallinity can be calculated as the sum of the integrals in position 1 and position 3. The integrals of ^{13}C CP MAS spectra depend on the ^{13}C amount, but also on the efficiency of the ^1H to ^{13}C magnetisation transfer is

influenced by spatial proximity of protons to carbons (structure and conformation of the sample) and several measurement parameters, especially MAS frequency (spinning speed of the sample) and the contact time.

2.17 References

1. M. Devanney, CEH marketing report, Low density polyethylene resin, May 2012
2. A. Borruso, CEH marketing research report, Linear low density polyethylene resin July 2011
3. F. X. Kromm, Tensile and creep properties of ultra high molecular weight Polyethylene fibres, *Journal of Polymer testing* 22 (2003) : p 463 - 470.
4. Y. Imanishi and N. Naga, Recent developments in olefin polymerisations with transition metal catalysts. *Progress in Polymer Science*, 26 (2001) : p 1147-1198.
5. H. v. Pechmann . Ueber Diazomethan. *Berichte der deutschen chemischen Gesellschaft* 27 (1892): p 1888 -1891.
6. R. Mulhaupt, Catalytic polymerisation and post polymerisation catalysis fifty years after the discovery of Ziegler-Natta, *Macromolecular chemistry and physics*, 204 (2003): p: 289.
7. K. Nashima, Y.Nakayama and A. Nakamura, Recent traces in the polymerisation of α - olefins, catalysed by organometallic complexes of early transition metals, *Advances in Polymer science*, 133 (1997), p: 7 -16.
8. P. Galli and G. Vecellio, Technology: Driving force behind innovation and growth of Polyolefins. *Progress in Polymer science*, 26 (2001), p: 1287.
9. A.F. Hill, *Organotransition metal chemistry*, Wiley Interscience: New York, 2002: pp: 136.
10. Chem systems POPS program, technology review report, December 2011.
11. J Hartwig,. *Organotransition Metal Chemistry, from Bonding to Catalysis*; University Science Books: New York, 2010.
12. Y. Imanishi and N. Naga, Recent developments in olefin polymerisations with transition metal catalysts. *Progress in Polymer Science*, 26 (2001): p. 1147-1198.
13. Kirk-Othmer, *encyclopaedia of chemical technology*, vol 16, Page 79, 3rd edition.
14. M.J Clarke and P.J Sadler, *Metallopharmaceuticals: Diagnosis and therapy*. Berlin: Springer. (1999)

15. C.J Jones and J Thornback, *Medicinal Applications of Coordination Chemistry*. Cambridge, UK RSC Publishing.
16. Internet article accessed on 1 March 2012,
http://wikipedia.org/wiki/organochromium_chemistry
17. Internet article accessed on 1 March 2012,
<http://www.univation.com/technology.catalyst.php>
18. M. Sweed, Free volume properties of semi-crystalline polymers, Sweed, PhD Dissertation, University of Stellenbosch March 2011
19. P. Starck, Studies of the Comonomer Distributions in Low Density Polyethylenes Using Temperature Rising Elution Fractionation and Stepwise Crystallisation by DSC. *Polymer International*, 40 (1996) p. 111-122.
20. L. Keulder, The effect of molecular composition on the properties of linear low density polyethylene. MSc Thesis, University of Stellenbosch: Stellenbosch 2008.
21. G. W Harding, The structure property relationship of polyolefins, PhD thesis, University of Stellenbosch, March 2009.
22. J.Minick, J. Moet, A Hiltener, E. Baer and S. P Chum, Crystallisation of very low density copolymers of ethylene with α olefins, *Journal of applied polymer science* 58 (1995) p 1371.
23. S. Anantawaraskul, J.B.P. Soares, P.M. Wood-Adams, The effect of operation parameters on TREF fractionation and Crystallisation analysis fractionation, *Journal of Polymer science: Part B: Polymer plastics*, 41 (2003), p 1762 -1778
24. P. Starck, Studies of the comonomer distributions in Low density Polyethylenes using Temperature rising elution fractionation and stepwise Crystallisation by DSC, *Polymer International* 40 (1996) p 111 -122.
25. J.T. Xu, X., R. Xu. L. S. Chen and L. X. Feng, The effect of short chain branching distribution on crystallisation of ethylene-butane copolymers, *Journal of materials science letters* 19, 2000, p 1541 – 1543.
26. E.S. Watson and M. O'Neil, Differential microcalorimeter, United States Patent, patent number 3, 263. Filed 4 April 1962, Patented 2 August 1966.
27. **Internet article accessed on 1 March 2012**
<http://www.friedli.com/research/PhD/DSC/chap3.html>
28. E. Schroder, G.Muller, K. Arndt , *Polymer Characterisation*, 1988
29. L. Konstanski, D. M Keller, S Hamdac, Size exclusion chromatography – a review of calibration methodologies, *Journal of biochemical and biophysical methods*, 58 (2004), p159.

30. Yu Zhibin, Positron and Positronium annihilation lifetime and free volume in polymers, PhD Thesis, Cape Western Reserve University: January, 1995.
31. Internet article accessed on 6 October 2012, New Age hardness testers, <http://www.hardnesstesters.com/applications/vickers-hardness-kooptesting.aspx>
32. Internet article accessed on 23 November 2012, Solid state NMR, http://en.wikipedia.org/wiki/solid_state_nuclear_magnetic_resonance

CHAPTER 3**3 EXPERIMENTAL TECHNIQUES****3.1 Materials****3.1.1 Polymer**

Linear low density polyethylene was studied. The grade was a copolymer of ethylene and 1-hexene with a nominal MFI of 2 g/10min and a nominal density of 0.9200 g/cm³. All three samples namely the catalyst trial and the reference samples were the same grade of polymer samples.

3.1.2 Stabiliser

A mixture of Irganox 1010 and Irgafos 168 (refer to Figure 3.1 and Figure 3.2) was used as thermal stabilisers during the TREF procedure to prevent degradation of the polymer during the slow cooling of the TREF phase. During the elution step of the TREF procedure, the elution solvent (xylene) was stabilised with 2,6 - di-tert-butyl-4-methylphenol (BHT).

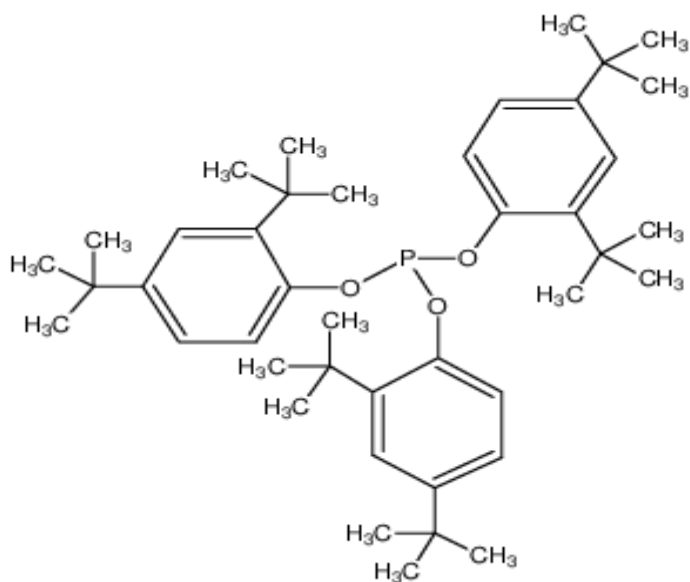


Figure 3.1: Tris (2, 4 - di-tert-butylphenyl) phosphate Irgafos 168 [1]

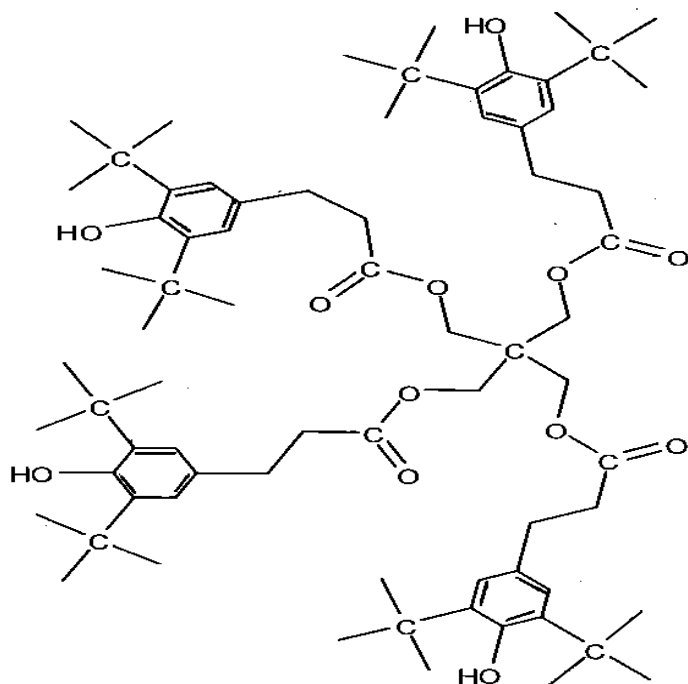


Figure 3.2: Irganox 1010 [1]

3.1.3 Solvent

The solvent, xylene (Aldrich, 99 % purity) was used in all the TREF experiments.

3.2 Analytical techniques

3.2.1 Temperature Rising Elution fractionation (TREF)

Temperature rising elution fractionation (TREF) technique fractionates semi-crystalline polymers according to their ability to crystallise from solution. This process is independent of molecular weight effects [2]. The in-house Preparative TREF method comprises of cooling, elution and recovery steps [3].

The cooling stage

The cooling stage entails dissolution of polymer in a xylene solvent and subsequent cooling of polymer solution. Approximately 3 g of linear low density polymer and 0.06 g stabiliser (combination of Irganox 1010 and Irgafos 68) were dissolved at 130 °C in 300 ml of xylene in a glass reactor. An inert crystallisation support, (washed sand white quartz - 50 + 70 mesh)

which was preheated at a temperature of 130 °C was then added to the reactor. The preheating was necessary in order to prevent premature crystallisation onto the cold support. Enough sand was added to the reactor vessel in order to ensure that no polymer solution was visible above the level of the sand. The reactor was then placed in a preheated oil-bath at a temperature of 130 °C, and fitted with a condenser.

The configuration of the cooling system was such that four TREF reactors could be simultaneously cooled from 130 °C to 20 °C at a rate of 1 °C/h. The simultaneous cooling of the four reactors saved time and allowed for bulk fractionation of the multiple samples sequentially.

The elution stage

Upon cooling the polymer solution, the polymer material together with the support is transferred to a stainless steel column. The column has a length of 15 cm and an internal diameter of 7 cm. The column is designed with a hole at the bottom, which allows for a temperature probe to be inserted through the bottom. This allows for the accurate monitoring of the temperature during the fractionation process. The column packing is illustrated in the Figure 3.3.

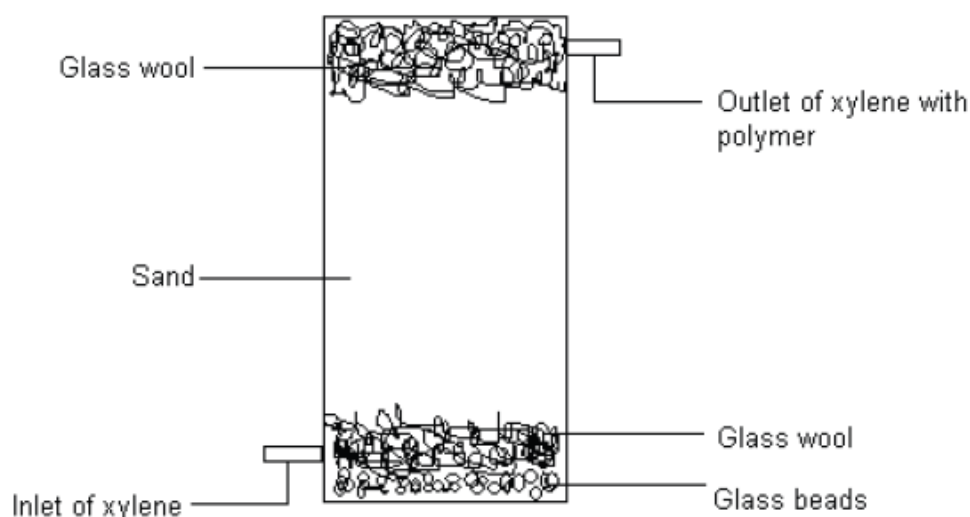


Figure 3.3: Illustration of the packing of a single TREF column [3]

The column is equipped with a coiled copper tube which is 6 mm in diameter. The solvent flows along the outside of the column in the tube, allowing the solvent to reach the required temperature before being passed into the column. Glass wool was packed into the top and the bottom of the column. The glass wool packing allows for the even distribution of the

solvent through the polymer support. The column is subsequently placed into a modified GC oven (Varian Model 3700) and heated at 10 °C temperature intervals to the required fractionation temperatures. At specific temperature intervals, the column was flushed with 300 ml xylene solvent at a flow rate of 40 ml/min. The flow rate was maintained by a solvent pump (FML 'Q' Pump, Model QG150).

Recovery Stage

The fractions that were collected at respective temperature intervals were rotor evaporated to remove the xylene solvent and crystallise the polymer fractions. The residual polymer fractions were recovered with acetone, air dried for 3 days and vacuum dried in an oven overnight.

3.2.2 CRYSTAF

The reference sample and catalyst trial samples were analysed on the Varian CRYSTAF 2000 instrument. The crystallisation profiles of the samples were determined on the CRYSTAF instrument in a nitrogen atmosphere. The samples were cooled from 100 °C to 30 °C at a rate of 0.1 °C/min. Approximately 10 mg of sample was used in the analysis. Ortho-dichloro benzene was used as crystallisation solvent for the reference sample and the catalyst trial sample comparisons.

3.2.3 Differential scanning calorimetry

The crystallisation and melting profiles of the bulk reference sample and catalyst trial samples were determined by DSC. The analysis was conducted on TA Instruments Q100 DSC. The instrument was calibrated using indium metal according to standard laboratory calibration procedures. Heating and cooling rates were maintained at a standard 10 °C /min. The sample was weighed off and sealed in a standard Aluminium DSC pan. The sample was then heated to 150 °C at a rate of 10 °C/min and then equilibrated at 150 °C for 5 minutes. The sample was then cooled down to - 40 °C at a rate of 10 °C/min and then left to equilibrate at that temperature for 5 minutes. The sample was then heated again to 150 °C at a rate of 10 °C. The second heating was used for analysis of the melting behaviour of the polymer.

3.2.4 Size exclusion chromatography

Molecular weight and polydispersity were determined with high temperature SEC. 1.5 - 2 mg of polymer was dissolved in 2 ml of 1, 2, 4 -trichlorobenzene containing 0.0125% 2, 6-di-tert-butyl-4-methylphenol (BHT) and dissolved at 160 °C. Molecular weights were determined on a PL-SEC 220 High Temperature Chromatograph from Polymer Laboratories at 145 °C. The 3 columns were PLgel OXLEXIS columns with dimension 300mm and diameter of 7.5mm. The particle size was 10 µm. A differential refraction index detector was used. The calibration of the instrument was done with monodisperse polystyrene standards (Easical from Polymer Laboratories).

3.2.5 Solution state carbon 13 nuclear magnetic resonance spectroscopy (NMR)

The ¹³C NMR spectra of the unfractionated polymers, as well as the fractions obtained by TREF were recorded. These spectra were used to determine the comonomer content present in each sample. Typically, about 65 mg of each sample was placed in a NMR tube and dissolved in 5 ml of 1, 2, 4-trichlorobenzene/C6D6. The 1, 2, 4-trichlorobenzene/C6D6 was used in 5:1 ratio.

The ¹³C and ¹H spectra were obtained on a Varian VXR 300 MHz instrument. A pulse angle of 45° and an acquisition time of 0.82 s were used.

The comonomer percentage was calculated according to equation 1 where Br is indicative of carbon units branched from the backbone of the polymer chain (branching carbons).

$$\text{Comonomer} = \frac{\alpha \text{ Br carbon}/2 + \text{Br carbon}}{\text{Total backbone carbons}} \quad (1)$$

The resonances associated with all the backbone carbons were integrated and the integrals of the peaks assigned to the branching carbon and the carbons α to branching were then used to determine the comonomer content (mole %) using the equation above. The percentage of the carbons α to branching was divided by two because there are two carbons α branching and the percentage of the branching carbons are added together.

3.2.6 Solid state carbon 13 nuclear magnetic resonance spectroscopy (NMR)

The solid state (SS) NMR spectra were acquired on a Varian VNMRs 500 MHz two channel spectrometer using 4 mm zirconia rotors and a 4 mm Chemagnetics T3 HX MAS probe. The cross-polarization (CP) spectrum was recorded at ambient temperature with proton decoupling using a recycle delay of 4s. The power parameters were optimised for the Hartmann-Hahn match. The radio frequency fields were $\gamma_{CB1C} = \gamma_{HB1H} \approx 55$ kHz. The contact time for cross-polarization was 0.5 ms.

Magic-angle-spinning (MAS) was performed at 7 kHz and Adamantane was used as an external chemical shift standard where the downfield peak was referenced to 38.3 ppm.

The integrals assigned to the carbon signals in position 1 and position 3 were added to give the total crystallinity of the polymer samples. The integral assigned to position 2 was not taken into account.

Different solid state ^{13}C NMR approaches are possible making use of the different relaxation behaviour or different distributions of isotropic chemical shifts of carbons in a crystalline or an amorphous environment. Here the latter approach is used by lineshape analysis of ^{13}C CP MAS spectra. The solid state ^{13}C CP MAS spectra can be deconvoluted into three Lorentzian lines (position 1-3). Position 1 and position 3 are signals of carbons in the monoclinic and an orthorhombic crystalline environment. Position 2 is the signal of the carbon on the amorphous environment. The total crystallinity can be calculated as the sum of the integrals in position 1 and position 3.

The integrals of ^{13}C CP MAS spectra depend on the ^{13}C amount, but also on the efficiency of the ^1H to ^{13}C magnetisation transfer is influenced by spatial proximity of protons to carbons (structure and conformation of the sample) and several measurement parameters, especially MAS frequency (spinning speed of the sample) and the contact time.

3.2.7 Micro hardness analysis

Hardness testing was performed on the LLDPE samples using a UHL Micro hardness tester with the Vickers indenter. Ten measurements were obtained using 25 $\mu\text{m/s}$ as the indentation speed and a dwell time of 15 s. Samples were analysed at an indentation load of

10 gf. The samples were first melted at 200 °C for 6 min before applying 3 mPa pressure for 3 min.

3.2.8 Positron annihilation lifetime spectroscopy (PALS)

The positron annihilation lifetime measurements were carried out using a standard fast-fast coincidence system with timing resolution of 240.34 ps full width of half-maximum (FWHM) and total of 1024 channels. The ²²NaCl positron source was placed between two pieces of sample and the sample was covered by Aluminium foil. The duration of each measurement was about 80 min maximum, during which time a total of 1106 counts were collected. All measurements were made in air at room temperature.

3.3 References

1. M. Pinto, Quantitative analysis of antioxidants from high density polyethylene (HDPE) by off-line supercritical fluid extraction coupled high performance liquid chromatography. MSc thesis, Virginia Polytechnic Institute, Virginia, 1997.
2. L.J. Britto, J.B.P Soares, A. Penlids, and B. Monrabal, Polyolefin Analysis by single step crystallisation fractionation by Crystaf. *Journal of polymer science: Part B: Polymer physics*, 37 (1999),p 539 - 552.
3. A.J Rabie, Blends with Low-Density Polyethylene (LDPE) and Plastomers. MSc thesis, University of Stellenbosch, Stellenbosch, 2004.

CHAPTER 4**4 RESULTS AND DISCUSSION**

Catalyst trials were performed on LLDPE grade polymers with a nominal MFI of 2 g/10min and a nominal density of 0.920 g/cm³. Studies were conducted on these trial samples to investigate if the samples synthesised under the catalyst trial conditions showed any significant differences in terms of crystallinity and mechanical properties to the sample that was synthesised using the standard catalyst.

Catalyst trials were conducted on the LLDPE reactor where changes were made to the levels of cocatalyst in the LLDPE reactor. The reference sample (RS), was synthesised under normal operating conditions with a normal level of cocatalyst. Two additional catalyst trials were conducted. The first trial entailed the trialling of a third party catalyst with an optimised amount of cocatalyst for that catalyst. The Aluminium to Titanium ratio of the trial catalyst was the same as for the standard catalyst. The sample obtained from this trial is referred to as the catalyst trial sample 1 (CST1). The second trial entailed the trialling of the standard catalyst with low concentration of cocatalyst in comparison to the normal operating concentration of cocatalyst. The sample obtained from this trial is referred to as the catalyst trial sample 2 (CST2).

The macroscopic product properties, namely density, MFI and level of hexene extractables are different for the trial samples synthesised under different catalytic conditions. The differences observed in the trial samples in comparison to the reference sample infer that the catalyst trial samples were synthesised with differences on a molecular level. Although the material was produced within selling range specifications, the slight differences in the densities and level of hexane extractables indicate differences in the crystallinities of the materials. The level of hexene extractables also differ for the samples, indicating differences in the level of low molecular weight species of the samples. The differences in the chemical composition between the reference sample and the catalyst trial samples were fully explored using the following characterisation techniques, preparative TREF, CRYSTAF, DSC, ¹³C NMR, HT SEC and PALS. The macro product properties are indicated in Table 4.1.

Table 4.1: Macroscopic product properties for bulk reference sample, bulk catalyst trial sample 1 and bulk catalyst trial sample 2

Sample	Density (g/cm ³)	MFI (g/10min)	% Hexene extractable
Reference sample	0.9200	2.02	3.59
Catalyst Trial sample 1	0.9188	2.14	3.11
Catalyst Trial sample 2	0.9214	2.01	2.35

The main objective of this study is to compare the catalyst trial LLDPE samples produced with the changes to the catalyst system (CTS1 and CTS2) against the reference sample (RS) synthesised under normal catalyst conditions.

4.1 Characterisation of bulk material

4.1.1 CRYSTAF analyses

CRYSTAF analyses on the samples were conducted to measure the crystallisation profile of the samples in order to determine if the samples could be fractionated at the same TREF temperature intervals. The CRYSTAF results of the bulk LLDPE samples indicate a unimodal chemical distribution. A crystallisation peak was observed with a sharp peak between 80 °C - 90 °C. The fraction soluble at 30 °C is indicated by the rectangle portion of the graph relative to the percentage of polymer remaining in solution. The soluble fraction is indicated in the 25 °C - 30 °C temperature region and the less crystalline fraction is located between the 30 °C - 70 °C region. All samples show the similar crystallisation profiles indicating that they can be fractionated at the same temperature intervals. The CRYSTAF spectra are indicated in Figure 4.1.

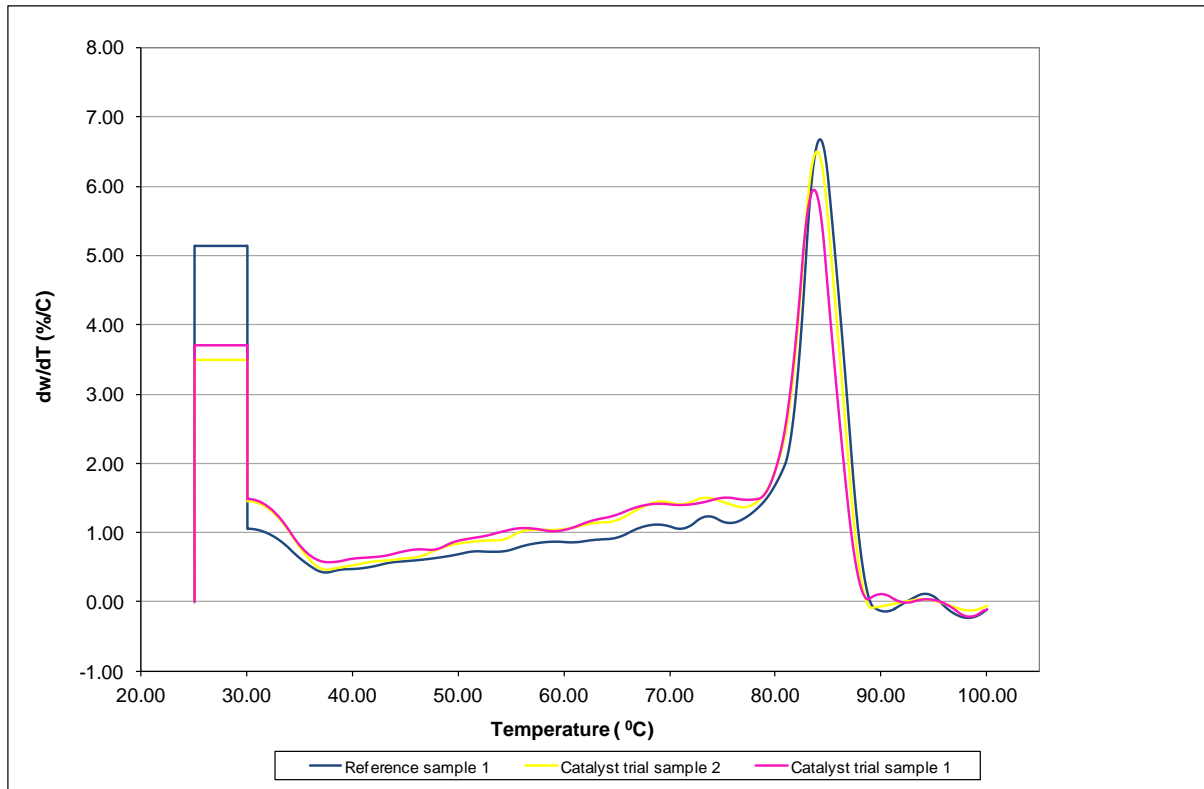


Figure 4.1: CRYSTAF analysis of bulk LLDPE samples

The percentage of soluble fraction measured at 30 °C is indicated in Table 4.2. The results indicate that the catalyst trial sample 2 which has the lowest amount of cocatalyst exhibits the lowest percentage soluble fraction. The peak temperature for the samples at the point of maximum crystallisation for the reference sample, catalyst trial sample 1 and catalyst trial sample 2 are 84.2 °C, 83.2 °C and 83.9 °C respectively.

Table 4.2: CRYSTAF results of bulk Reference sample, Catalyst Trial sample 1 and Catalyst Trial sample 2

Sample	% Soluble fraction at 30 °C
Reference sample	37.5
Catalyst Trial sample 1	18.5
Catalyst Trial sample 2	17.5

4.1.2 TREF Analysis

Preparative TREF was used to fractionate the reference sample, catalyst trial sample 1 and catalyst trial sample 2. The results of a typical TREF fractionation experiment are show in

Table 4.3. It should be noted that the amount of material collected from one TREF fraction cannot always be compared to the amount of material collected from another fraction due to the slight differences in the fractionation temperature gap. Therefore the weights of the fractions are divided by the temperature interval between the fractions to give a more accurate representation of the mass of the fraction. Results of the TREF experiment conducted on the reference sample is indicated in Table 4.3 where W_i is the weight of the fraction divided by the original total weight of the sample and $W_i / \Delta T$ is the weight of a fraction divided by the temperature interval between the two successive fractions.

Table 4.3: TREF fractionation results of reference sample

Temperature (°C)	W_i %	$W_i / \Delta T$
20	7.6	0.8
30	4.4	0.4
40	5.4	0.5
50	8.2	0.8
60	8.3	0.8
70	8.4	0.8
80	14.2	1.4
90	11.7	1.2
100	19.6	2.0
110	7.9	0.8
120	4.3	0.4

The results from Table 4.3 shows that most of the material elutes between 70 °C - 110 °C.

The distribution of the fractions is illustrated in Figure 4.2.

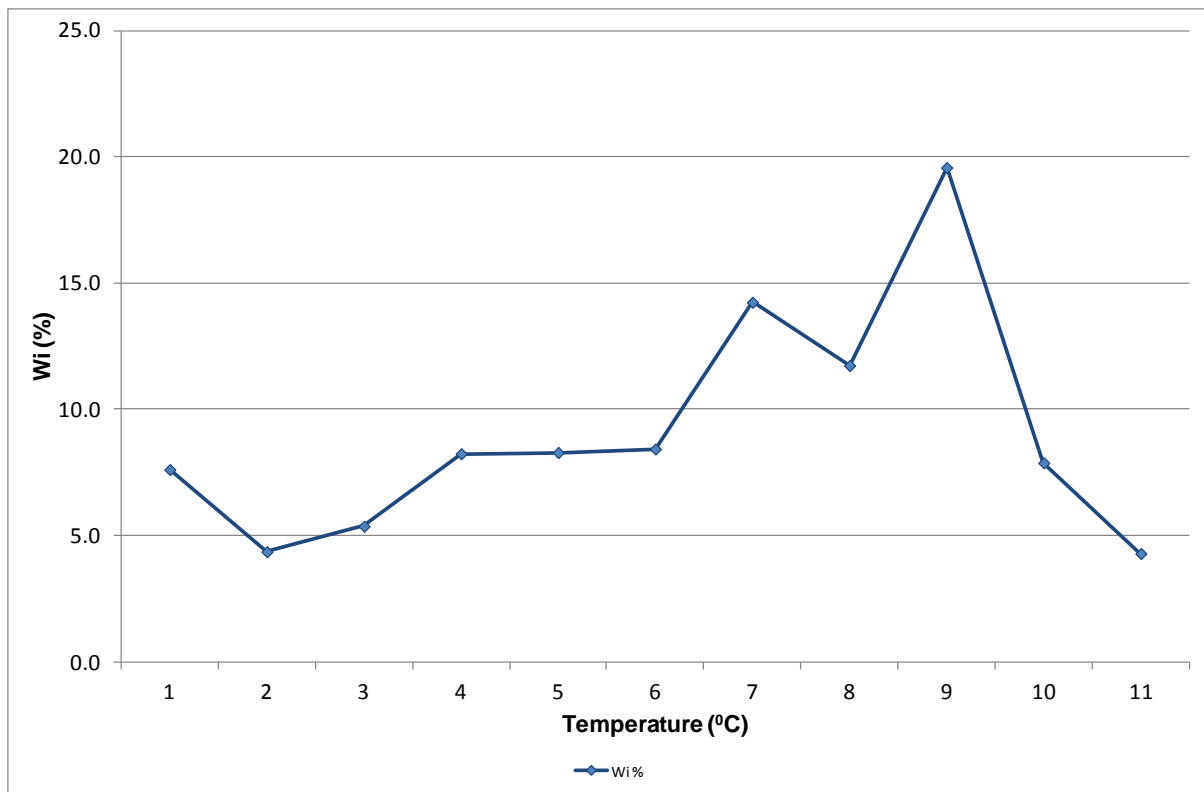


Figure 4.2: TREF elution weight distribution for the reference sample

The distribution of the material is broad which indicates a broad distribution in the chemical composition of the sample. TREF fractionates polymer chains according to their ability to crystallise from solution. The general observation is that amorphous polymer chains elute at low temperature and the more crystalline polymer chains elute at higher temperature ranges. Studies conducted by Monrabel *et.al* also verified this trend [1]. The most crystalline material with a low level of branching elutes at higher temperature ranges and the least crystalline material with the most branching elutes at lower temperatures. Branching in LLDPE is due to the amount of comonomer insertion. Side chain branching in LLDPE also affects crystallinity. Highly branched LLDPE with a high level of comonomer is less crystalline than LLDPE with low levels of branching and a low level of comonomer. The schematic representation of the data further indicates that the bulk of the material elutes between 70 °C - 110 °C.

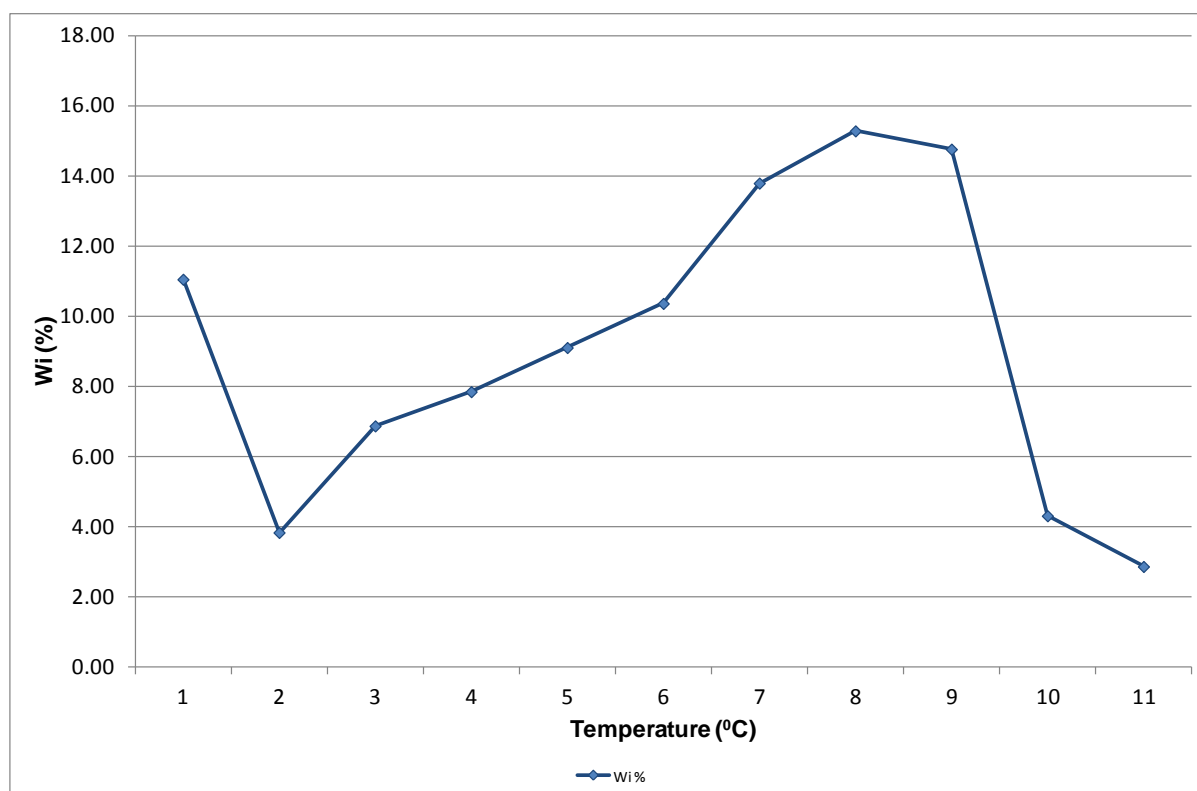
A similar TREF profile is observed with the catalyst trial sample 1. The distribution of the TREF data is indicated in Table 4.4.

Table 4.4: TREF fractionation results for catalyst trial sample 1

Temperature (°C)	Wi %	Wi / ΔT
20	11	1.1
30	3.8	0.4
40	6.9	0.69
50	7.8	0.78
60	9.1	0.91
70	10.4	1.04
80	13.8	1.38
90	15.3	1.53
100	14.8	1.48
110	4.3	0.43
120	2.9	0.29

The data indicates that the bulk of the material elutes between 70 °C - 100 °C.

The distribution of fractions is illustrated in Figure 4.3.

**Figure 4.3: TREF elution profile for the catalyst trial sample 1**

The catalyst trial sample 2 exhibited similar TREF profiles as the reference sample and catalyst trial sample 1. The bulk of the material is shown to elute between 70 °C - 100 °C. The distribution of the TREF fractionation data is indicated in Table 4.5.

Table 4.5: TREF fractionation data for catalyst trial sample 2

Temperature (° C)	Wi %	Wi / Δ T
20	5.1	0.5
30	3.0	0.3
40	4.2	0.4
50	4.1	0.4
60	6.4	0.6
70	9.5	1.0
80	14	1.4
90	17	1.8
100	17	1.7
110	5.9	0.6
120	1.3	0.1

The distribution of fractions is illustrated in Figure 4.4.

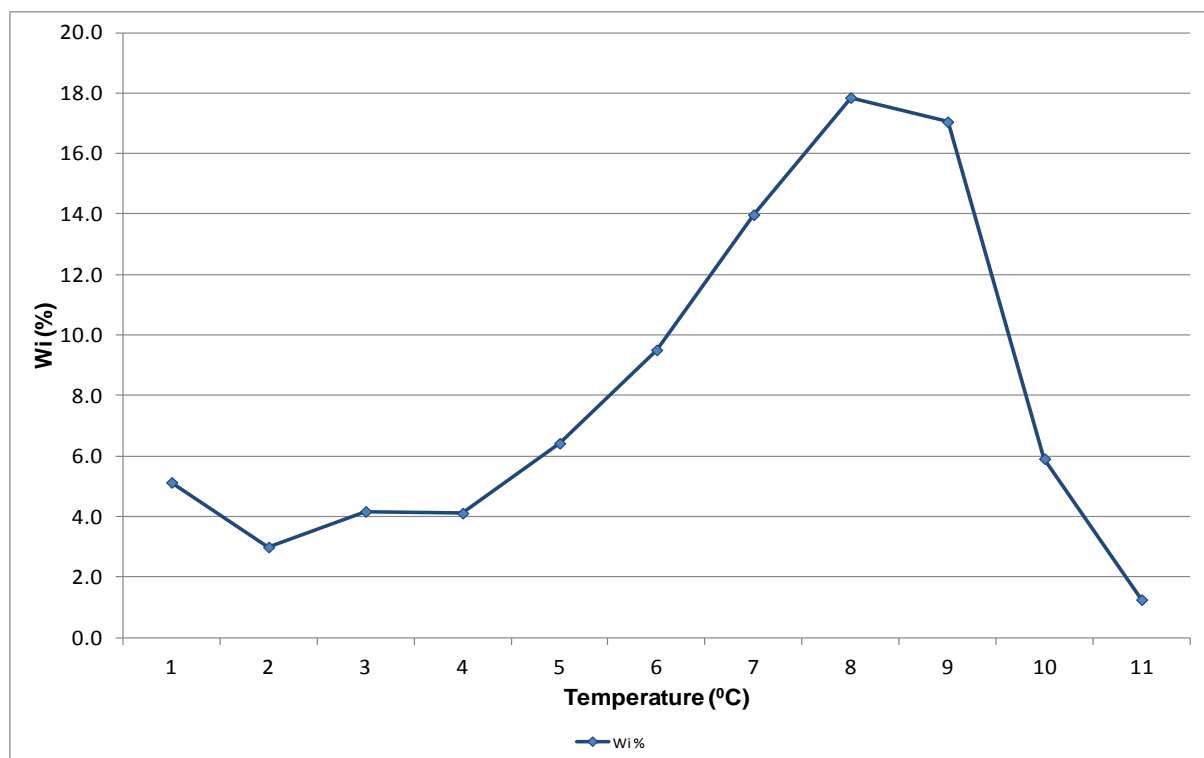


Figure 4.4: TREF fractionation data for the catalyst trial sample 2

In summary, the reference sample, catalyst trial sample 1 and catalyst trial sample 2 have different TREF profiles. The catalyst trial sample 1 has a much higher soluble content. To further explore these differences on a molecular level, it is recommended that the samples be bulk fractionated at the same temperature intervals. An overlay of the samples showing comparative TREF fraction distributions is indicated in Figure 4.5.

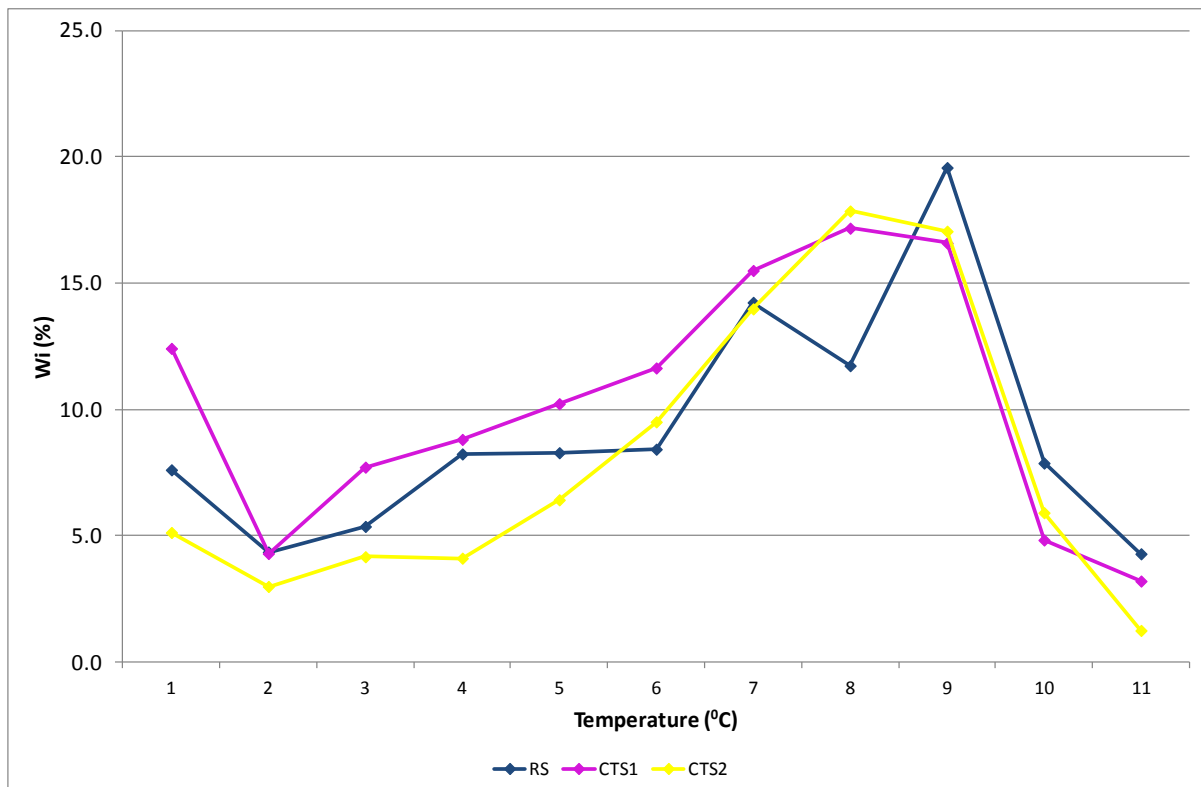


Figure 4.5: TREF profile comparisons for reference sample, catalyst trial sample 1 and catalyst trial sample 2

The overlays of the TREF fractionations indicate that the samples have similar crystallisation profiles can be fractionated at the same temperature intervals. This allows for a more direct comparative study between the samples.

4.1.3 DSC Analysis

The results of the DSC analyses of the three bulk LLDPE samples are shown in Table 4.6.

Table 4.6: DSC results of bulk samples

Sample	Tm (°C)	Hm (J/g)	% Crystallinity
Reference sample	125.2	98.55	33.0
Catalyst Trial sample 1	123.6	102.5	34.9
Catalyst Trial sample 2	118.8	117.4	40.1

The catalyst trial sample 2 contains the highest degree of crystallinity, followed by the catalyst trial sample 1 and then the reference sample. This is quite interesting, when the results are considered together with the solution crystallisation results obtained by CRYSTAF. The reference sample has the lowest crystallinity (according to DSC), and the highest soluble content (according to CRYSTAF), yet has the highest solution crystallisation temperature (CRYSTAF), and the highest melting point. The CTS 1 has a much lower soluble content than the reference sample (according to CRYSTAF), yet appears to have a very similar crystallinity according to DSC. The CTS 2 sample has the lowest soluble content, the highest crystallinity, and yet has the lowest melting temperature of the three samples. These results indicate that the type of crystallinity present (and by extension the chemical composition distribution) in the three samples must be significantly different. The DSC graphs showing the DSC integration for crystallinity are indicated in Appendix A.

DSC data indicates an increase in crystallinity with an increase in the elution temperature. An overlay of the Bulk LLDPE samples is indicated in Figure 4.6.

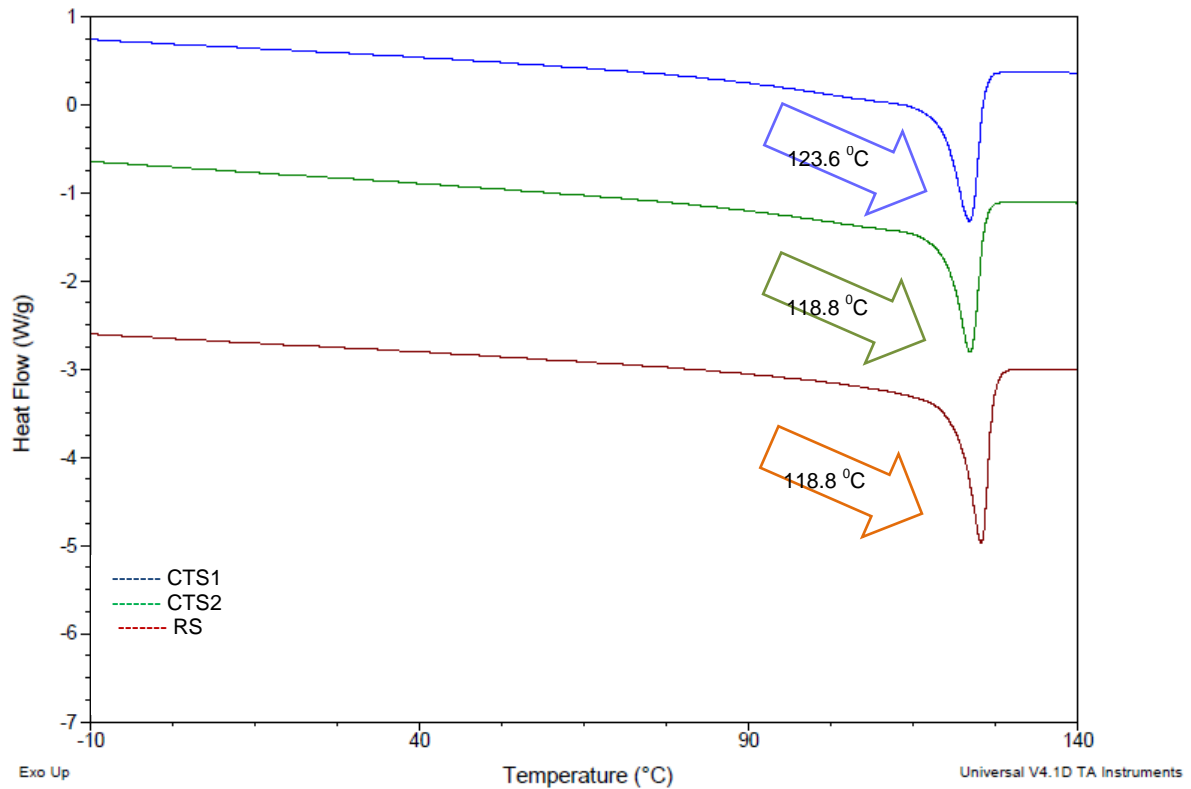


Figure 4.6: DSC analyses of reference sample, catalyst trial sample 1, catalyst trial sample 2

An increase in the crystallinity with an increase in the fractionation temperature is also observed as shown in Figure 4.7. This reinforces the trend of an increase in % crystallinity with an increase in fractionation temperature. A comparison can be drawn between the comonomer content and the crystallinities. It can be concluded that the more branching a fraction contains, the less crystalline that fraction is and the lower the melting point will be [1]. This trend has been observed and accounted for elsewhere in the literature as well [2 - 5].

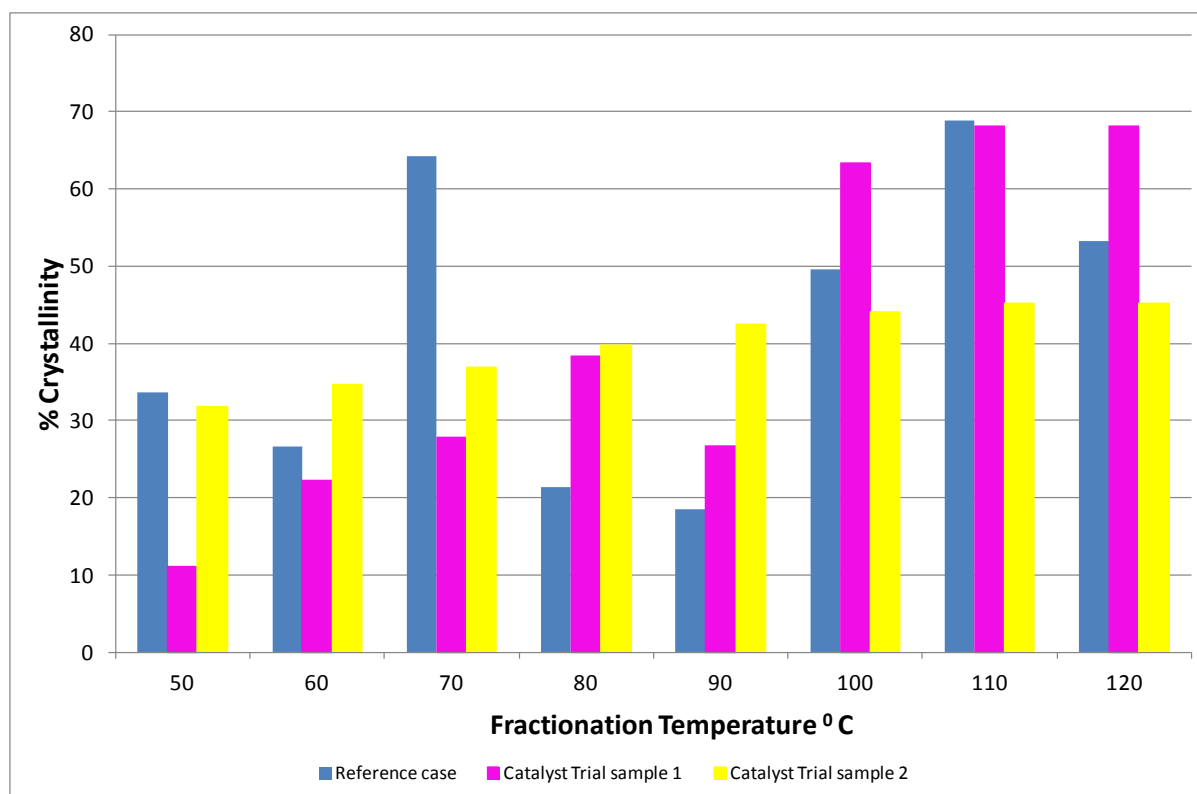


Figure 4.7: Crystallinity of the reference sample, catalyst trial sample 1 and catalyst trial sample 2

4.1.4 SEC Analysis

The molecular weight trends are given in Figure 4.8 and the molecular weight values are given in Table 4.7 for the reference sample, catalyst trial sample 1 and catalyst trial sample 2 respectively. The SEC profiles of the bulk samples and the respective fractions of the bulk samples are shown in Appendix B.

Table 4.7: Molecular weight and dispersity index of bulk samples

Sample	Mn (g/mol)	Mw (g/mol)	DI
Reference sample	52000	256000	4.92
Catalyst Trial sample 1	58900	211200	3.58
Catalyst Trial sample 2	57300	216900	3.78

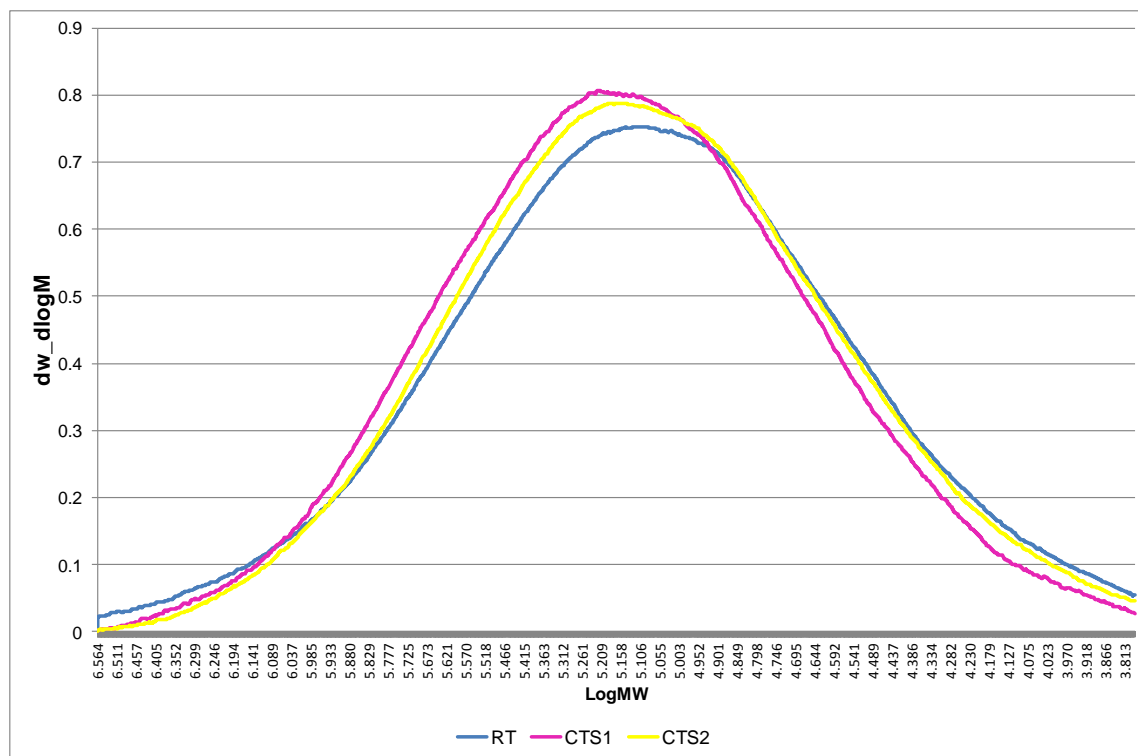


Figure 4.8: Molecular weight trends for reference sample, catalyst trial sample 1 and catalyst trial sample 2

The samples display similar molecular weight values and dispersity (DI) profiles.

The molecular weight of the fractions of the reference sample, catalyst trial sample 1 and catalyst trial sample 2 are indicated in Figure 4.9.

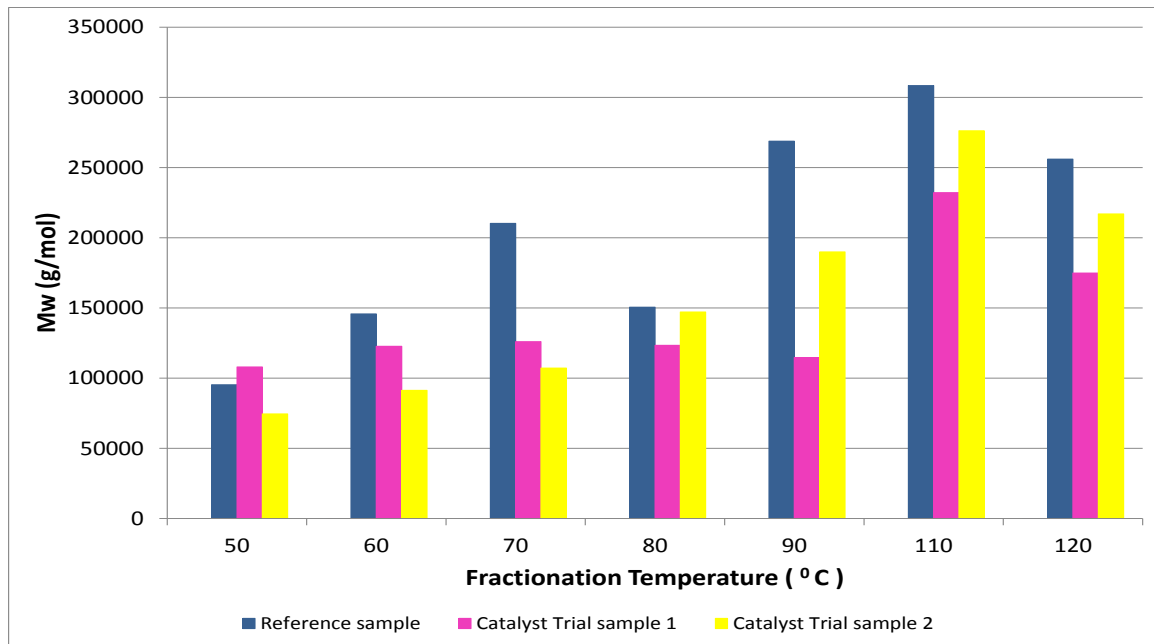


Figure 4.9: Molecular weight distribution across fractions

The dispersity indices values (DI) is indicated in Figure 4.10.

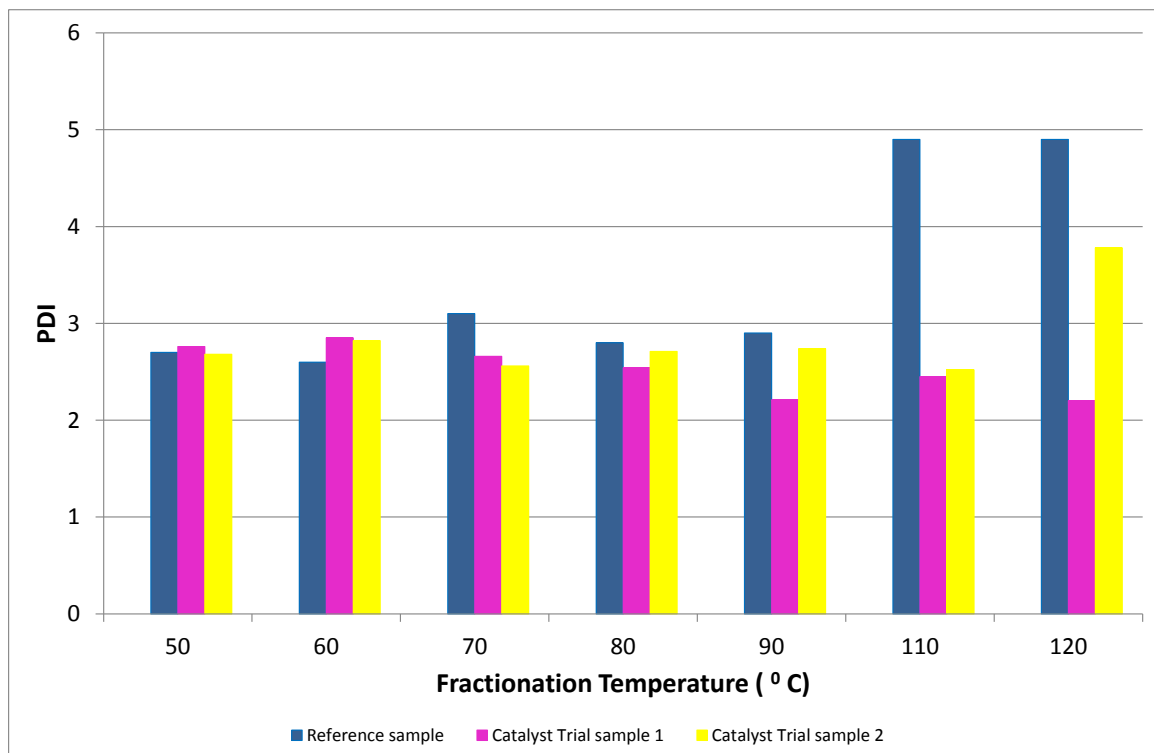


Figure 4.10: Distribution of DI across fractions

It is well known from literature that molecular weight increases with an increase in fractionation elution temperature [6]. This trend is clearly depicted by the catalyst trial sample 2. The increase in the molecular weight with the increase in the elution temperature is due to crystallisability effects, since the polymer chains with longer crystallisable sequences are generally higher in molar mass. The DSC results of the TREF fractions indicate that the more crystalline material elutes at higher temperature ranges. The TREF results also indicate that the fractions which are least crystalline have the lowest molecular weights and highest dispersity indices. The highly crystalline fractions have the lowest level of short chain branching (least comonomer content) allowing for more compact packing of the polymer chains.

4.1.5 ^{13}C NMR Analyses

The comonomer concentration of the bulk samples were analysed by the ^{13}C NMR technique to further gain an indication of the crystallinity profiles of the samples for comparison purposes. The samples were analysed by both the solution state and solid state NMR techniques.

The results of both the solid state and solution state analyses for the bulk samples are indicated in Table 4.8. The solid state NMR spectra of the bulk samples and fractions of the bulk samples are shown in Appendix C.

Table 4.8: Comonomer content of bulk samples

Sample	Solid state ^{13}C NMR % crystallinity	Solution state ^{13}C NMR % comonomer
Reference sample	63.0	5.87
Catalyst trial sample 1	69.0	4.43
Catalyst trial sample 2	68.1	6.00

The results of the solution state ^{13}C NMR show the total comonomer content of the bulk polymer sample. The general trend indicates that the catalyst trial sample 2 with the low amount of cocatalyst is more crystalline than the catalyst trial sample 1 and the reference sample. In the solid state ^{13}C NMR technique the sum of the integrals of the carbon atoms in the monoclinic and orthorhombic crystalline environments of the polyethylene polymer make up the total crystallinity of the polymer. The theoretical explanation of the principles of the solid state NMR analytical technique has already been discussed in chapter 2, section 2.16. The integrals and crystallinity is shown in Table 4.9. The monoclinic region is represented by position 1 and the orthorhombic region is represented by position 3. Although

the final solid state ^{13}C NMR results show no significant differences between the samples, the individual assignments to the carbons in the monoclinic region of the crystalline environment show that the catalyst trial sample 2 has the highest relative integral. This data is indicated in Table 4.9. Previous studies conducted by Assumption *et al* [7] show that both solution state and solid state NMR characterisation correlate differences in chemical composition well. In addition studies conducted by C Yannoni and Kuwabara *et al* on the solid state ^{13}C NMR show that the cross polarisation magic angle spinning (CPMAS) experiment is an effective technique for the determination of crystallinity in semi-crystalline polymers [8 -9].

Table 4.9: Fitting parameters for the deconvolution of the CP MAS spectra of the LLDPE polymers and the determined values of crystallinity

Sample	Position	(^{13}C)/ppm	Line width (Hz)	Relative Integral	Crystallinity (%)
RS	1	3.6	65	50.0	63.0
	2	31	248	37.0	
	3	33.2	215	13.0	
CTS1	1	32.6	66	57.0	69.0
	2	30.9	214	32.0	
	3	33.6	226	12.0	
CTS2	1	32.6	66	60.0	68.1
	2	30.9	247	31.8	
	3	33.7	113	8.2	

The comonomer concentration of the fractions of the samples were also analysed by the solution state ^{13}C NMR technique. The results are shown in Table 4.10. The analyses were important to understand the distribution of crystallinity across the fractions. The distribution of crystallinity across certain fractions would give an indication of which fractions to remove for comparative purposes.

Table 4.10: Comonomer content of fractions of samples

Temperature (°C)	Reference sample	Catalyst Trial sample 1	Catalyst Trial sample 2
20	30.6	39.4	-
30	-	-	-
40	-	-	18.5
50	-	-	-
60	16	15.3	17.9
70	8	9.4	14.9
80	8.9	9.9	7.7
90	3.7	-	5.4
100	8.6	-	1.1
110	5.5	1.3	1.1

The results indicated that four groups of fractions could be selectively removed from a sample and the bulk of the sample recombined. The 20 °C - 40 °C, 60 °C, 80 °C and 100 °C fractions were identified as fractions with distinct comonomer content which could be removed. The TREF experiment was performed in the following manner in order to collect the specific fractions. All other fractions were recombined to form the bulk recombined material. The 20 °C - 40 °C fraction was obtained by collecting all material that eluted from 20 °C up until 40 °C. The 60 °C fraction was obtained by collecting all material that eluted from 57 °C up until 60 °C. The 80 °C fraction was obtained by collecting all material that eluted from 77 °C up until 80 °C. The 100 °C fraction was obtained by collecting all material that eluted from 97 °C up until 100 °C.

CRYSTAF, DSC and ¹³C NMR results all indicate that the catalyst trial sample 2 is more crystalline than reference sample and the catalyst trial sample 1. Catalyst trial sample 2 has the lower amount of cocatalyst in comparison to the reference sample. Studies have been conducted on catalyst systems used in the polyethylene polymerisation environment [6, 10 and 11]. The effect of the catalyst - cocatalyst interactions have also been studied in detail [12 -18]. The type, concentration and combination of cocatalysts strongly influence the overall catalyst activity and final product crystallinity. Research conducted by Kojah *et al* showed that an increase in cocatalyst concentration decreased the number average molecular weight and decreased the melting point of the final product [12]. The type of cocatalyst has an effect on the number average molecular weight and molecular weight distribution. In particular, mixtures of cocatalyst increase catalyst activity. The exact

mechanism of active site formation, resulting in an increase in the catalyst activity and corresponding increase in the crystallinity is given in Figure 4.11.

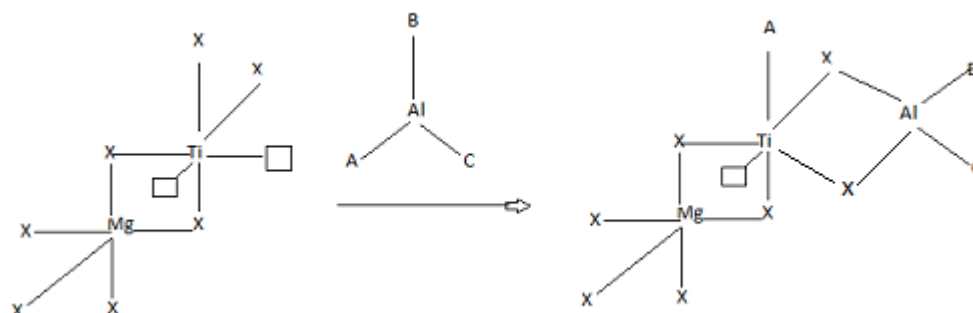


Figure 4.11: Suggested mechanism for active site formation activated by alkyl aluminium type (X: -Cl, A, B or C; ethyl, n-hexyl or Cl) [12]

The mechanism of active site formation is related to the reducing ability of the cocatalyst towards the catalyst.

4.2 Characterisation of bulk material recombined with fractions removed

4.2.1 TREF Analysis: Removal of TREF fractions

For the fractionation removal and bulk recombination experiments, selected fractions were removed from the sample after the completion of a TREF run. For the four selected fractions which were identified to be removed, four samples of the selective LLDPE sample had to be fractionated by TREF. From each sample a single fraction was removed, and the remainder of the material recombined and analyzed. The removed fractions were characterised by the NMR, DSC, SEC and PALS techniques.

4.2.1.1 TREF Analysis

The weight distribution for the selected fractions for the reference sample, catalyst trial sample 1 and catalyst trial sample 2 are indicated in Table 4.11. The various fractions that were removed have varying weight percentages. This needs to be taken into account during the comparative study.

Table 4.11: Weight percentages of selected fractions removed for the reference case sample, catalyst trial sample 1 and catalyst trial sample 2

Temperature of fraction removed (°C)	Weight percentage (wi %) of fractions		
	Reference sample	Catalyst Trial sample 1	Catalyst Trial sample 2
20 - 40	22.9	12	4.8
57 - 60	9.8	9.2	7.6
77 - 80	31.7	31.7	17.3
97 -100	24.1	24.1	30.7

4.2.2 Molecular weight and dispersity index distribution

The molecular weight and dispersity index of the bulk recombined samples with the selected fractions that are removed are shown in Table 4.12, Table 4.13 and Table 4.14 respectively. A general decrease in the molecular weight and a decrease in the dispersity index for the bulk recombined material have been observed for the higher temperature fractions that were removed.

Table 4.12: Molecular weight distributions for the reference sample

Temperature of fraction removed (°C)	Recombined reference sample upon fraction removal		
	Mn (g/mol)	Mw (g/mol)	DI
20 - 40	42000	145200	3.5
57 - 60	39800	135200	3.4
77- 80	19000	727000	3.8
97 -100	26900	102000	3.8

Table 4.13: Molecular weight distributions for the catalyst trial sample 1

Recombined catalyst trial sample 1 upon fraction removal			
Temperature of fraction removed (°C)	Mn (g/mol)	Mw (g/mol)	DI
20 - 40	43600	223600	5.2
57 - 60	43600	181200	4.2
77 - 80	32700	141100	4.3
97 -100	29200	143500	4.9

Table 4.14: Molecular weight distributions for the catalyst trial sample 2

Recombined catalyst trial sample 2 upon fraction removal			
Temperature of fraction removed (°C)	Mn (g/mol)	Mw (g/mol)	DI
20 - 40	44000	159200	3.6
57 - 60	28400	97600	3.4
77 - 80	28880	139700	4.8
97 -100	26100	109000	4.2

4.2.3 Crystallinity and comonomer content

The crystallinity and comonomer content of the reference sample, catalyst trial sample 1 and catalyst trial sample 2 are shown in Table 4.15, Table 4.16 and Table 4.17 respectively. The general trend that is observed for all the samples is an overall decrease in the crystallinity of the bulk recombined material as highly crystalline fractions are removed. This trend can be explained by the corresponding comonomer content, highly crystalline fractions have a low comonomer content, as these fractions are removed, the bulk of the material recombined shows a higher comonomer content. There is a general correlation between the comonomer content and crystallinity. Upon fraction removal and bulk recombination, all of the LLDPE samples show similar crystalline behaviour.

Table 4.15: Comonomer content of reference sample fractions and bulk recombined material

Temperature of fraction removed (°C)	Comonomer % of fraction removed	Comonomer % of recombined material	Crystallinity of fraction removed (%)	Crystallinity of bulk recombined material (%)
20 - 40	30.6	3.3	14.9	46.5
57 - 60	16	19	18.9	42.3
77 - 80	8.9	12.7	30.8	42.5
97 -100	9	14	35.3	32.5

Table 4.16: Comonomer content of catalyst trial sample 1 fractions and bulk recombined

Temperature of fraction removed (°C)	Comonomer % of fraction removed	Comonomer % of recombined material	Crystallinity of fraction removed (%)	Crystallinity of bulk recombined material (%)
20 - 40	18.5	21.1	6.1	29.9
57 - 60	17.9	25.6	17	28.1
77 - 80	7.7	25.9	9.6	23.2
97 -100	1.1	14.9	25.6	27.8

Table 4.17: Comonomer content of catalyst trial sample 2 fractions and bulk recombined

Temperature of fraction removed (°C)	Comonomer % of fraction removed	Comonomer % of recombined material	Crystallinity of fraction removed (%)	Crystallinity of bulk recombined material (%)
20 - 40	39.4	19.5	12.3	28.4
57 - 60	15.3	21.8	12.8	24.4
77 - 80	9.9	17.1	13.9	25.3
97 -100	1.3	9.6	21.7	15.6

4.2.4 Crystallinity and melting

The crystallinity and melting temperature of the samples were determined by DSC. The percentage crystallinity for the fractions that were removed for the reference sample, catalyst trial sample 1 and catalyst trial sample 2 are indicated below in Table 4.18, Table 4.19 and Table 4.20. For the catalyst trial sample 2, not enough material of the 20 °C - 40 °C fraction was available to perform a DSC analysis and no result is shown.

Table 4.18: DSC data of fractions removed for the reference sample

Temperature of fraction removed (°C)	T _m (°C)	H _m (J/g)	% Crystallinity
20 - 40	101.2	43.6	14.9
57 - 60	96.2	55.6	18.9
77 - 80	114.3	90.3	30.8
97 -100	127.5	103.4	35.3

Table 4.19: DSC data of fractions removed for the catalyst trial sample 1

Temperature of fraction removed (°C)	T _m (°C)	H _m (J/g)	% Crystallinity
20 - 40	82.1	17.9	6.13
57 - 60	99.5	49.8	17
77 - 80	95.8	28.2	9.64
97 -100	123.3	75.1	25.6

Table 4.20: DSC data of fractions removed for the catalyst trial sample 2

Temperature of fraction removed (°C)	T _m (°C)	H _m (J/g)	% Crystallinity
20 - 40	-	-	-
57 - 60	100.7	37.5	12.8
77 - 80	106.3	40.8	13.9
97 -100	122.9	63.8	21.7

The crystallinity of the recombined material is shown in Figure 4.12. The data indicates that as more highly crystalline fractions are removed, there is a decrease in the total crystallinity of the bulk recombined material.

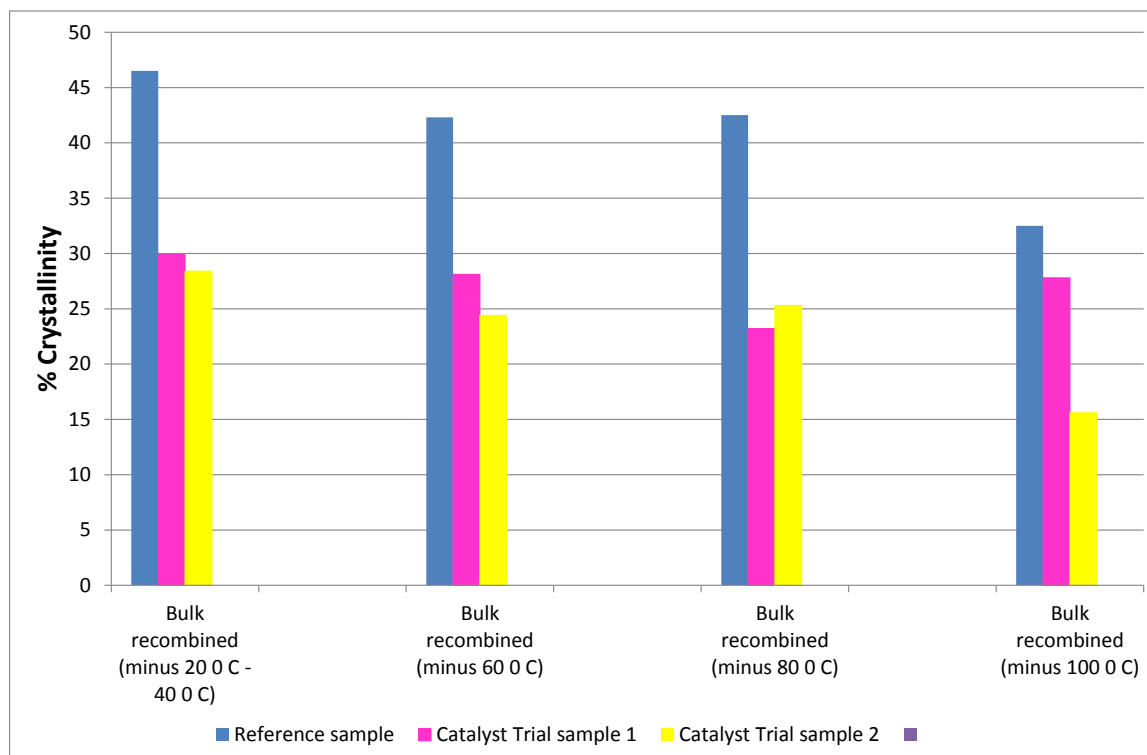


Figure 4.12: % Crystallinity of recombined material with selective fractions removed

This trend indicating the decrease in crystallinity of the total bulk recombined material upon the removal of highly crystalline fractions has been previously demonstrated in literature [19 - 21]. TREF studies have shown that highly crystalline material elutes at high temperature and that amorphous material is eluted at low temperature ranges [3, 22]. This is expected since at high TREF fractionation temperatures, the more easily the chains can crystallise from the solution as a result of a higher level of order in the polymer chains leading to the more perfect crystallites. There is a strong correlation between comonomer content and crystallinity. Removing low temperature fractions from the bulk of the polymer has a much less significant effect on the total crystallinity of the polymer than removing the highly crystalline fractions. The low temperature fractions have more short chain branches and the removal of these fractions results in an increase in the overall crystallinity of the bulk recombined material. This is attributed to the fact that there are less side chains that could impede crystallisation. Similarly the high temperature fractions have less short chain branches and are more highly crystalline. The removal of these highly crystalline fractions result in the overall decrease of the crystallinity of the bulk recombined material.

4.2.5 Free volume analysis

The theoretical and experimental principles of the novel analytical technique of Positron Annihilation lifetime spectroscopy (PALS) has been described in detail in chapter 2 and chapter 3 respectively. Several experimental and theoretical studies have been conducted to directly measure the free volume hole sizes in semi crystalline polymers [23 - 27].

The total free volume or mean hole size in the amorphous and crystalline regions has been determined using the Positron Annihilation lifetime spectroscopic technique (PALS). Previous work conducted by Sweed *et al* showed that the positron annihilation parameters change due to differences in the comonomer length and comonomer content [21]. Studies showed that a four lifetime component gave the best fit to raw positron lifetime data. The longest lifetime components designated as τ_3 and τ_4 represent the annihilation of the longer lived o-Ps localized within the open spaces in the polymer. The τ_3 lifetime interval is associated with the annihilation of the o-Ps in the crystalline regions (interface and/or defects) of the polymer. The τ_4 lifetime interval is associated with the annihilation of the o-Ps in the amorphous regions of the polymer. Both the τ_3 and τ_4 lifetime intervals were measured to determine the free volume in the crystalline regions and amorphous regions in the polymer samples.

4.2.5.1 Free volume analysis of the bulk samples

The free volume was measured for the bulk recombined material without the selective fractions for the reference sample, catalyst trial sample 1 and catalyst trial sample 2. The data showing the τ_3 and τ_4 values for the bulk samples are is shown in Table 4.21.

Table 4.21: PALS data for reference sample, catalyst trial sample 1 and catalyst trial sample 2

Sample	$\tau_3 \pm \Delta \tau_3$ (ns)	$I_3 \pm I_3$ (%)	$\tau_4 \pm \Delta \tau_4$ (ns)	$I_4 \pm I_4$ (%)
Reference sample	1.1 ± 0.19	7.0 ± 0.79	2.6 ± 0.5	22.0 ± 1.3
Catalyst Trial sample 1	1.2 ± 0.22	6.5 ± 0.93	2.8 ± 0.08	21.0 ± 1.9
Catalyst Trial sample 2	1.3 ± 0.23	8.0 ± 1.39	2.7 ± 0.06	21.5 ± 1.5

The data indicates a larger τ_3 and τ_4 value in the catalyst trial sample 1 in comparison to the catalyst trial sample 2 and the reference sample. In comparison to the catalyst trial sample 2, the reference sample shows the lowest values.

The comonomer content of the sample is the short chain branching content of the sample. The general tendency is that as the amount of short chain branching increases, there is an increase in free volume (space) in the molecular structure. This would be indicated by an increase in the amount in the τ_4 values associated with the free volume in the amorphous regions of the material. Free volume analysis for the bulk recombined material with the fractions removed for the reference sample was also conducted. The free volume analysis indicate a general increase in the τ_3 lifetime and τ_4 lifetime. As more crystalline material was removed, the total crystallinity of the bulk recombined material decreased.

4.2.5.2 Free volume analysis of the bulk recombined material

The free volume analysis of the bulk recombined samples with the selected fractions that are removed are shown in Table 4.22, Table 4.23 and Table 4.24 respectively.

Table 4.22: PALS data for the reference sample recombined with selected fractions removed

Temperature of fraction removed (°C)	$\tau_3 \pm \Delta \tau_3$ (ns)	$I_3 \pm I_3$ (%)	$\tau_4 \pm \Delta \tau_4$ (ns)	$I_4 \pm I_4$ (%)
20 - 40	1.32 ± 0.15	0.9 ± 1.1	2.81 ± 0.08	15.5 ± 1.5
57 - 60	1.21 ± 0.13	8.3 ± 0.6	2.91 ± 0.57	18.8 ± 1.0
77 - 80	1.13 ± 0.13	8.0 ± 0.6	2.85 ± 0.05	17.7 ± 0.9
97 -100	1.51 ± 0.23	9.9 ± 2.0	2.96 ± 0.15	16.7 ± 2.9

The free volume analysis of the bulk recombined material with the selected fractions removed for the catalyst trial sample 1 is shown in Table 4.23

Table 4.23: PALS data for the catalyst trial sample 1 recombined with selected fractions removed

Temperature of fraction removed (°C)	$\tau_3 \pm \Delta \tau_3$ (ns)	$I_3 \pm I_3$ (%)	$\tau_4 \pm \Delta \tau_4$ (ns)	$I_4 \pm I_4$ (%)
20 - 40	0.85 ± 0.14	6.5 ± 1.1	2.68 ± 0.03	19.5 ± 0.6
57 - 60	1.29 ± 0.22	6.6 ± 1.1	2.83 ± 0.67	20.6 ± 1.5
77 - 80	1.34 ± 0.16	8.4 ± 0.8	3.12 ± 0.06	20.7 ± 1.1
97 -100	1.2 ± 0.23	7.0 ± 0.9	2.95 ± 0.07	22.7 ± 4.0

The free volume analysis of the bulk recombined material with the selected fractions removed for the catalyst trial sample 2 is shown in Table 4.24

Table 4.24: PALS data for the catalyst trial sample 2 recombined with selected fractions removed

Temperature of fraction removed (°C)	$\tau_3 \pm \Delta \tau_3$ (ns)	$I_3 \pm I_3$ (%)	$\tau_4 \pm \Delta \tau_4$ (ns)	$I_4 \pm I_4$ (%)
20 - 40	1.12 ± 0.16	5.5 ± 0.5	2.81 ± 0.06	13.2 ± 0.8
57 - 60	1.27 ± 0.14	8.0 ± 0.7	2.95 ± 0.07	15.0 ± 0.10
77 - 80	1.12 ± 0.17	7.9 ± 0.7	2.98 ± 0.06	21.1 ± 1.1
97 -100	1.78 ± 0.26	11.4 ± 3.6	3.20 ± 0.23	14.9 ± 4.0

Free volume analyses of the bulk recombined material with the selective fractions removed for the reference sample, catalyst trial sample 1 and catalyst trial sample 2 all show that as the highly crystalline fractions are removed from the bulk material, there is a general increase in the free volume in the crystalline region and the amorphous regions.

4.2.6 Hardness analysis analysis

Hardness studies conducted on the Micro hardness tester with UHL VMHT instrument are indicated in Table 4.25.

Table 4.25: Micro hardness results of bulk LLDPE samples

Sample	Hardness (HV)
Reference sample	24
Catalyst Trial sample 1	13
Catalyst Trial sample 2	31

The results from the hardness analysis are consistent with the crystallinity trends indicated by the CRYSTAF, DSC, ¹³C NMR and PALS analyses. The results indicate that the catalyst trial sample 2 with the low amount of comonomer is the most crystalline sample in comparison to the reference sample and catalyst trial sample 1.

Hardness studies were also conducted on the bulk recombined samples with the crystalline fractions removed. The results are indicated in Table 4.26. The results indicate that there is

an observed decrease in the hardness levels or mechanical strength of the bulk recombined material as the more highly crystalline fractions are removed. The mechanical data further supports the common trend of the results shown by the other analytical techniques.

Table 4.26: Micro hardness results of the bulk recombined LLDPE samples with selective fractions removed

Reference sample		Catalyst Trial sample 1		Catalyst Trial sample 2	
Temperature of fraction removed (°C)	Hardness (HV)	Temperature of fraction removed (°C)	Hardness (HV)	Temperature of fraction removed (°C)	Hardness (HV)
20 - 40	29	20 - 40	66	20 - 40	34
57 - 60	20	57 - 60	29	57 - 60	23
77 - 80	15	77 - 80	5.1	77 - 80	12
97 -100	10	97 -100	-	97 -100	5.2

It is to be noted that due to the amorphous nature of the bulk recombined material specifically for the catalyst trial sample 1, a smooth surface could not be obtained for the focusing of the microscope to make an indentation. Hence a hardness value could not be obtained for the bulk recombined sample with the 100 °C fraction removed.

4.3 References

1. B. Monrabel, Temperature rising elution fractionation and Crystallisation analysis fractionation. Encyclopaedia of analytical chemistry. 2000. p:8074 – 8084.
2. J.T. Xu, X.R. XY, L.S. Chen and L.X Feng, Effect of short chain branching distribution on crystallisation of ethylene-butene copolymers, Journal of Materials science letters 19, 2000, p:1541- 1543.
3. P. Starck, Studies of the comonomer distributions in low density Polyethylenes using temperature rising elution fractionation and stepwise crystallisation by DSC, Polymer international journal, 40, No 2. 1996.
4. M.Y Keating, E.F McCord, Evaluation of comonomer distribution in ethylene copolymers using DSC fractionation, Thermochemica Acta, 243, Issue 2, 15 September 1994, p:129 -145.

5. M. R Nouri, Studies of comonomer distributions and molecular segregations in metallocene prepared polyethylenes by DSC, 25, Issue 8, December 2006, p:1052 - 1058.
6. L. Wild, Temperature rising elution fractionation, *Advances in Polymer science journal*, 98, 1990, p: 1 - 47
7. H. J Assumption, J.P Vermeulen, W. L Jarrett, L.J Mathias, A. J van Reenen, High resolution solution and solid state NMR characterisation of ethylene/1-butene and ethylene/1-hexene copolymers fractionated by preparative temperature rising elution fractionation, *Journal of polymer science, Part A: Polymer chemistry*, 47, 2006, 67 - 74.
8. C. S Yannoni, High resolution NMR in Solids: The CPMAS Experiment, *Journal of American chemical society*, 1982, 15, 201 – 208.
9. K. Kuwabara, H. Kaji, M. Tsuji and F. Horii, Crystalline-noncrystalline structure and chain diffusion associated with 180° Flip motion for Polyethylene single crystals as revealed by solid state ^{13}C NMR Analyses, *Journal of Macromolecules*, 2000, 33, 7093 - 7100.
10. E. Puhakka, T. Pakkanen, T.A Pakkanen and E. Iiskola, Theoretical investigations on Ziegler-Natta catalysis: models for the cocatalyst components, *Journal of organometallic chemistry* 511 (1996) 19 – 27.
11. R. Mulhaupt, Catalytic Polymerisation and the post polymerisation catalysis fifty years after the discovery of Ziegler's Catalysts, *Journal of macromolecular chemistry and physics*, 2003, 204, 289 – 327.
12. S. Kojoh, M. Kioka and N. Kashiwa, The influences of cocatalyst on propylene polymerisation at high temperature with an MgCl_2 -supported TiCl_4 catalyst system, *European polymer journal* 35 (1999) 751 – 755.
13. N.Senso, S. Khaubunsongserm, B. Jongsomjit and P. Praserttham, The influence of mixed activators on ethylene polymerisation and ethylene-1-hexene copolymerisation with silica supported Ziegler- Natta catalyst, *Open access molecules* 2010, 15, 9323 – 9339.
14. T. Garoff, P.Waldvogel, K. Kallio, V. Eriksson, A. Aittola and E. Kokkol, Linear low density Polyethylene with a uniform or reversed comonomer composition distribution, International patent classification C08F 10/00 (2006.01), International publication number WO 2010/125022 A1, International application number PCT/EP2010/055519, International publication date, 4 November 2010.
15. S. Xia, Z. Fu, B. Huang, J. Xu and Z. Fan, Ethylene 1- hexane copolymerisation with MgCl_2 supported Ziegler- Natta catalysts containing aryloxy ligands. Part 1: Catalysts

- prepared by immobilizing $TiCl_3(OAr)$ onto $MgCl_2$ in batch reaction. *Journal of molecular catalysis A: Chemical* 355 (2012) 161 – 167.
16. S. Matui, T. Fujita, FI catalysts: super active new ethylene polymerisation catalysts, *Journal of catalysis today* 66 (2001) 63 – 73.
 17. Q. Wang, Y. Lin, Z. Zhang, B. Liu and M. Terano, High temperature polymerisation of propylene catalyzed by $MgCl_2$ supported Ziegler-Natta catalyst with various cocatalysts, *Journal of applied polymer science*, Vol 100, 1978- 1982 (2006).
 18. B. Liu, T. Nitta, H. Nakatani and M. Terano, Specific roles of Al- Alkyl cocatalyst in the origin of Isospecificity of active sites on donor- free $TiCl_4/MgCl_2$ Ziegler- Natta catalyst, *Journal of macromolecular chemistry and physics*, 2002, 203, 2412 - 2421.
 19. L. Keulder, The effect of molecular composition on the properties of linear low density polyethylene, MSc thesis, University of Stellenbosch, March 2008.
 20. G. W Harding, The structure property relationship of polyolefins, PhD thesis, University of Stellenbosch, March 2009.
 21. M. Sweed, Free volume properties of semi-crystalline polymers, PhD Thesis, University of Stellenbosch, March 2011.
 22. S. Anantawaraskul, J.B.P Soares, P.M. Wood- Adams, The effect of operation parameters on TREF fractionation and Crystallisation analysis fractionation, *Journal of Polymer science: Part B: Polymer physics*, Vol 41, 1762 -1778 (2003).
 23. P. Hautojavri, ed, *Positrons in solids*, Springer- Verlag Berlin Heidelberg, 1979
 24. Y. Kobayashi, W. Xheng, E.F. Meyer, J.D. McGervey, A.M. Jamieson, R. Simha, *Macromolecules*, 22, 2302, 1989
 25. S. Tao, *Journal of Chemistry and Physics*, 56, 5499,1972
 26. J.R. Stevens, *Methods of experimental physics*, 16A, 371, 1980
 27. D.M. Schrader and Y. C. Jean, eds, *Positron and Positronium chemistry*, Elsevier, 1988.

CHAPTER 5

5 CONCLUSIONS

5.1 Conclusions

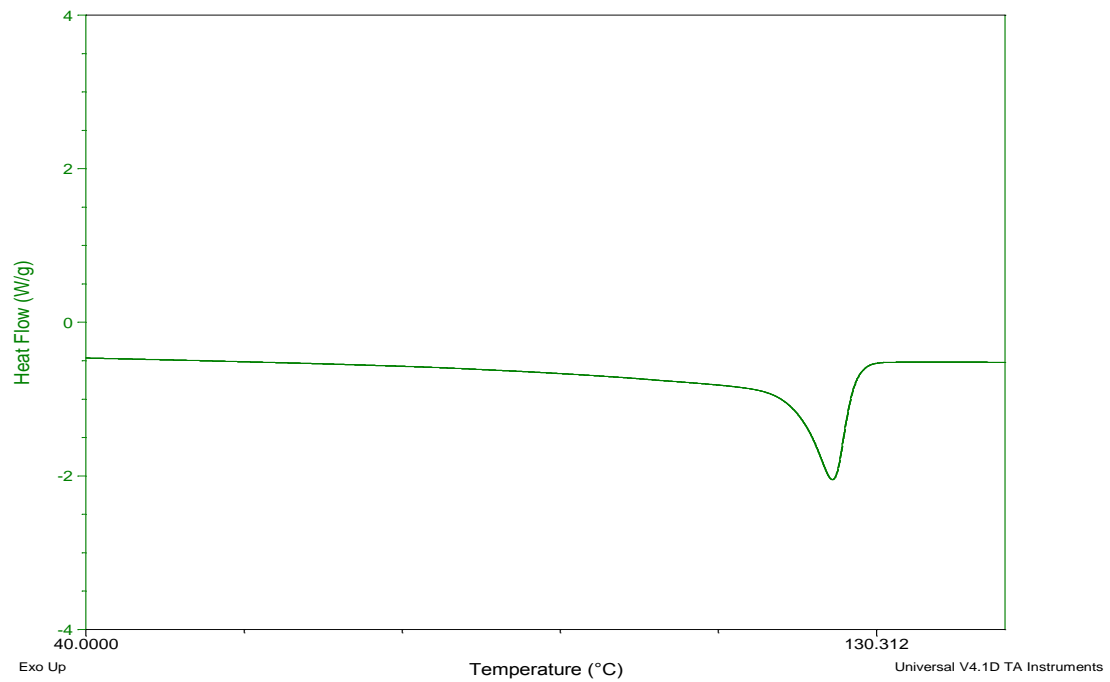
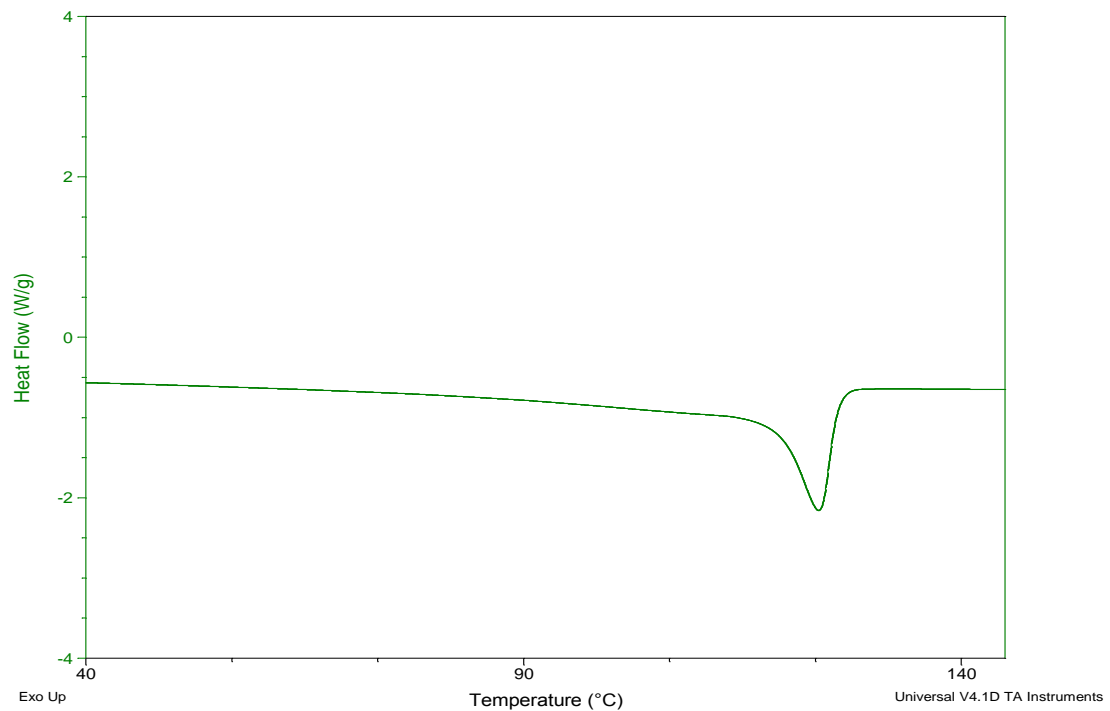
The aims of this study were to perform a characterisation study of LLDPE polymer and to compare LLDPE samples produced with changes to the catalyst system against a reference LLDPE sample produced under standard production conditions. In addition, further objectives were to ascertain whether selectively removing different polymer fractions from the bulk polymer material would result in significant changes in the product properties. The following objectives of the study were successfully achieved and can be summarised as follows:

- The bulk reference LLDPE sample, bulk catalyst trial sample 1 and bulk catalyst trial sample 2 were successfully analysed by CRYSTAF, DSC and ^{13}C NMR analytical techniques. The results indicate that the catalyst trial sample 2 is more crystalline than the reference sample and the catalyst trial sample 1. This was due to the low cocatalyst content of the catalyst trial sample 2.
- The bulk reference LLDPE sample, bulk catalyst trial sample 1 and bulk catalyst trial sample 2 were successfully fractionated using preparative TREF. The TREF results showed a broad chemical composition distribution of all of the bulk LLDPE samples. The TREF results indicated that TREF fractionates according to the ability of polymer chains to crystallise from solution and that the amount of comonomer branching influences the crystallinity. The catalyst trial samples were comparable to the reference sample.
- The individual fractions were characterised by using DSC, high temperature SEC and ^{13}C NMR. The results of DSC characterisation showed that the melting points of the TREF fractions increased with elution temperature. It was also observed that the molecular weight increases with an increase in fractionation temperature. ^{13}C NMR analyses showed a decrease in comonomer content with an increase in fractionation temperature.
- Selective fractions were successfully removed from the bulk samples and the bulk material recombined.

- DSC analysis of the bulk recombined material showed that there was an overall decrease in the total crystallinity of the bulk recombined material after removal of the highly crystalline fractions.
- PALS analysis of the bulk recombined material indicated a general increase in the τ_3 lifetime and τ_4 lifetime intervals. Free volume analysis further confirmed a decrease in crystallinity of the bulk recombined material as highly crystalline material was removed.
- Hardness studies conducted on the bulk recombined material after removal of selected crystalline fractions, indicated a decrease in the hardness levels or mechanical strength of the bulk recombined material as more highly crystalline fractions are removed.

5.2 Future work

In the current study the DMA analysis of the bulk recombined material was challenging in that the TREF technique did not generate enough bulk recombined material to fully prepare a sample for mechanical analysis on the DMA instrument. It is recommended that future studies can be focussed on mechanical studies of LLDPE polymer with hexene as copolymer, using the DMA analysis technique. It is recommended for future work that multiple TREF fractionations be performed so that sufficient mass of fractions can be generated for an extensive free volume analysis of the individual fractions by the PALS technique. The study can be further extended to investigate the chemical composition of another comonomer, for example 1 - octene of LLDPE which has not yet been researched.

Appendix A: DSC Data**Figure A 1. DSC of bulk Reference sample****Figure A 2. DSC of bulk Catalyst Trial sample 1**

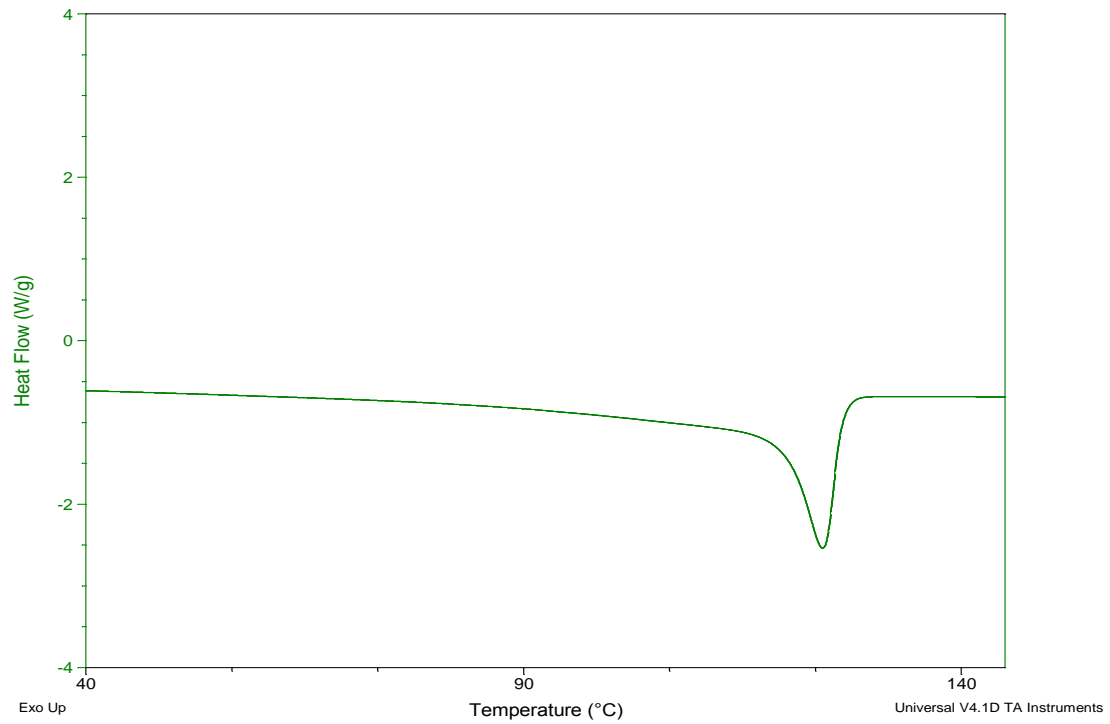


Figure A 3. DSC of bulk Catalyst Trial sample 2

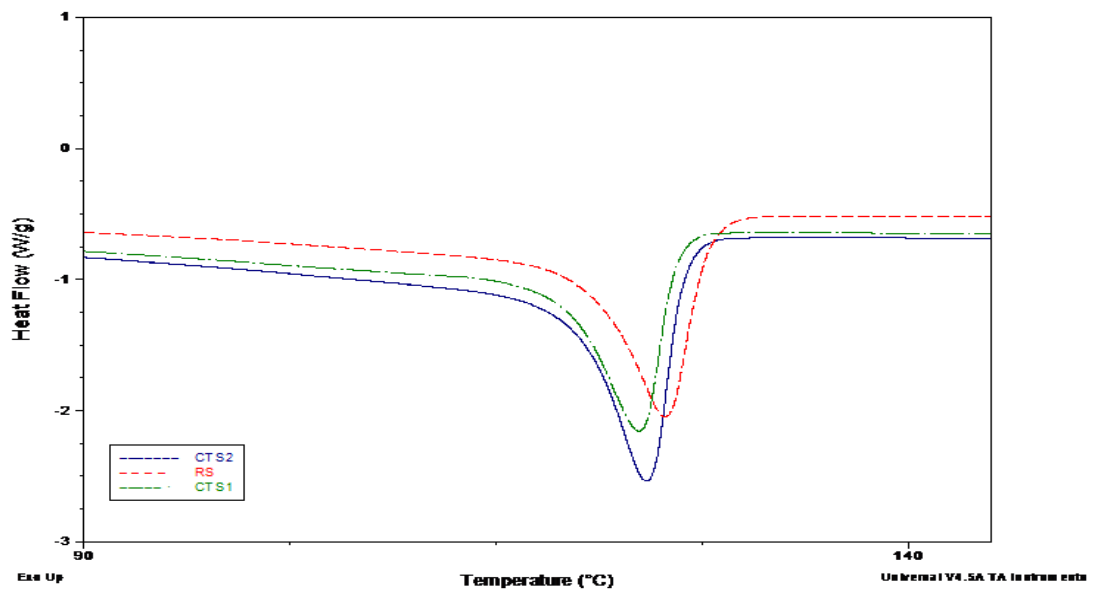


Figure A 4. Combined DSC of bulk samples RS, CTS1 and CTS2

Reference Sample Fractions

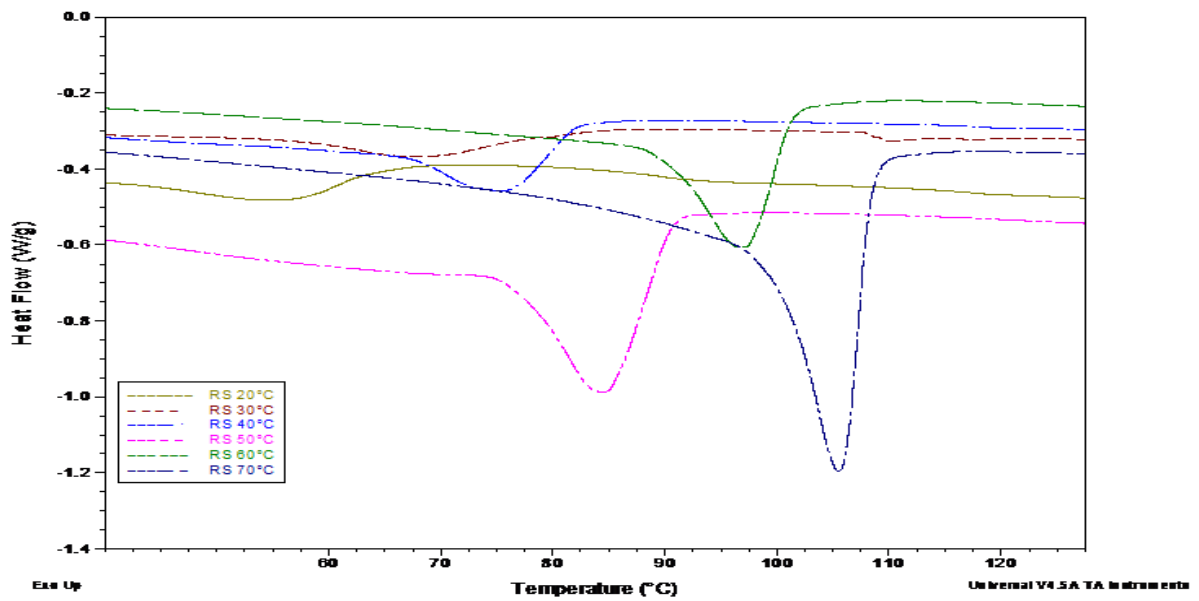


Figure A 5. DSC of Reference sample fractions (20 °C - 70 °C)

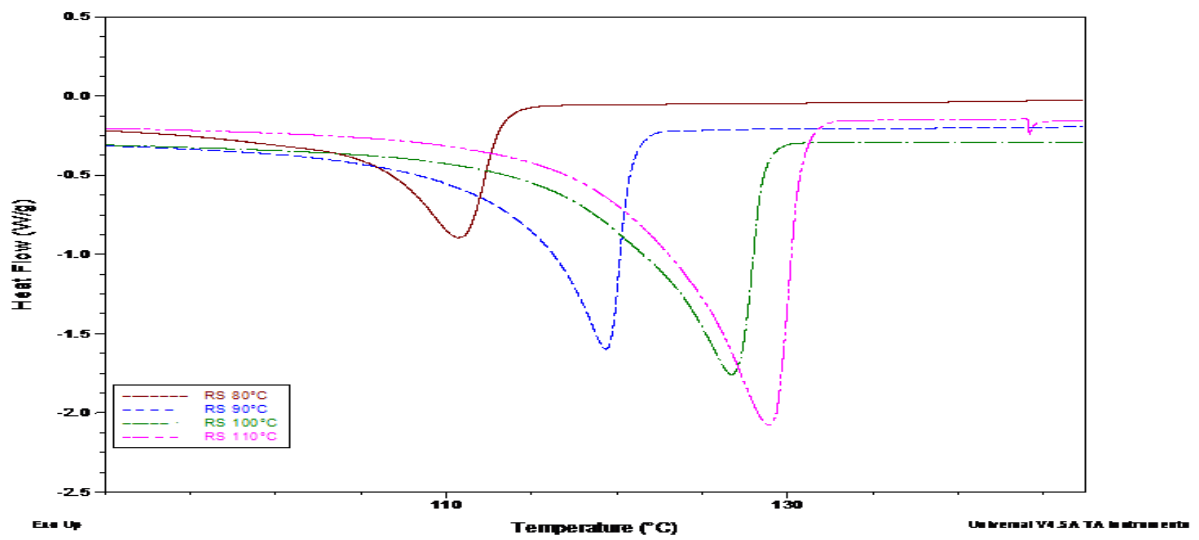


Figure A 6. DSC of Reference sample fractions (80 °C - 110 °C)

Catalyst Trial sample 1 Fractions

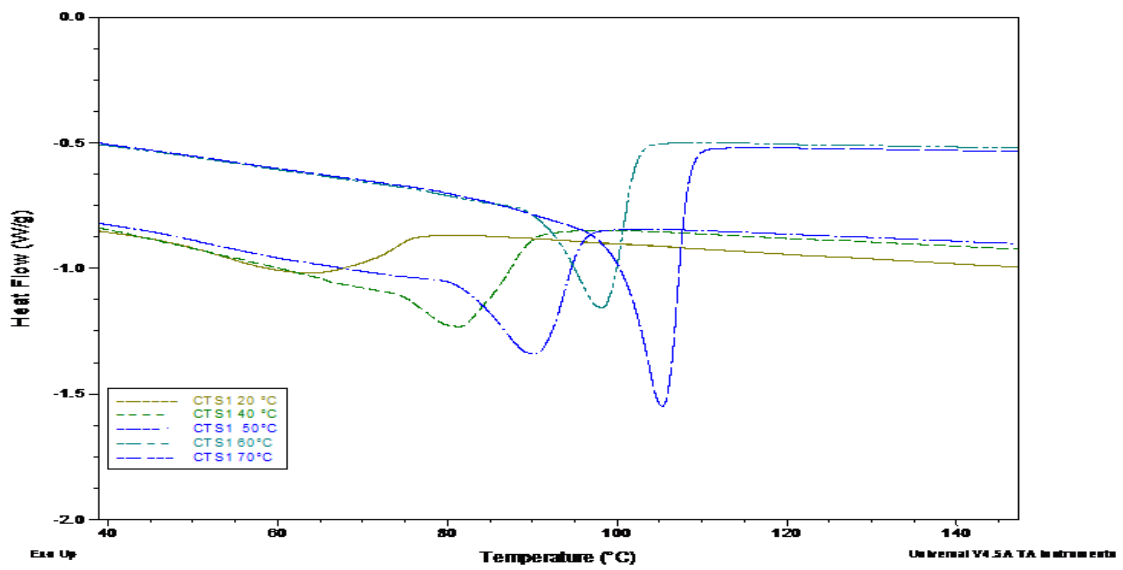


Figure A 7. DSC of catalyst trial sample 1 fractions (20 °C - 70 °C)

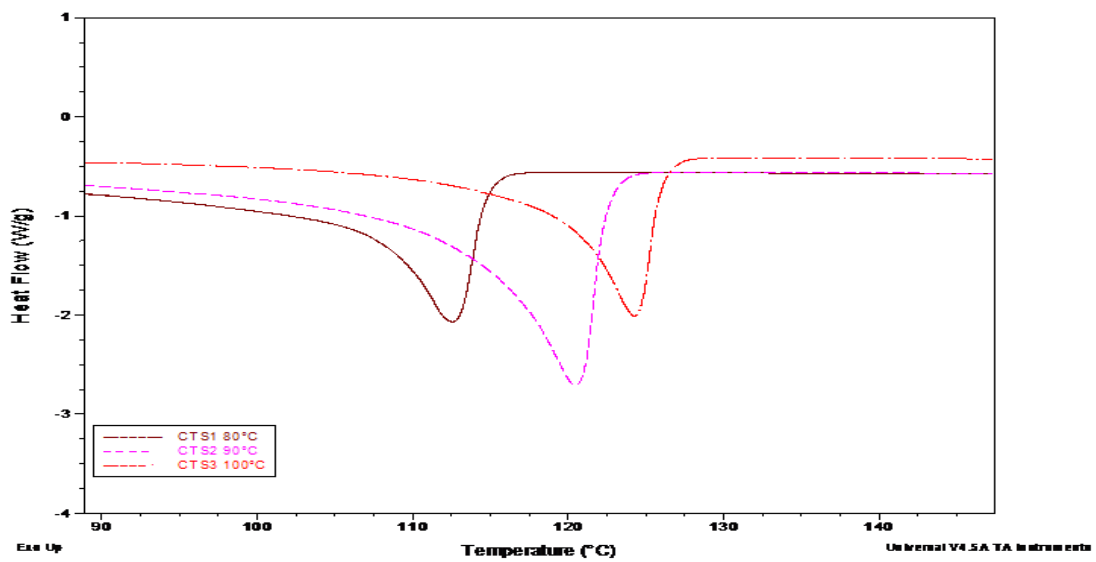


Figure A 8. DSC of catalyst trial sample 1 fractions (80 °C - 100 °C)

Catalyst Trial sample 2 Fractions

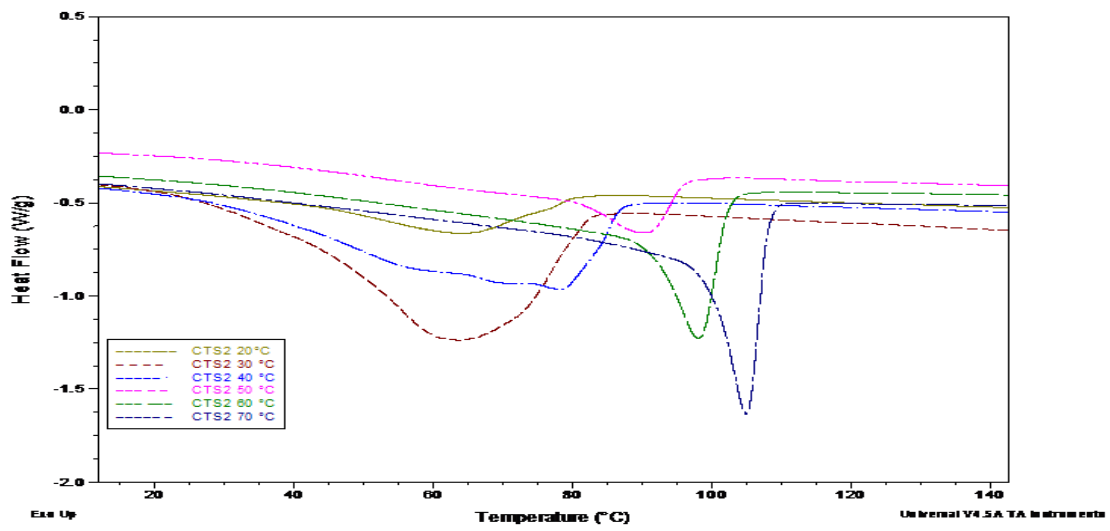


Figure A 9. DSC of catalyst trial sample 2 fractions (20 °C - 70 °C)

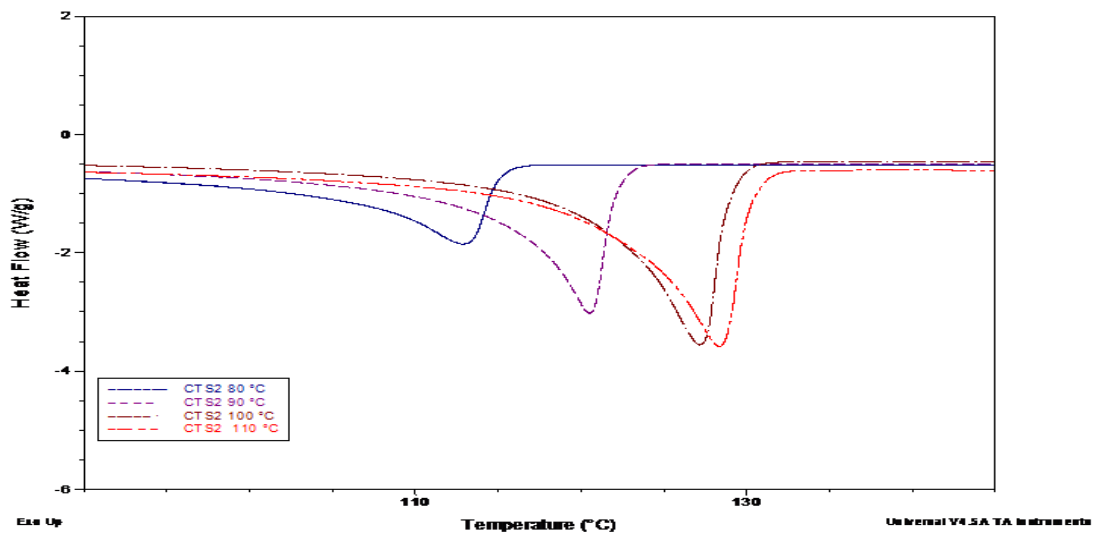


Figure A 10. DSC of catalyst trial sample 2 fractions (80 °C - 110 °C)

Appendix B: SEC Data

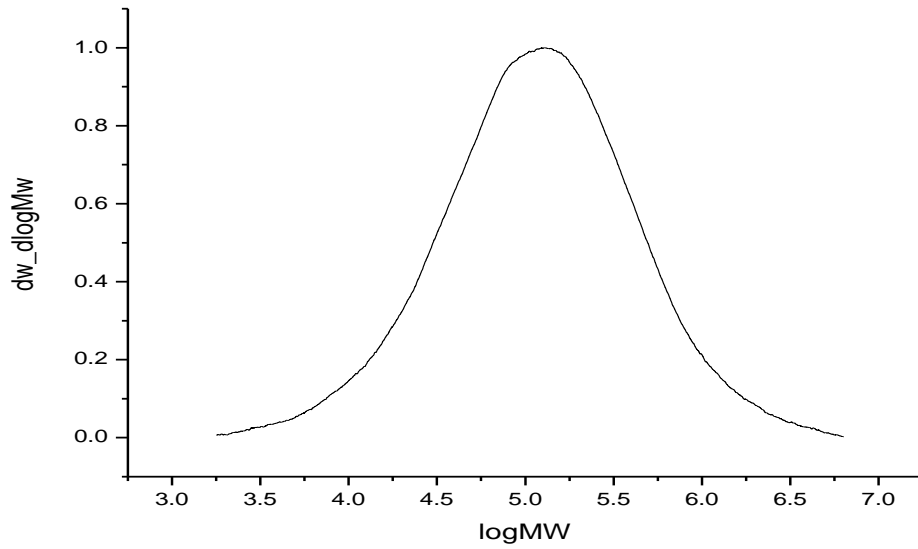


Figure B 1. SEC of bulk reference sample

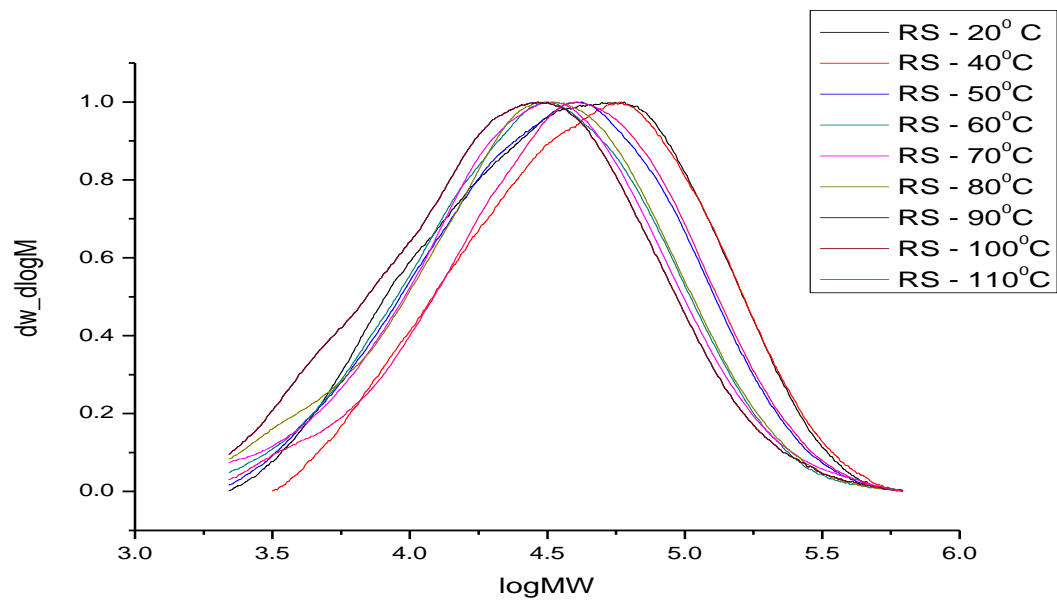


Figure B 2. SEC of reference sample fractions

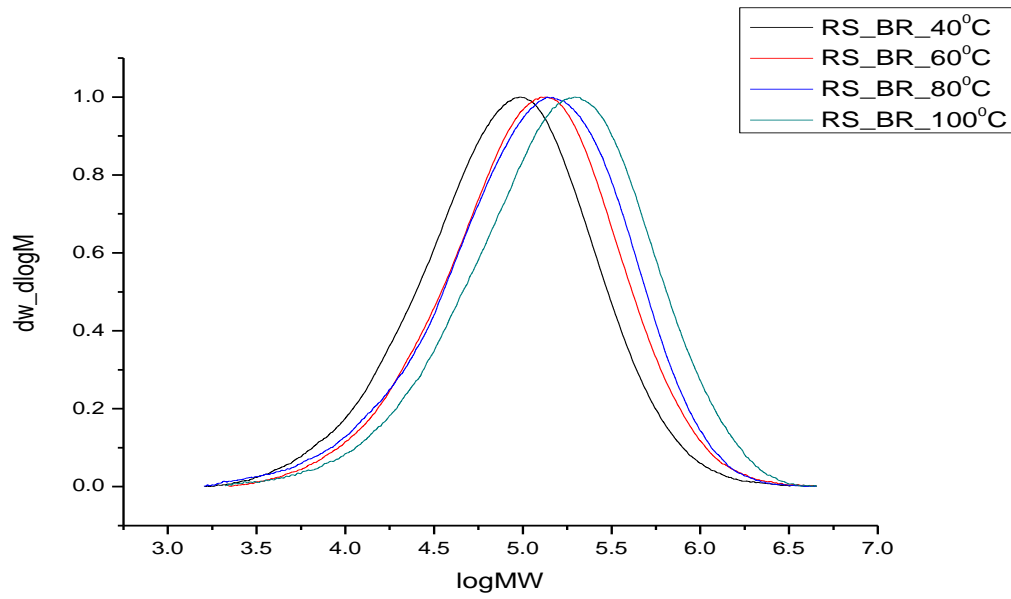


Figure B 3. SEC of reference sample bulk recombined with fractions removed

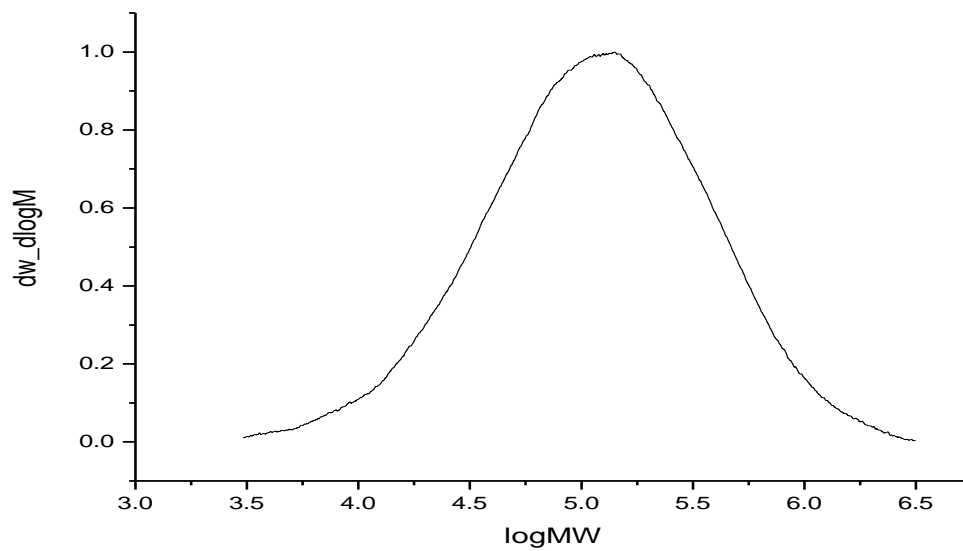


Figure B 4. SEC of bulk catalyst trial sample 1

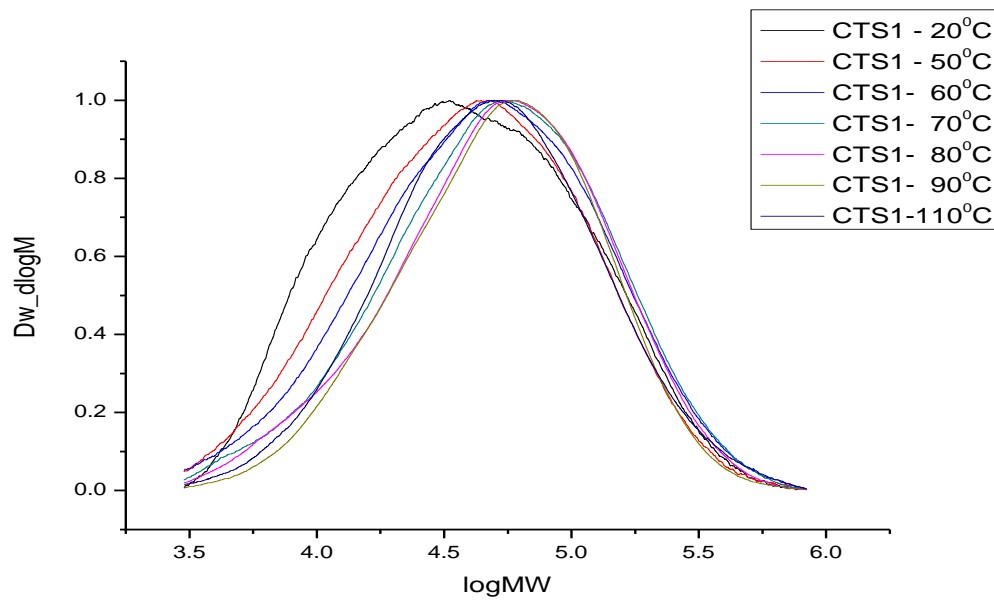


Figure B 5. SEC of catalyst trial sample 1 fractions

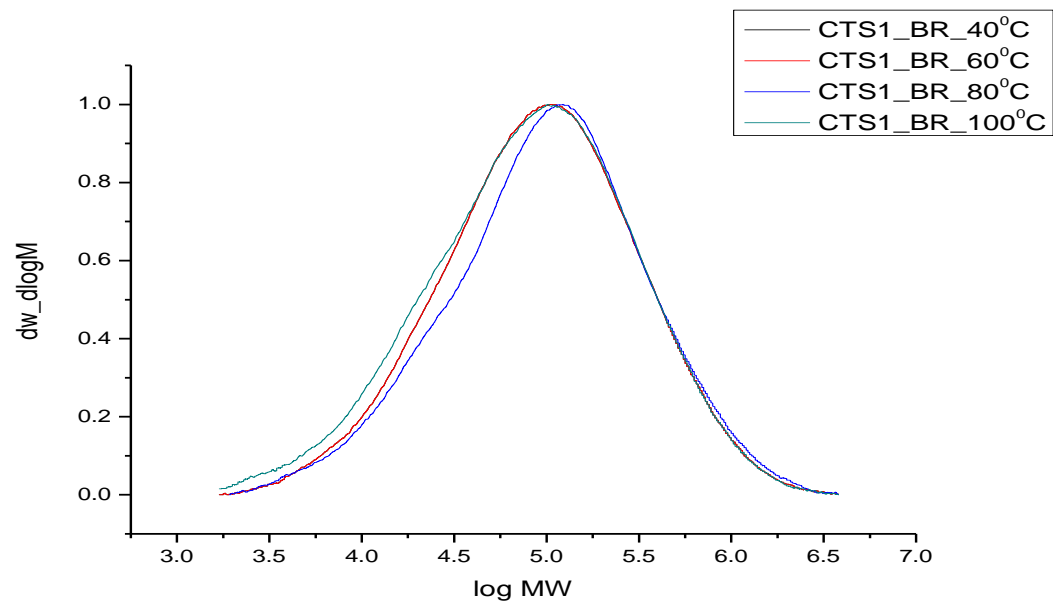
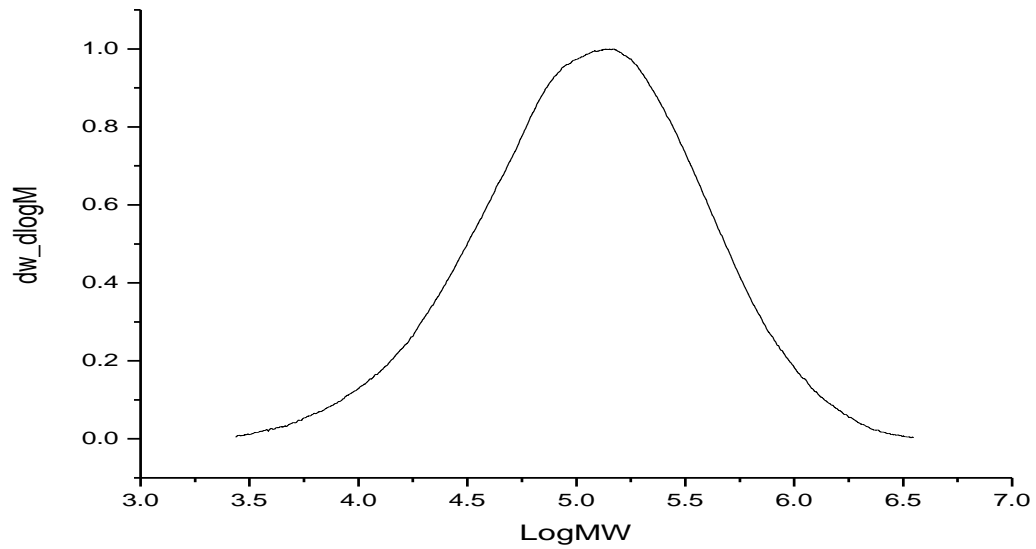
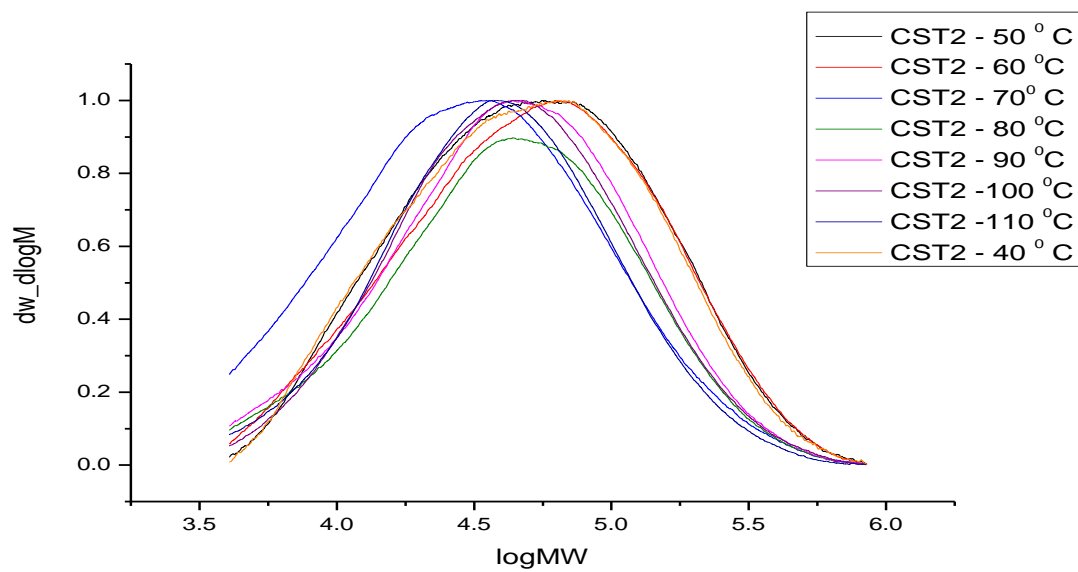


Figure B 6. SEC of catalyst trial sample 1 bulk recombined with fractions removed

**Figure B 7. SEC of bulk catalyst trial sample 2****Figure B 8. SEC of catalyst Trial 2 sample 2 fractions**

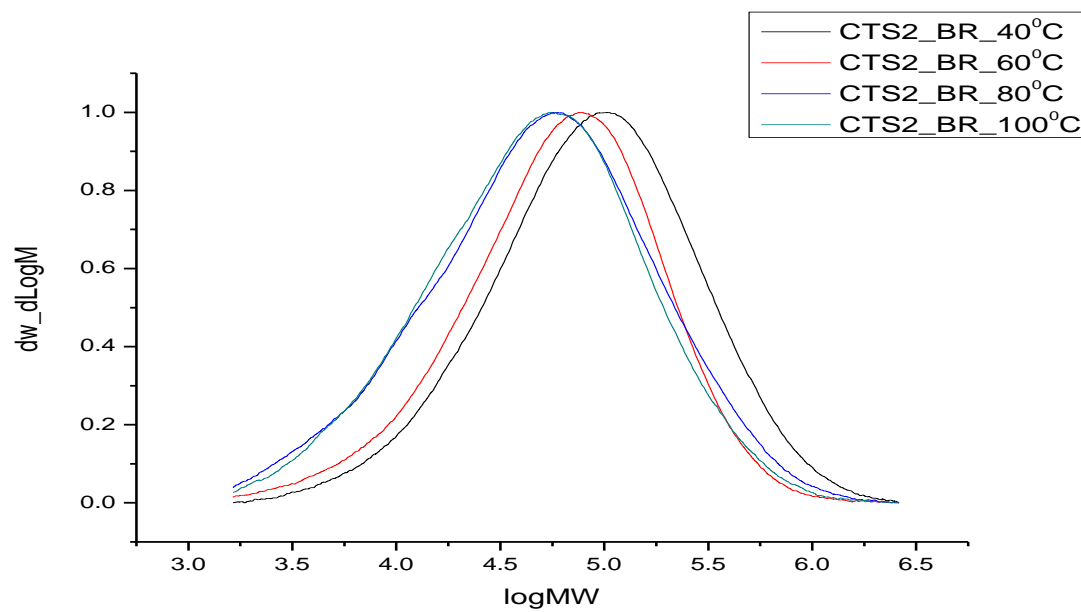
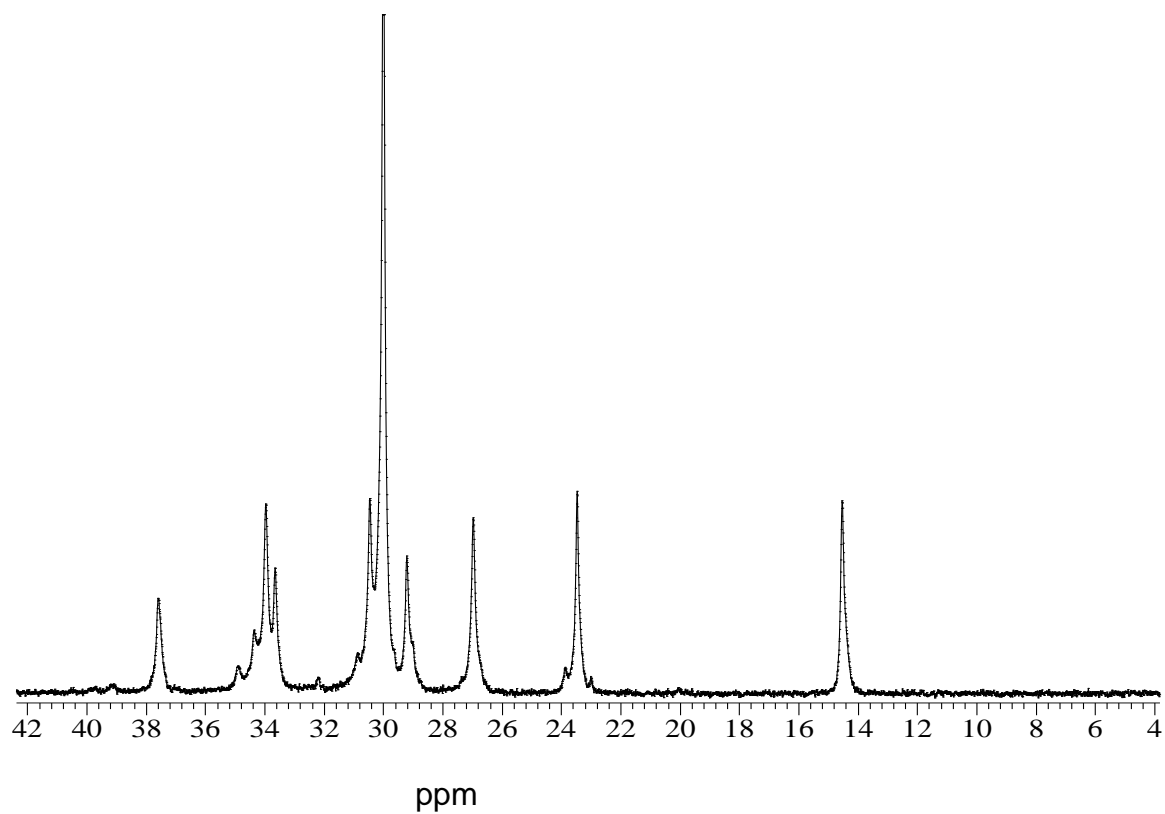
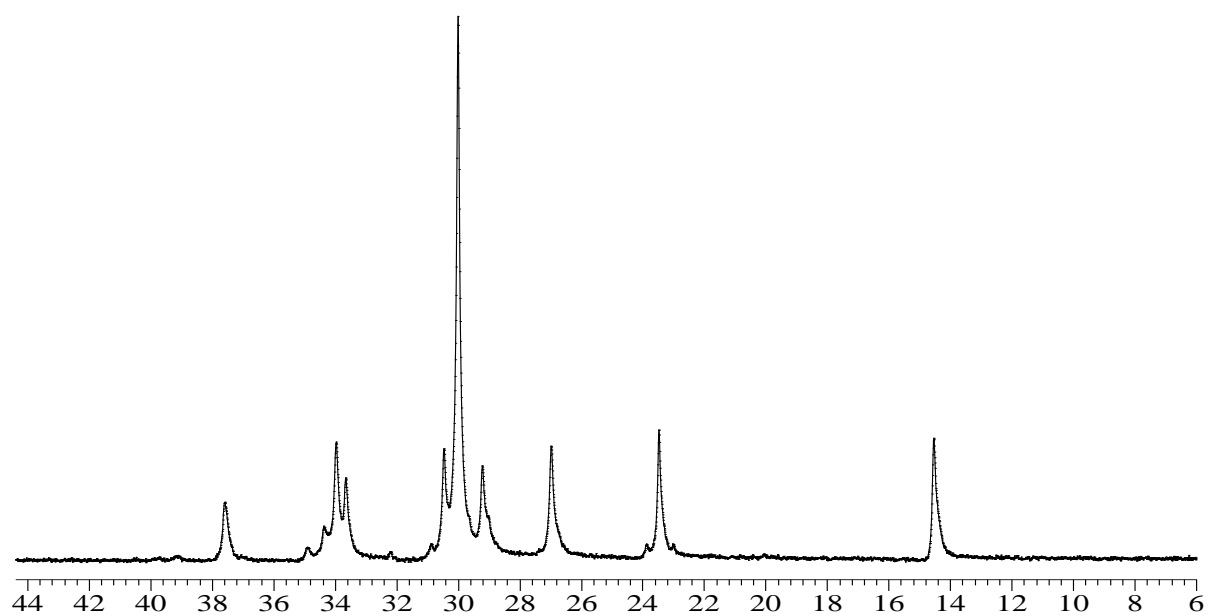


Figure B 9. SEC of catalyst trial sample 2 bulk recombined with fractions removed

Appendix C: NMR Data

Figure C1. ^{13}C NMR of bulk reference sampleFigure C2. ^{13}C NMR of 20°C ppm

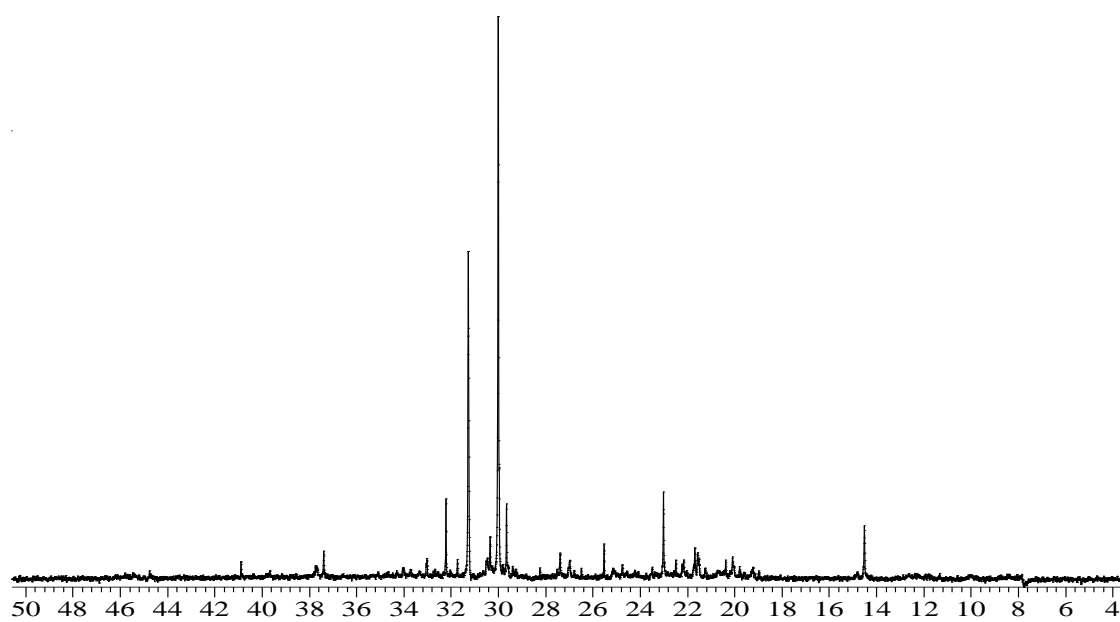


Figure C3. ^{13}C NMR of 30 $^{\circ}\text{C}$ fraction of reference sample

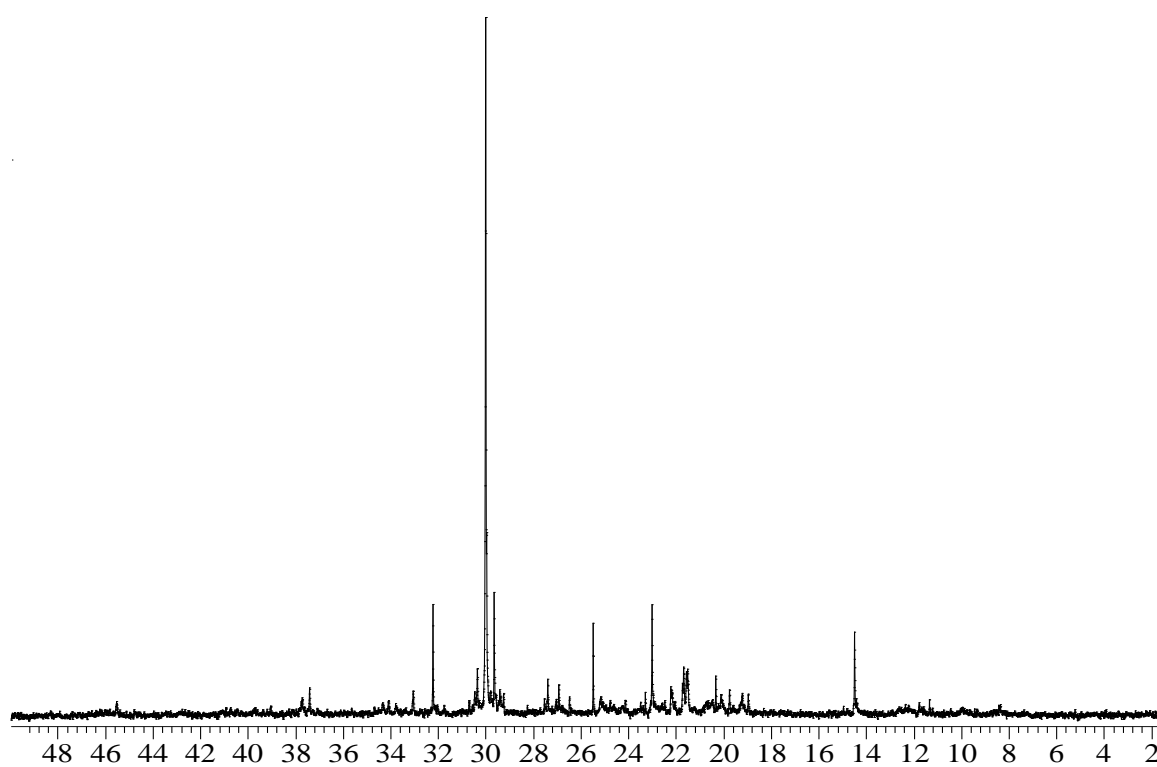


Figure C4. ^{13}C NMR of 40 $^{\circ}\text{C}$ fraction of reference sample

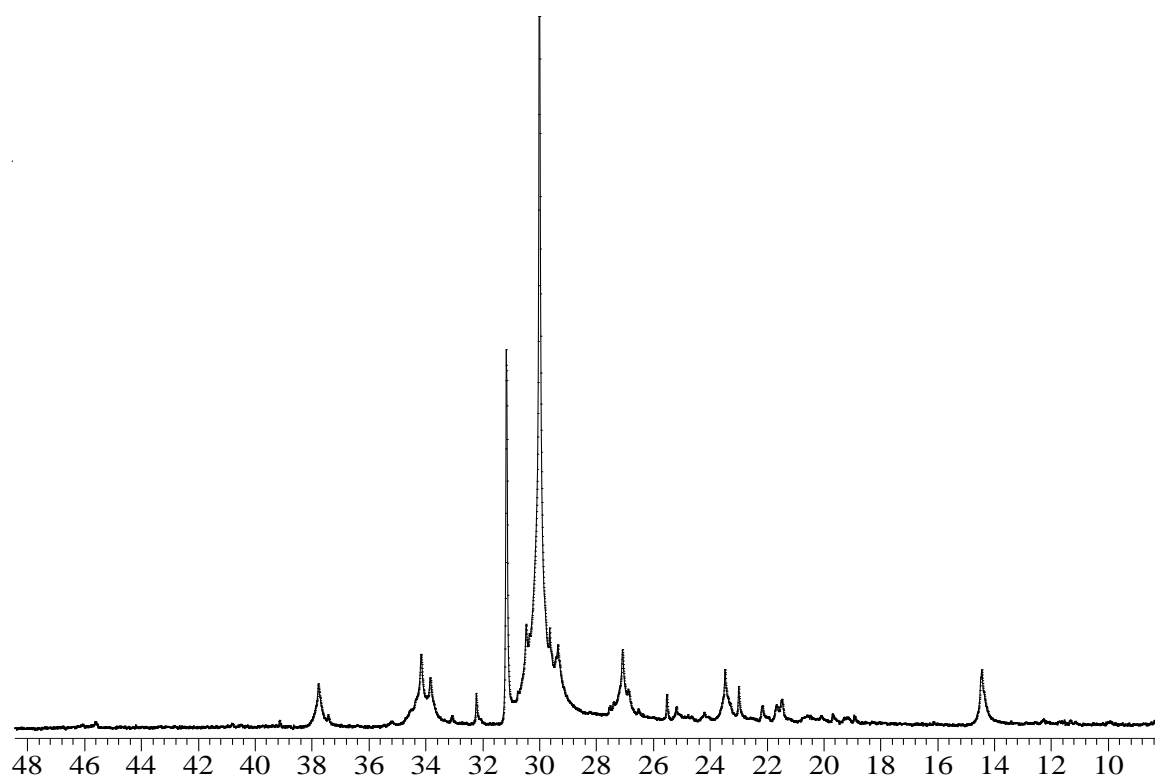


Figure C5. ^{13}C NMR of 50°C fraction of reference sample

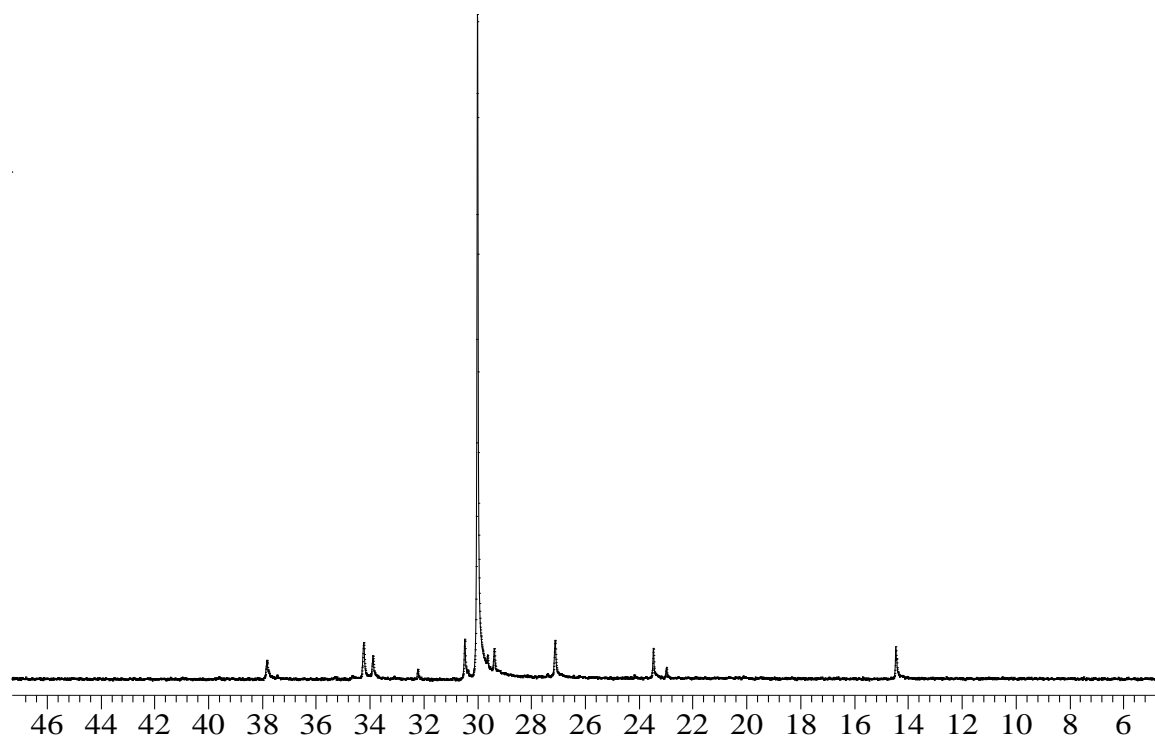


Figure C 6. ^{13}C NMR of 60°C fraction of reference sample

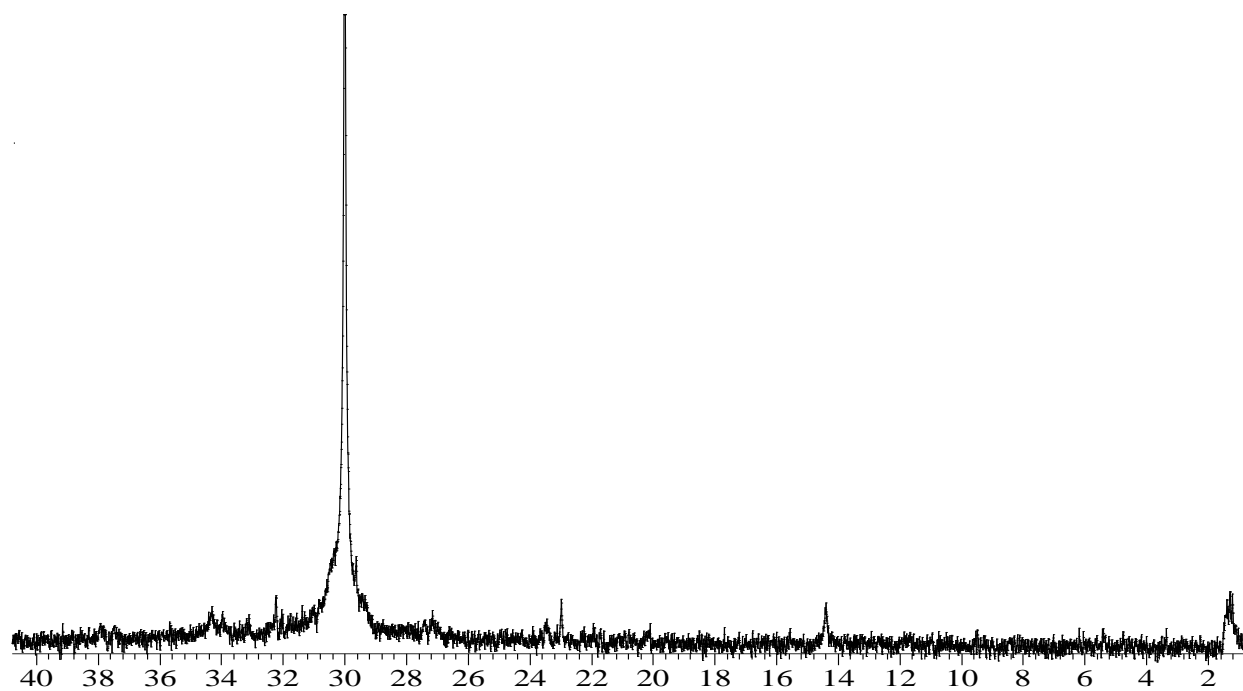


Figure C 7. ^{13}C NMR of 70 $^{\circ}\text{C}$ fraction of reference sample

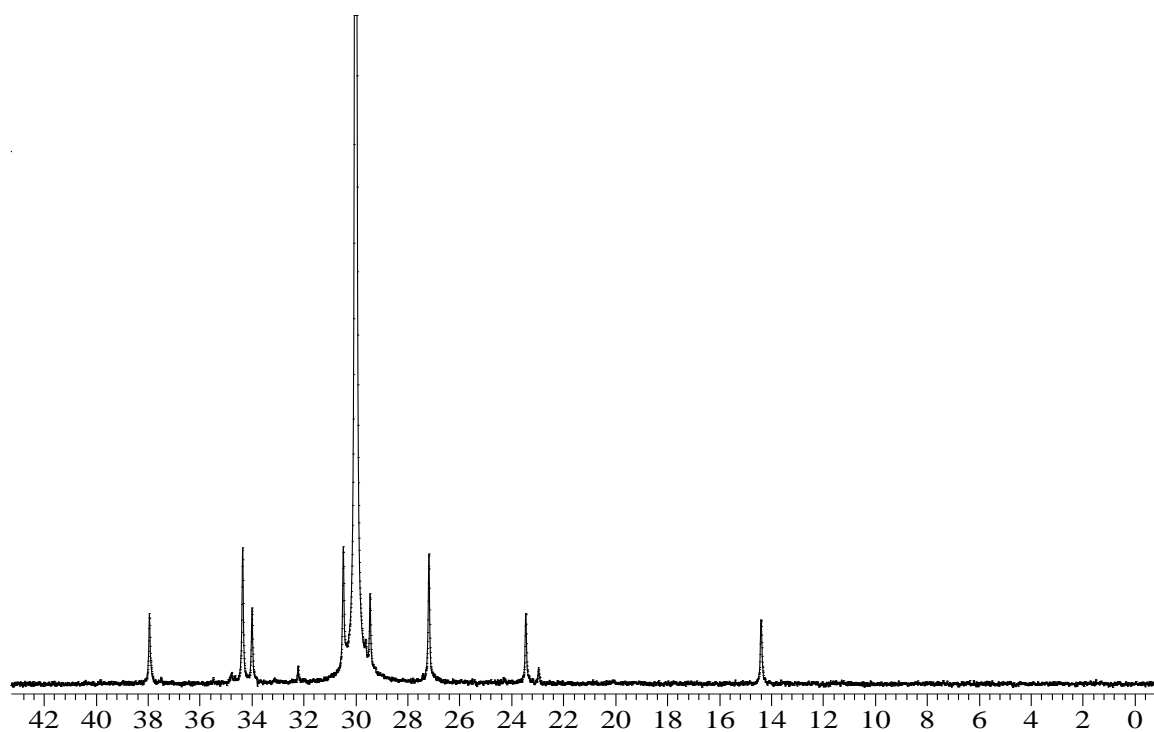


Figure C 8. ^{13}C NMR of 80 $^{\circ}\text{C}$ fraction of reference sample

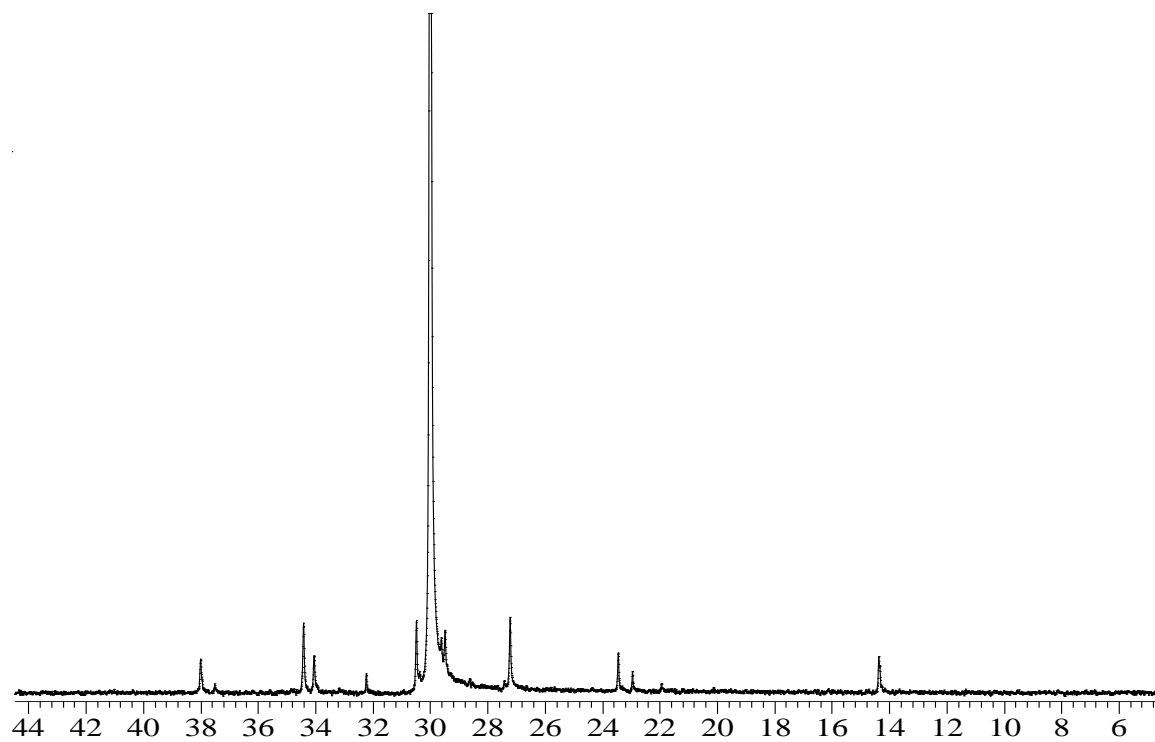


Figure C9. ^{13}C NMR of 90 $^{\circ}\text{C}$ fraction of reference sample

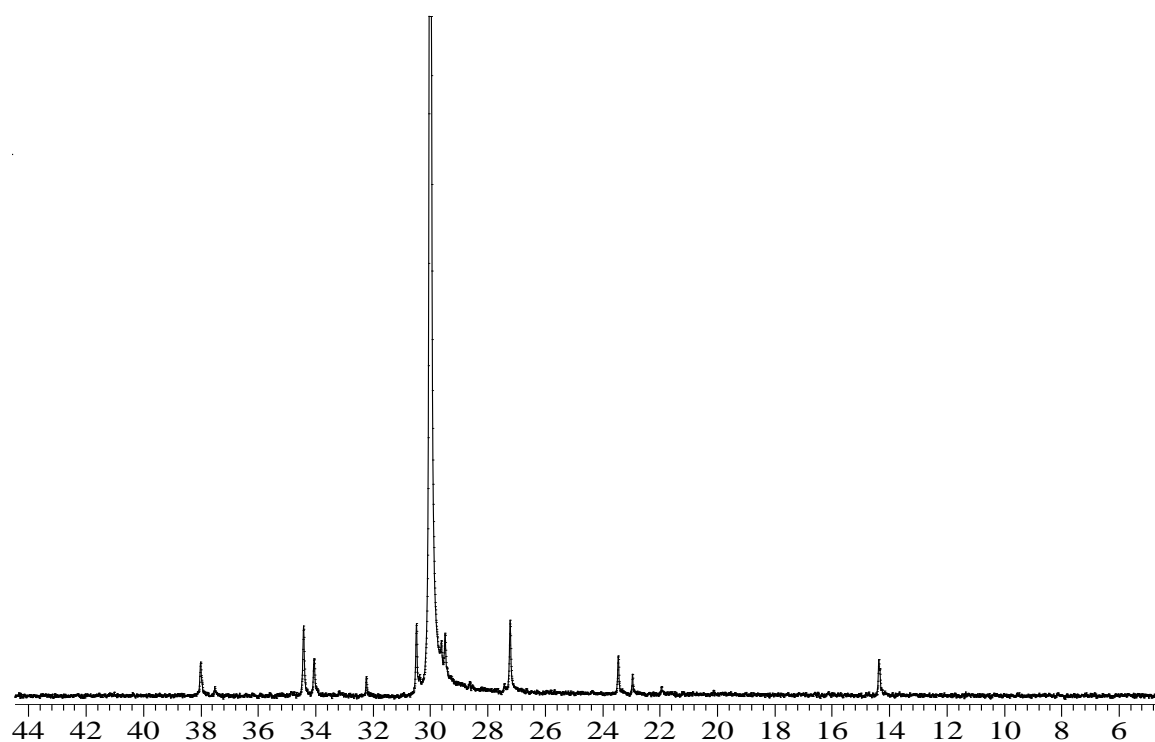


Figure C10. ^{13}C NMR of 100 $^{\circ}\text{C}$ fraction of reference sample

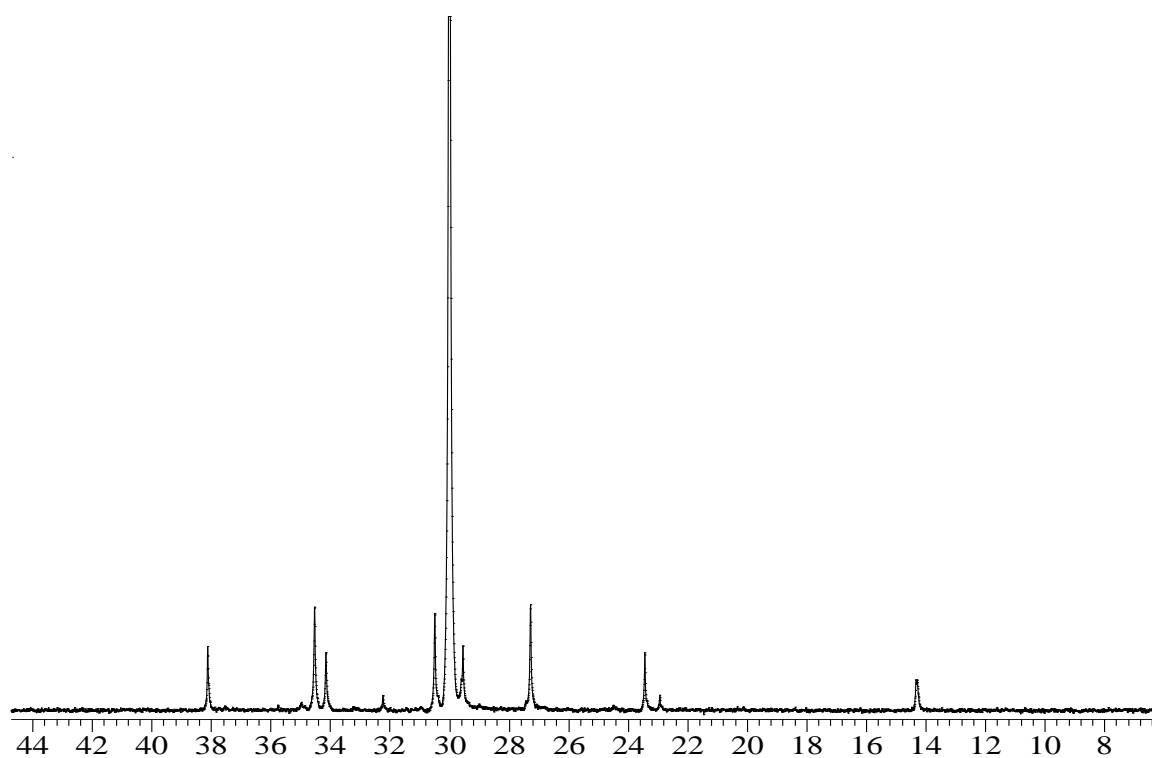


Figure C11. ^{13}C NMR of 110 $^{\circ}\text{C}$ fraction of reference sample

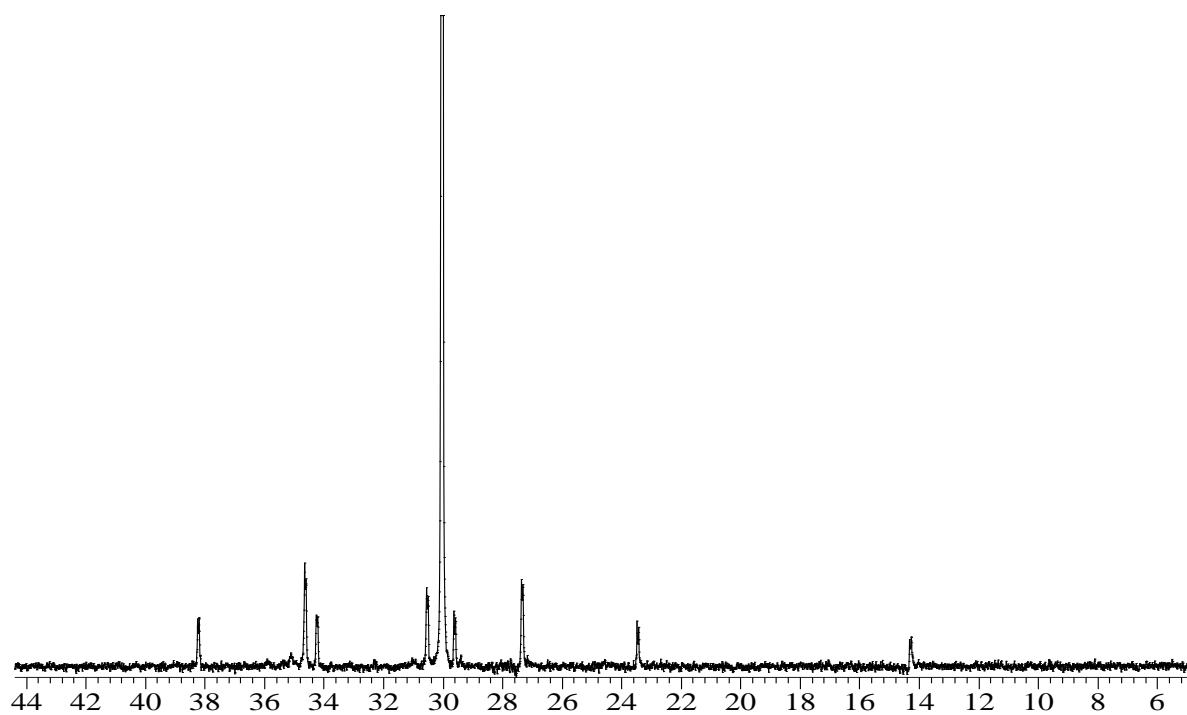


Figure C12. ^{13}C NMR of bulk catalyst trial sample 1

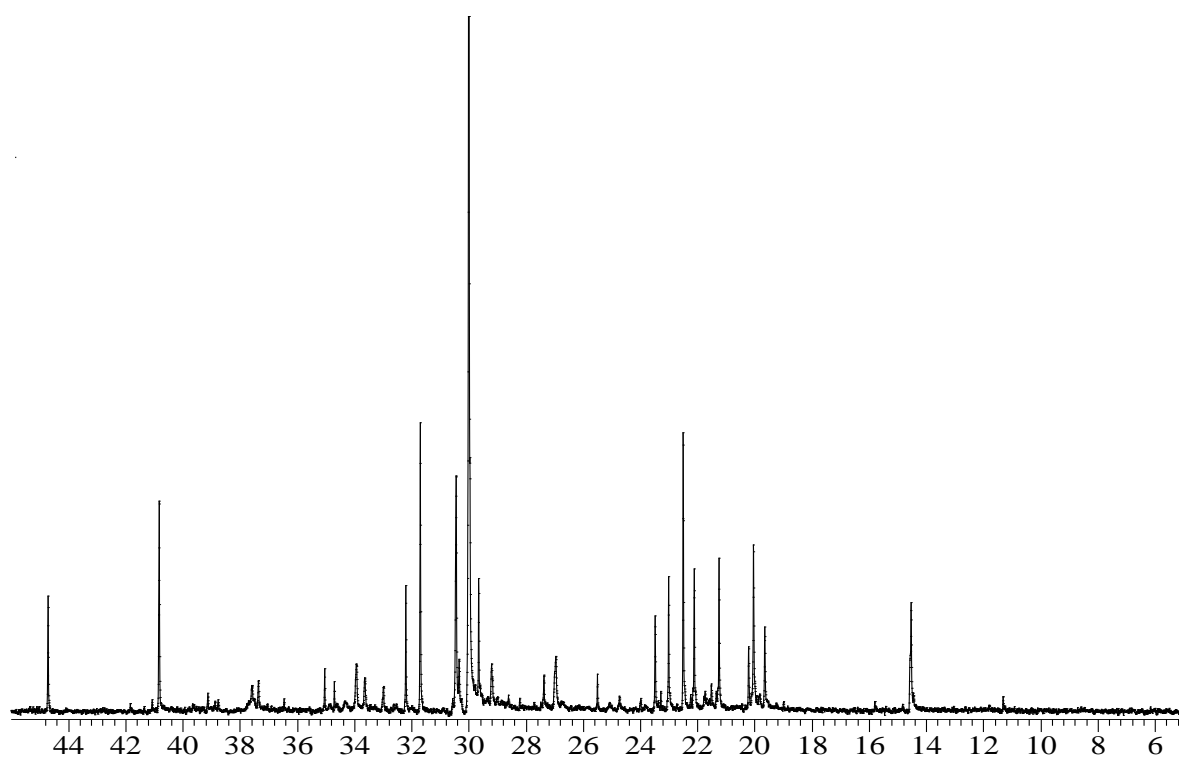


Figure C13. ^{13}C NMR of 20 $^{\circ}\text{C}$ fraction of catalyst trial sample 1

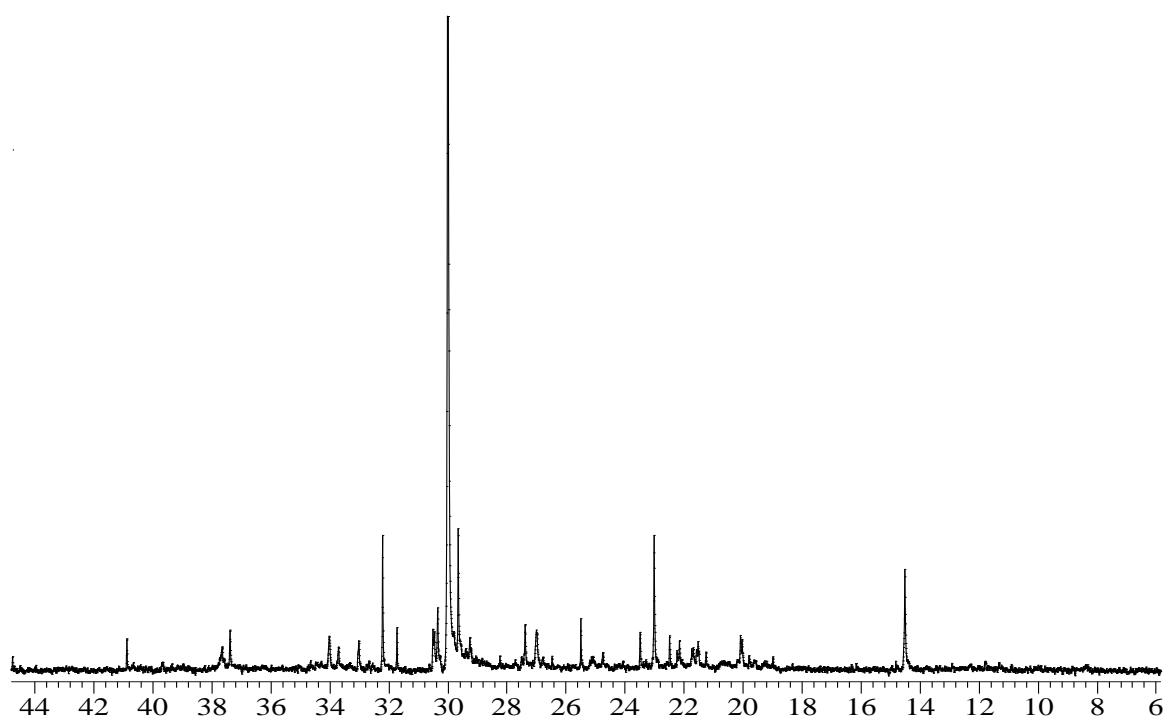


Figure C14. ^{13}C NMR of 30 $^{\circ}\text{C}$ fraction of catalyst trial sample 1

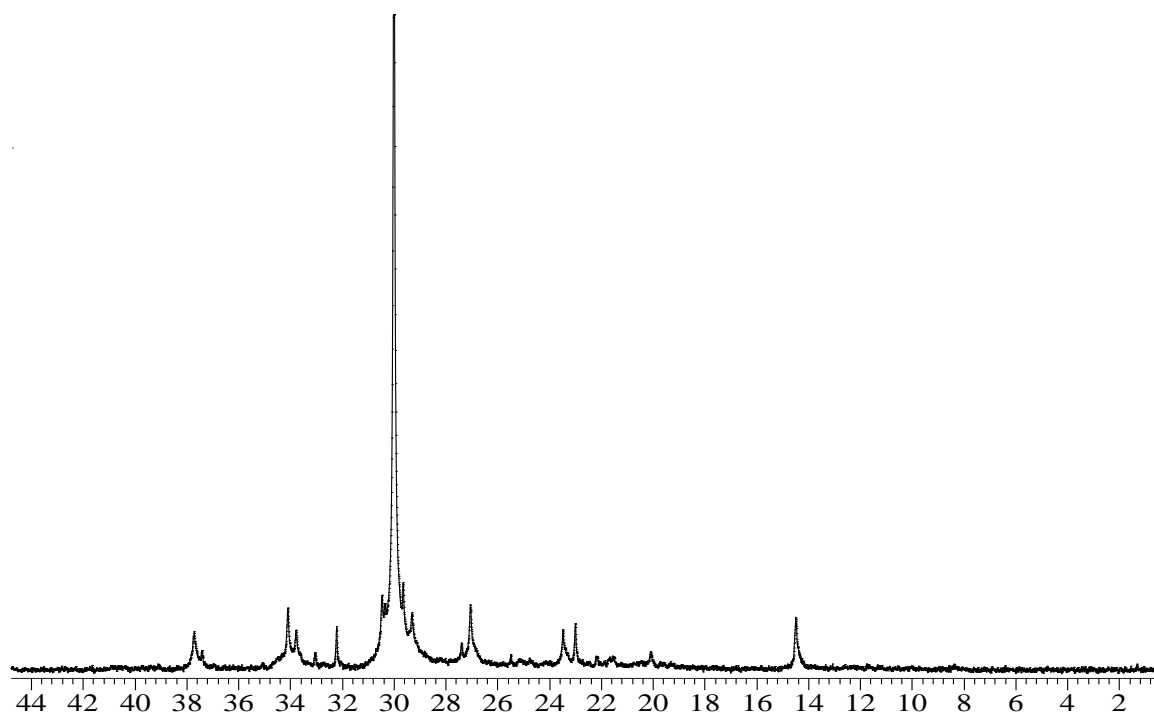


Figure C15. ^{13}C NMR of 40 $^{\circ}\text{C}$ fraction of catalyst trial sample 1

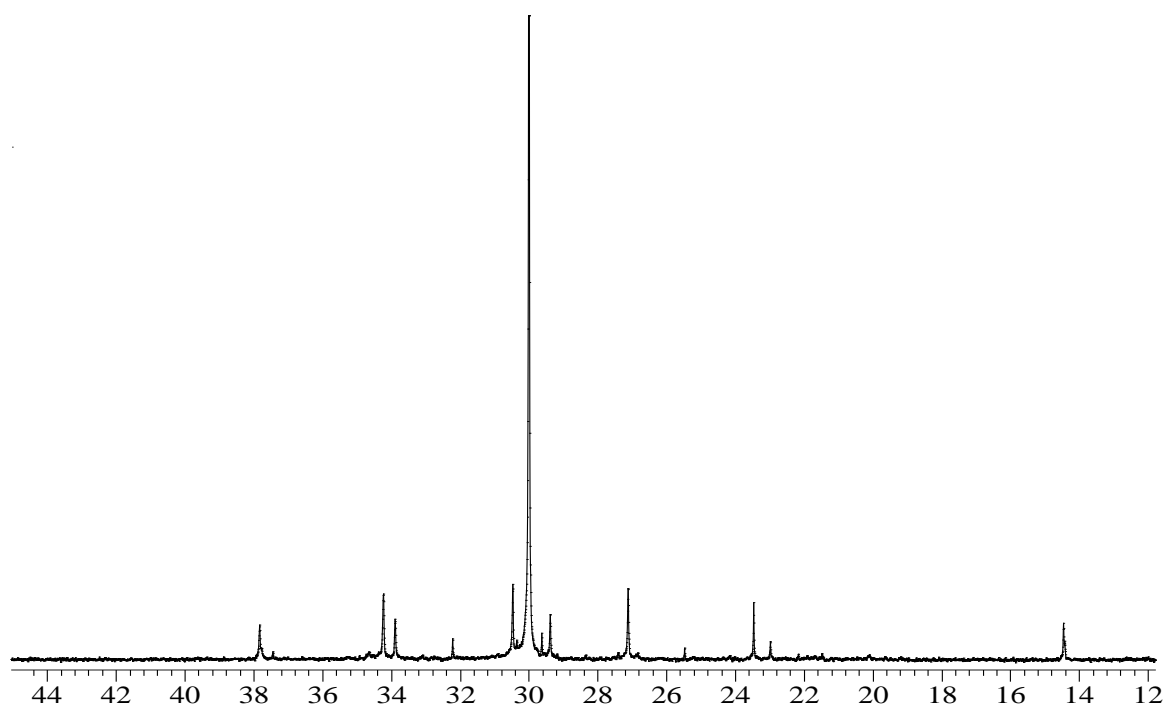


Figure C16. ^{13}C NMR of 60 $^{\circ}\text{C}$ fraction of catalyst trial sample 1

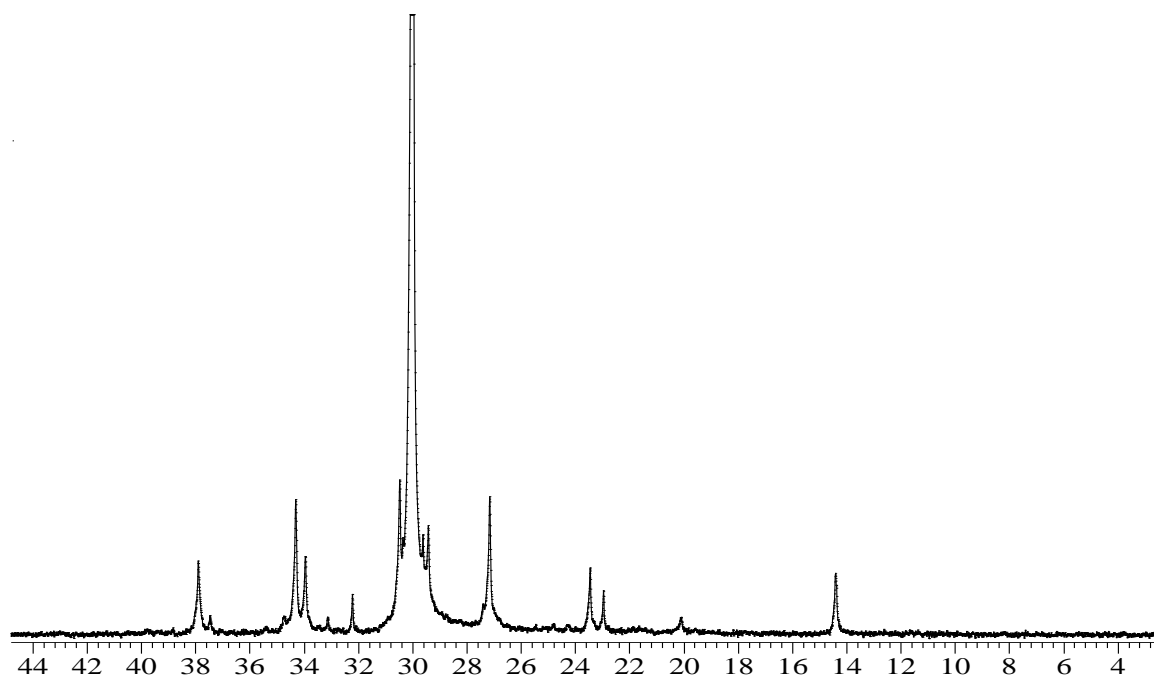


Figure C17. ^{13}C NMR of 70 $^{\circ}\text{C}$ fraction of catalyst trial sample 1

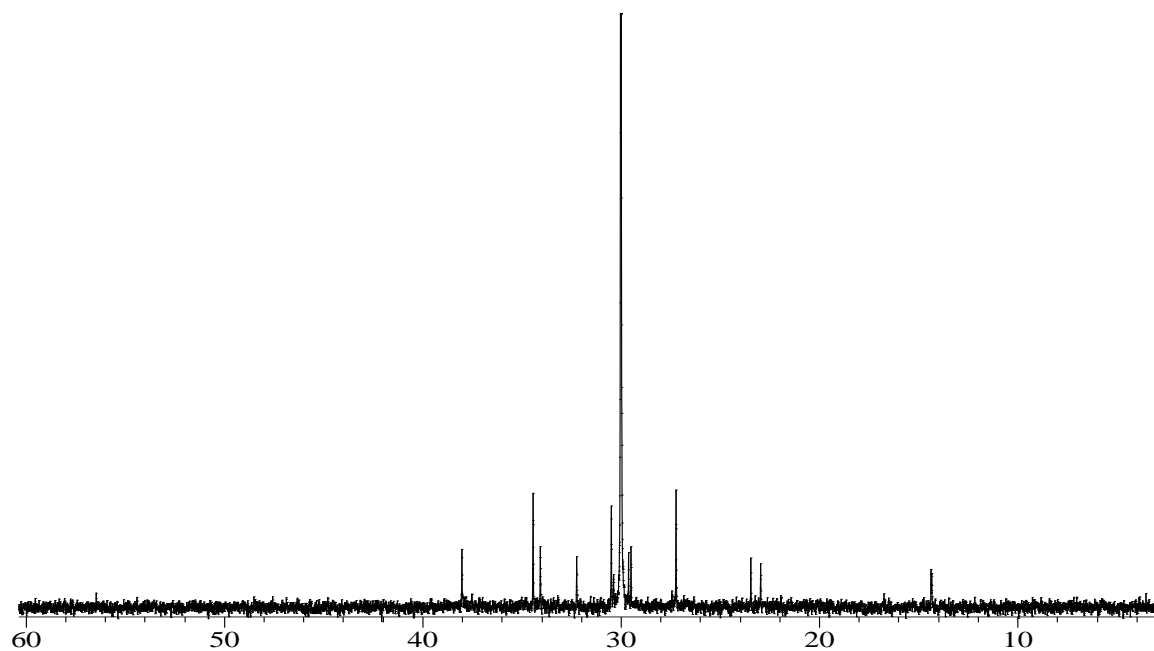


Figure C18. ^{13}C NMR of 90 $^{\circ}\text{C}$ fraction of catalyst trial sample 1

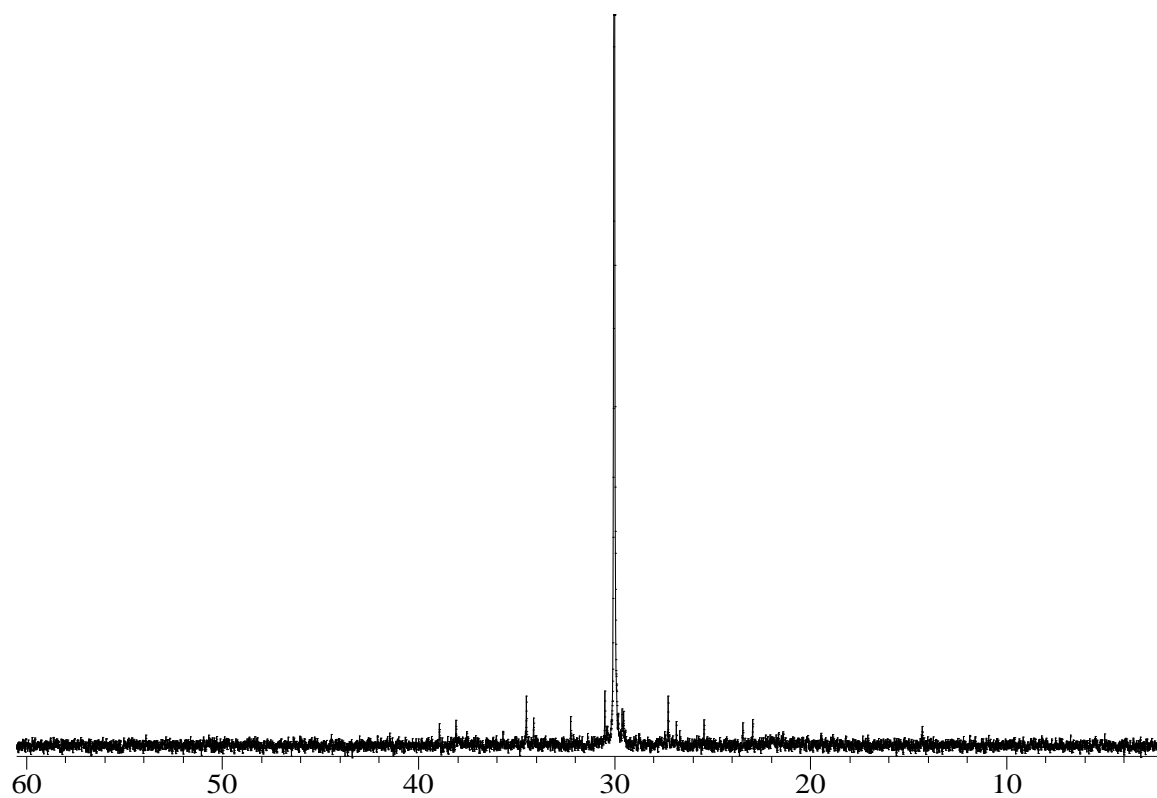


Figure C19. ^{13}C NMR of 100 $^{\circ}\text{C}$ fraction of catalyst trial sample 1

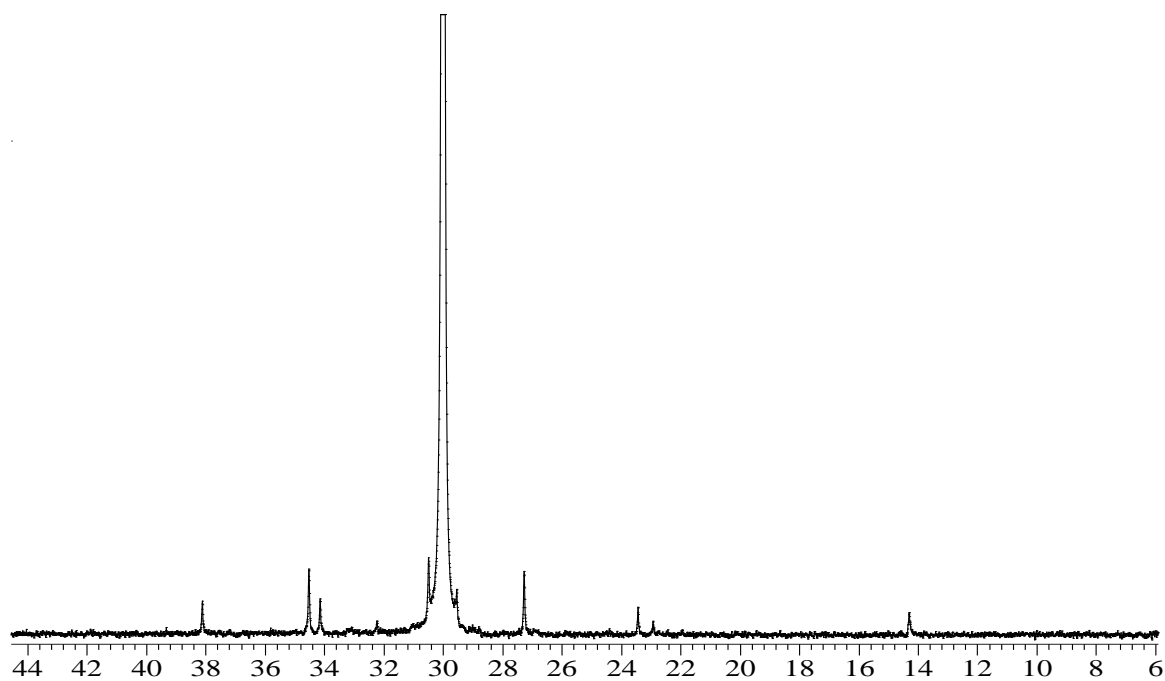


Figure C20. ^{13}C NMR of 110 $^{\circ}\text{C}$ fraction of catalyst trial sample 1

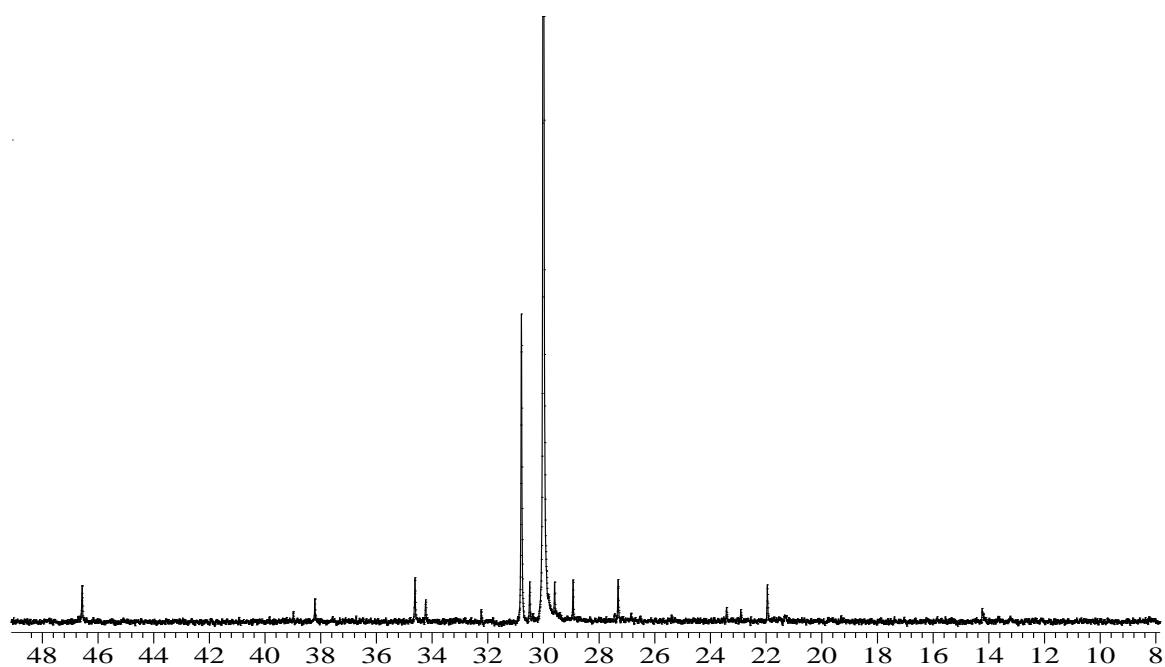


Figure C21. ^{13}C NMR of 120°C fraction of catalyst trial sample 1

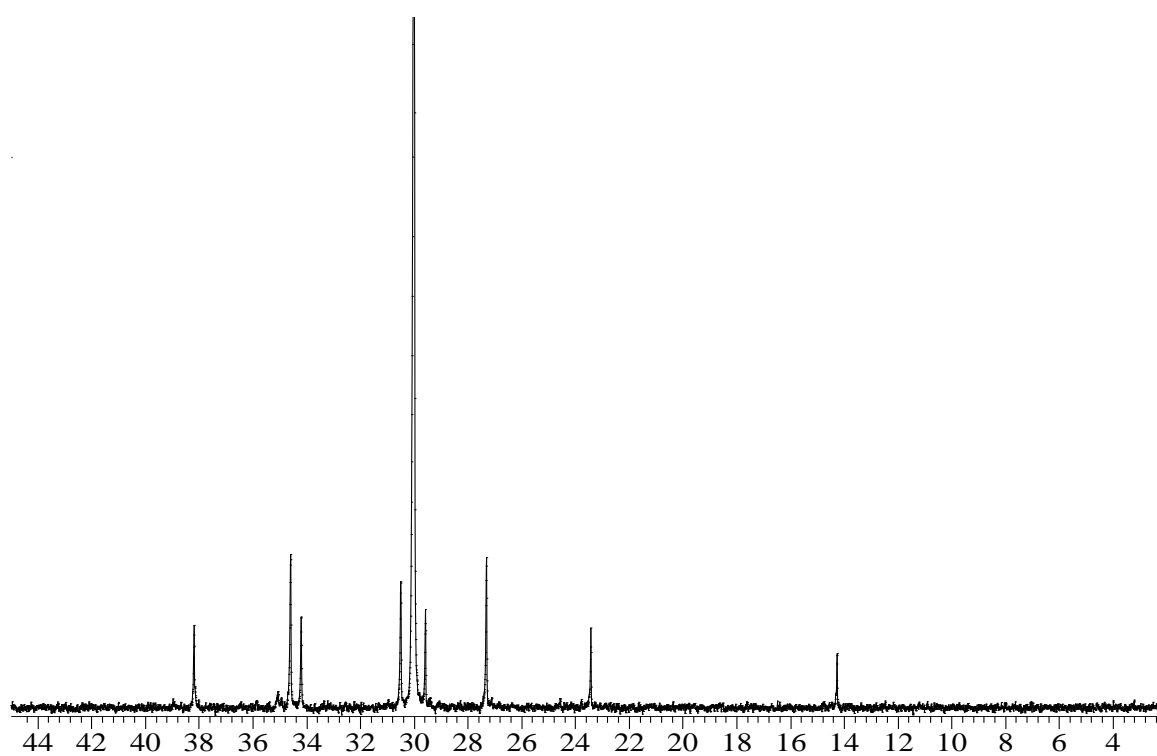


Figure C22. ^{13}C NMR of Catalyst Trial sample 2

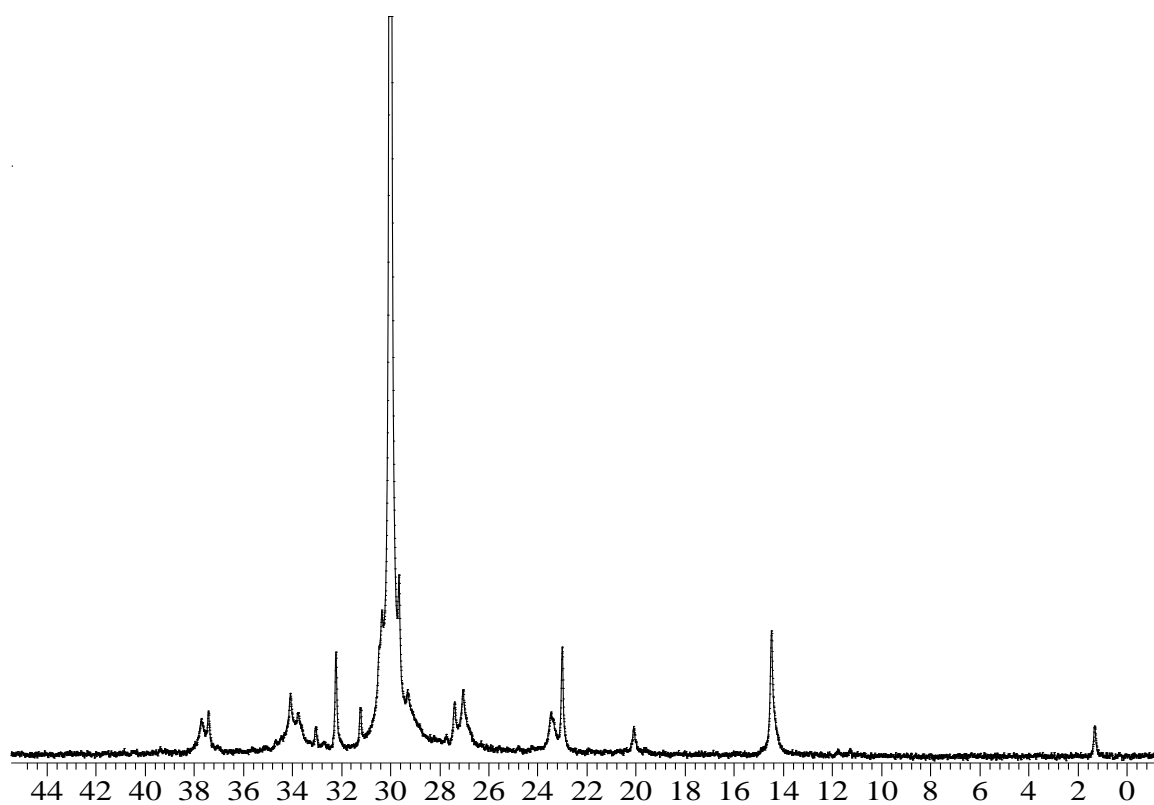


Figure C23. ^{13}C NMR of 40 $^{\circ}\text{C}$ fraction of catalyst trial sample 2

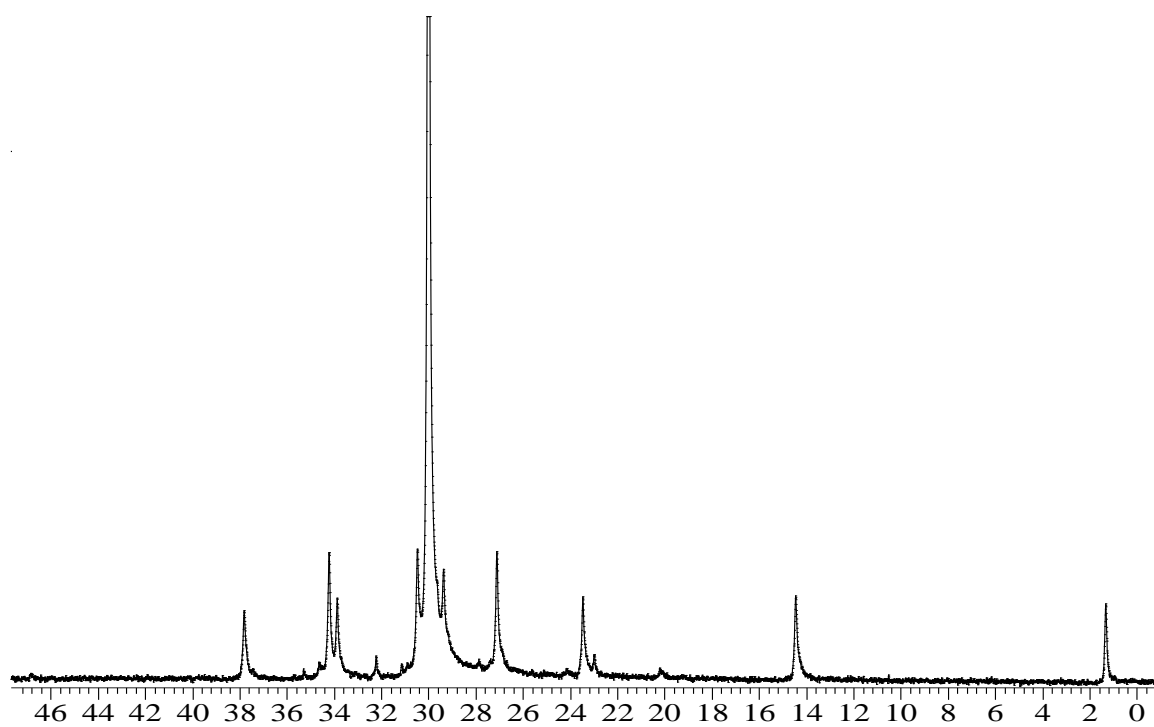


Figure C24. ^{13}C NMR of 60 $^{\circ}\text{C}$ fraction of catalyst trial sample 2

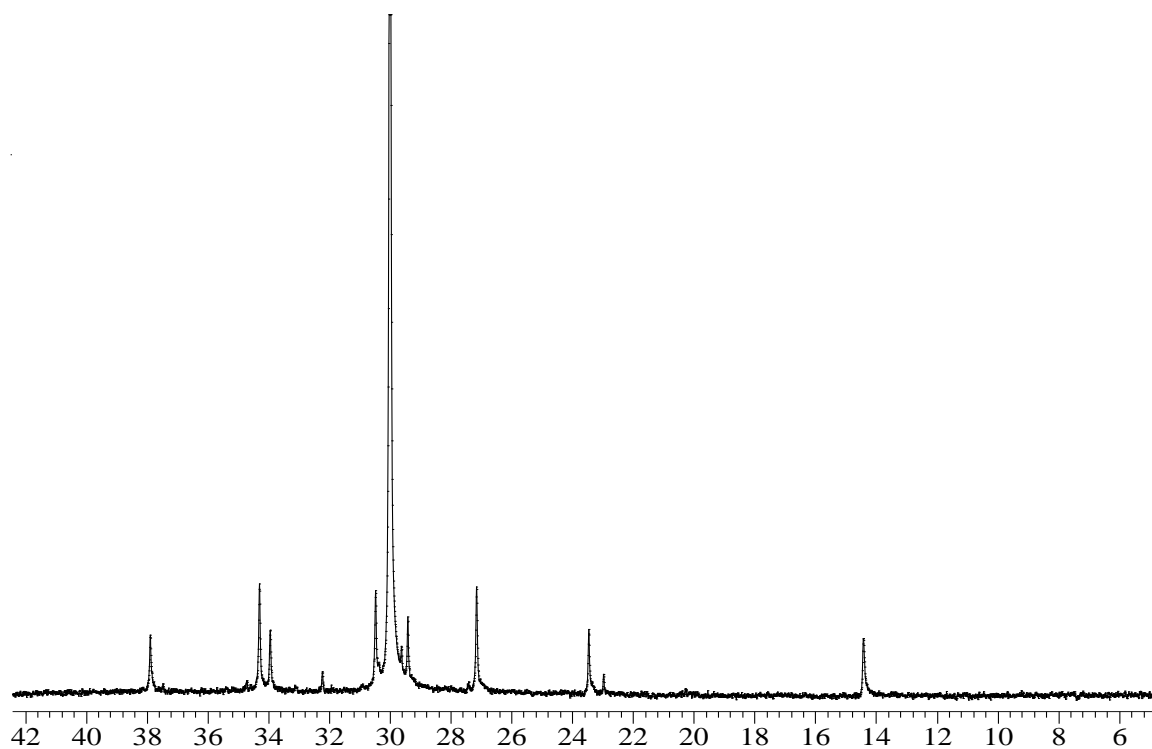


Figure C25. ^{13}C NMR of 70 $^{\circ}\text{C}$ fraction of catalyst trial sample 2

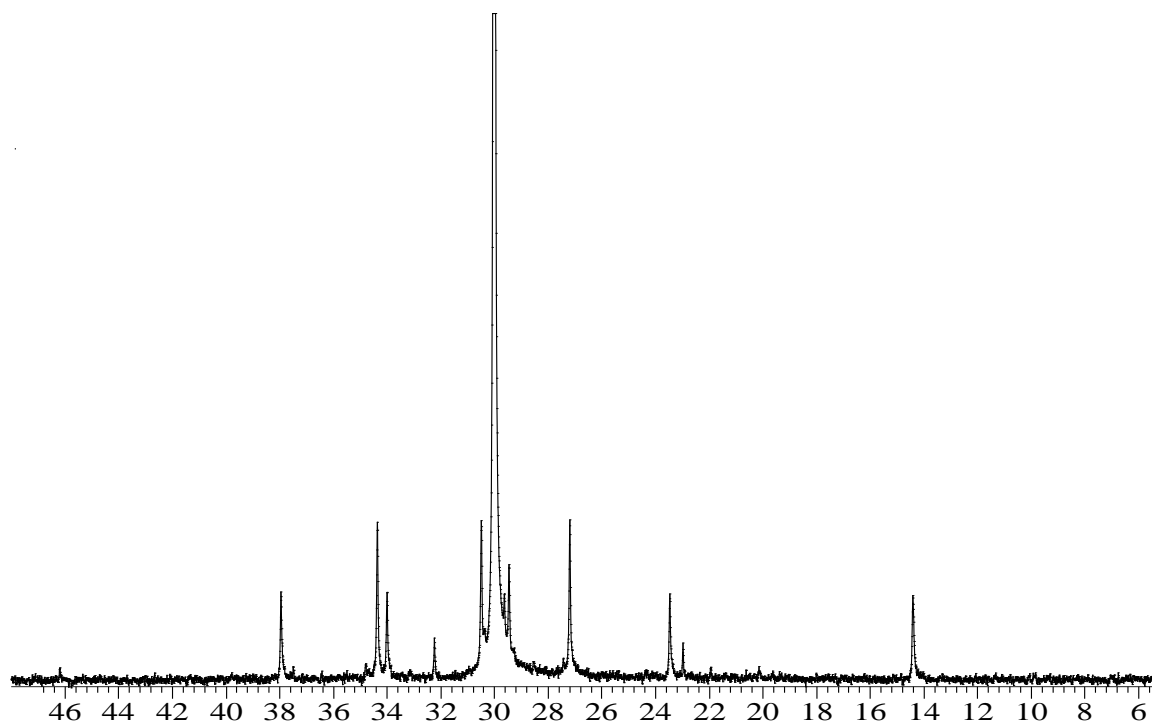


Figure C26. ^{13}C NMR of 80 $^{\circ}\text{C}$ fraction of catalyst trial sample 2

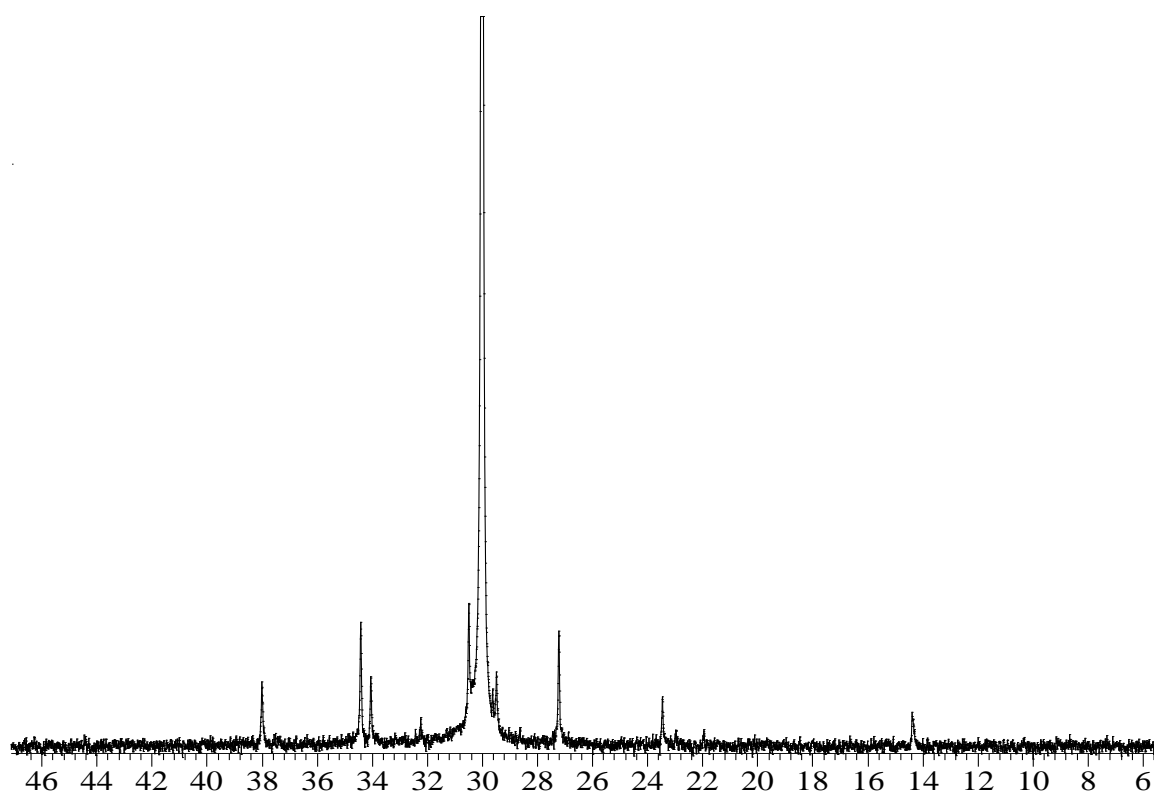


Figure C27. ^{13}C NMR of 90°C fraction of catalyst trial sample 2

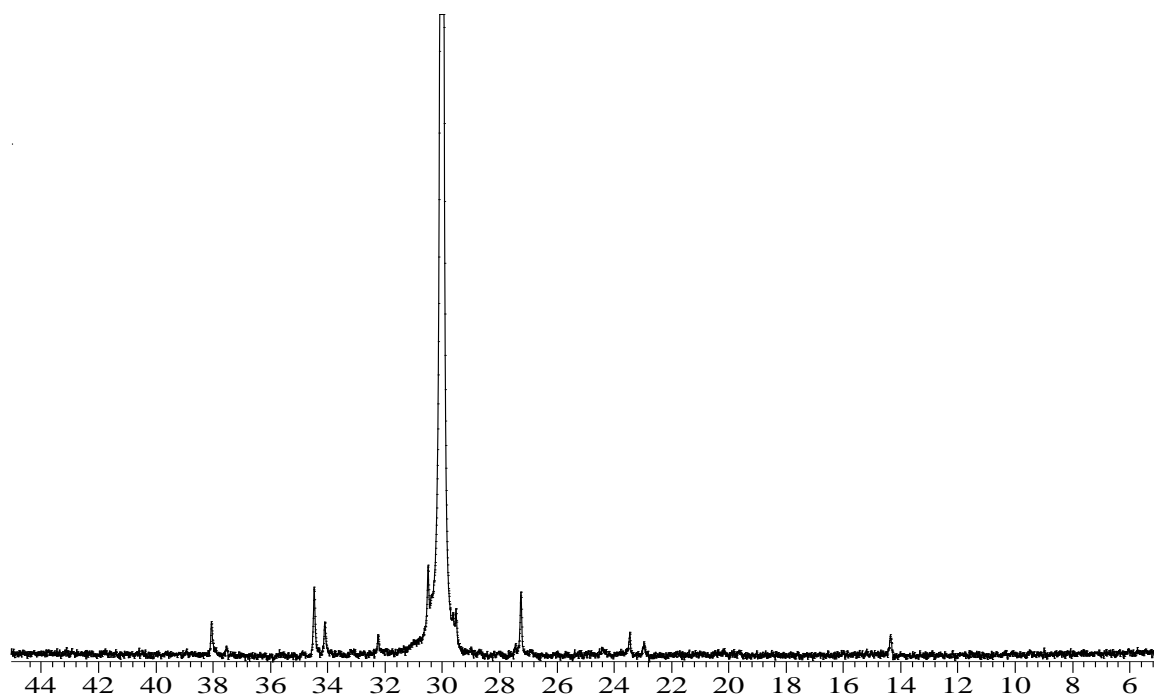


Figure C28. ^{13}C NMR of 100°C fraction of catalyst trial sample 2

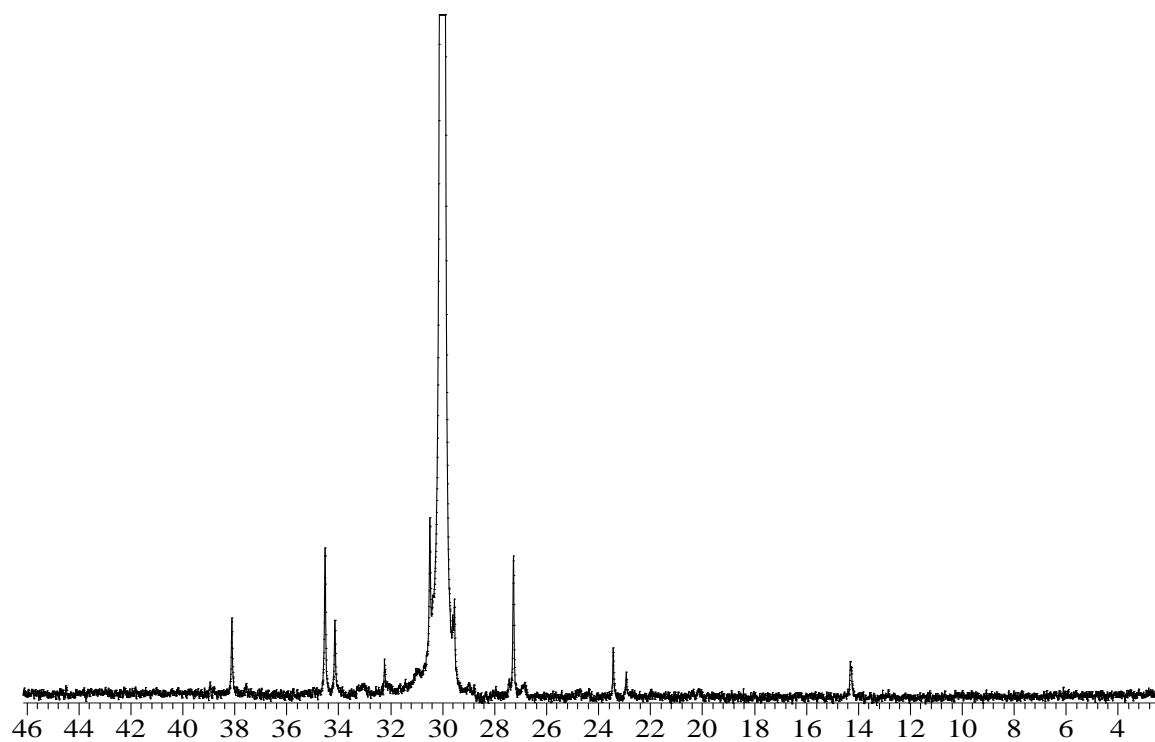


Figure C29. ^{13}C NMR of 110 $^{\circ}\text{C}$ fraction of catalyst trial sample 2